THESIS ENTITLED

SYNTHESES, CHARACTERIZATION AND CYTOTOXIC ACTIVITY OF SOME METAL COMPLEXES WITH PYRIDYLPYRAZOLE LIGAND

SUBMITTED TO
THE MAHARAJA SAYAJIRAO UNIVERSITY OF BARODA

For the Degree of

DOCTOR OF PHILOSOPHY

IN

CHEMISTRY

By

Mr. ZALA MAHENDRASINH GAJUBHA, M.Sc.

DEPARTMENT OF CHEMISTRY FACULTY OF SCIENCE
THE M. S. UNIVERSITY OF BARODA,
VADODARA-390002
GUJARAT
INDIA

AUGUST-2011

THESIS ENTITLED

SYNTHESES, CHARACTERIZATION AND CYTOTOXIC ACTIVITY OF SOME METAL COMPLEXES WITH PYRIDYLPYRAZOLE LIGAND

SUBMITTED TO
THE MAHARAJA SAYAJIRAO UNIVERSITY OF BARODA

For the Degree of

DOCTOR OF PHILOSOPHY

IN

CHEMISTRY

By

Mr. ZALA MAHENDRASINH GAJUBHA, M.Sc.

DEPARTMENT OF CHEMISTRY FACULTY OF SCIENCE
THE M. S. UNIVERSITY OF BARODA,
VADODARA-390002
GUJARAT
INDIA

AUGUST-2011

Dr. Sujit Baran Kumar
Assistant Professor,
Department of Chemistry

Department of Chemistry
Centre of Advanced Studies in Chemistry
& DST-FIST sponsored Department
Faculty of Science, Vadodara 390 002 India
Tel: +91-265-2795552
E-mail: chemistry_msu@yahoo.com

The Maharaja Sayajirao University of Baroda

CERTIFICATE

This is to certify that the thesis "**Syntheses, Characterization and Cytotoxic Activity of Some Metal Complexes with Pyridylpyrazole Ligand**" incorporate the results of original investigation carried out by Mr. Zala Mahendrasinh Gajubha, M.Sc., who has registered his name in The M. S. University of Baroda, Vadodara since June 2008 for the award of Doctor of Philosophy under the supervision of Dr. Sujit Baran Kumar, Assistant Professor, Department of Chemistry, Faculty of Science, The Maharaja Sayajirao University of Baroda, Vadodara-390002. This work neither in part nor whole has been submitted for any other degree by Mr. Zala Mahendrasinh Gajubha or others.

It is also certified that he has fulfilled all the requirements of the regulations relating to the nature and period of research.

Guiding Teacher

(**Dr. Sujit Baran Kumar)**

DEDICATED TO MY FAMILY

CONTENTS

Acknowledgements

This thesis would not have been possible without the guidance, support and encouragement of my Guide Dr. Sujit Baran Kumar. I am sincerely grateful to him for always believing in me and my ideas. It is their belief that pushed me to explore more and more about coordination chemistry research. He is amongst the people who not only deserves acknowledgements but shall be remembered for life time.

I am deeply grateful to Prof. B.V. Kamath Head, Department of Chemistry for providing me infrastructure facilities to carry out my research work and continuously encouragement for research work.

Special thanks to Dr. Parimal Paul and Dr. E. Suresh for his practical advice and helping for X-ray diffraction for single crystal Analysis from CSMCRI, Bhavnagar.

I am also thankful to Prof. S. Bhattacharya and Mr. Suryabhan Singh helping me for X-ray diffraction for single crystal Analysis from Banaras Hindu University, Varansi,U.P .

I am thankful to Prof. N. D. Kulkarni and Dr. Bhavna Trivedi for helping me for Room temperature Magnetic study and Cyclic Voltammetry Study.

I sincerely like to thank UGC, New Delhi for their financial support in the form of RFSMS and also C.C Shroff fellowship.

I am also thankful to Dr. P.H. Parikh and Mr. Ayaz Rangrej for their help in Cytotoxic Activity experiments.

I am thankful to Dr. Nikunj Bhatt and Dr. Pratyush Patankar for their kind support and guidance during my work. . Dr. Nikunj Bhatt had been more than a senior to me, He was with me irrespective of time and situation.

I would like to thank Mr. S. P. Shahoo for helping me in carrying out elemental analysis from SPARC and Mr. Rohit Jadav for helping me in carrying out ^{1}H NMR and ESI-MASS analysis from TRC.

I am heartily thankful to my juniors Mehul and Ankita for their immense efforts in accomplishing the writing of my thesis. I am also thankful to Mr. Dinesh Bhavsar and Mrs. Revthi Ganesh for their kind support during the long journey of my thesis.

I express my sincere gratitude to my family, for their kind support during the long journey of my thesis. My parents really work hard for my completion of ph.D.

LASTLY, I AM THANKFUL TO ALL MY TEACHERS STARTING FROM MY FIRST TEACHER, MY PARENTS TO MY GUIDE, FOR PUSHING ME TO WHAT I AM. I WOULD LIKE TO DEDICATE THIS THESIS TO THEIR SELFLESS EFFORTS IN EDUCATING ME.

Department of Chemistry
Faculty of Science (Zala Mahendrasinh Gajubha)
The Maharaja Sayajirao University of Baroda

PREFACE

The work embodied in this thesis entitled "Syntheses, Characterization and Cytotoxic Activity of Some Metal Complexes with Pyridylpyrazole Ligand" was initiated in January 2007, to explore the transition metal chemistry of pyridylpyrazole compounds. The characterizations of different compounds have been done using X-ray crystallography, other spectroscopic, cyclic voltammetry, variable temperature magnetic study and other physicochemical techniques. This thesis consists of six chapters on the studies of complexes of copper(II), cobalt(II), nickel(II), zinc(II) and cadmium(II) with pyridylpyrazole ligand and their cytotoxic activity. Metal complexes of pyridylpyrazole compounds have been the centers of attraction in coordination chemistry due to the bioactivity.

A brief survey of the known chemistry and application of different N-substituted pyrazole based ligands are outlined in introductory Chapter I along with the purpose of present investigation. In Chapter II we describe "Synthesis and characterization of pyridylpyrazole ligand and some mononuclear complexes of Cu(II), Ni(II) and Co(II) and binuclear Cu(II) complexes with Pyridylpyrazole ligand". "Synthesis and characterization of thiocyanate and selenocyanate containing complexes with pyridylpyrazole ligand" are described in Chapter III. The chapter IV describes the 'Synthesis, characterization, structure and magnetic study of azido and cyanato bridged nickel(II) and copper(II) complexes and it has two sections. In section IVA, we describes the "Synthesis, characterization, structure and magnetic properties of azido bridged binuclear complexes of Cu(II) and Ni(II) with pyridylpyrazole ligand" and in section IVB, we described the "Synthesis, characterization, structure and magnetic properties of cyanate bridged binuclear complexes of Cu(II) and Ni(II) with pyridylpyrazole ligand". The Chapter V deals with the "Synthesis, characterization and structure of Zn(II) and Cd(II) complexes with pyridylpyrazole ligand". In Chapter VI, we describe "Study of cytotoxic activity of copper(II), nickel(II), cobalt(II), cadmium(II) and zinc(II) complexes with pyridylpyrazole ligand" In brief, this thesis accounts the chemistry of copper(II), cobalt(II), nickel(II), zinc(II) and cadmium(II) complexes pyridylpyrazole ligand and

their cytotoxic activity. I am happy to note that the work has been published in some International journals (List of Publications).

In keeping with the general practice of reporting scientific observation, due acknowledgement has been made whenever the work described as based on the findings of other investigators. I must take the responsibility of any unintentional oversights and errors which might have kept in spite of due precautions.

Department of chemistry
Faculty of Science
The M. S. University of Baroda **(Zala Mahendrasinh Gajubha)**

CHAPTER-I

INTRODUCTION

A Partial review on the Coordination Chemistry of Multidentate Nitrogen-containing Pyrazolyl ligand and their Complexes

Introduction

The coordination chemistry of heterocyclic nitrogenous chelating ligands was started by F. Blau [1] and he first described the transition metal complexes of nitrogen containing heterocyclic 2,2'-bipyridine (bpy) [1]. Later bidentate and tridentate nitrogen containing heterocyclic compounds 1,10-phenanthroline and 2,2':6',2''-terpyridine have been extensively used in transition and non-transition metal complexes [2-3]. The important feature of these heterocyclic is that they behave as an excellent π-acceptors ligand. Therefore they provide soft metal coordination sites. The tremendous development of coordination chemistry of bidentate and tridentate ligands and their applications in the field of chemical, structural, catalysis etc. have inspired to design multi *N*-donor centers in which one of the donor center is coming from pyridine or *N*-heterocyclic. In most cases heterocyclic pyridine ring along with five membered heterocyclic system such as imidazole, pyrazole, thiazole, oxazoles are generally used to design polydenated nitrogen donor ligands. Imidazole and pyrazole derivatives are extensively studied because of their appearance in biomolecules.

Pyrazole containing anionic tripodal poly(pyrazole)borate ligand was introduced by Trofimenko in 1966 and it has been extensively employed to stabilize a variety of organometallic and coordination compounds [4]. Transition metal complexes with this ligand have wide application in different areas in chemistry. A number of review articles on pyrazole containing ligand and their complexes are available in the literature [5-11]. A new method for the synthesis of a large variety of N-substituted pyrazole derivatives was reported by Driessen and he discussed coordination properties of the new series of N-substituted pyrazole derivatives of different amines towards several first-row transition metal ions [12-18]. The nature and properties of these compounds was a good base for studies of more complex chelating ligands and their compounds. To design appropriate multidentate polynucleating ligands, besides the binding sites, the spacer groups between them play a very important role. These spacers group connect the different coordination moieties at a desired distance from each other, thus regulating the steric and electronic properties of the metal complexes. For example, when a spacer such as methylene group is incorporated between the rings, the electronic communication between these two

heterocyclic is prevented and the complexes of such ligands give rise to significantly different electronic properties. A number of other pyrazole-based chelating ligands, which consist of pyrazole heterocycles linked by NR (R = H or alkyl or benzyl or pyridine-CH_2) with incorporation of 'insulating spacer(s)' between the coordinating sites have also been synthesized and their coordination chemistry well-developed and the complexes of such ligands give rise to significantly different electronic properties. The design of such ligands must take into account the factors influencing the stability and molecular geometry of the complexes.

Review of the present status of the chemistry of pyrazolyl containing multi Nitrogen-coordination ligands and their compounds

It is clear from the foregoing discussion that pyrazole containing multi donor ligand have rich coordination environment and form variety of complexes with transition metal ions with varying coordination geometry and nuclearity. In the following we have, therefore, collected information that are available for nitrogen containing pyrazole based ligands and their complexes. In the recent times many interesting papers dealing with the chemistry of pyrazole containing multidentate ligands have appeared in the literature [19-41]. We, therefore, have restricted our discussion only to those systems that are relevant to the subject presented in this dissertation.

1. Pyrazole containing bidentate ligand and their complexes

There are few types of pyrazole-based bidentate chelating ligands reported in the literature. The number of ligands as well as complexes is very limited. In this type of bidentate ligand, chelation sites are available from (A). One pyrazole and one pyridine e.g. pyrazolylmethylpyridine or (B). Two pyrazole molecules e.g. bis(pyrazole-1-yl)methane.

A. One pyrazole and one pyridine containing chelating ligand

In this type of ligand, there are two chelating nitrogen atoms- one from pyrazole and another from pyridine nitrogen atoms. Pyrazolylmethylpyridines ligands (L_1) having both

pyrazole and pyridine group [Fig.1] and it form 1:1 complexes with different metal ions e.g. $PdCl_2$, $CoCl_2$, $NiCl_2$ and also form complexes of the types such as $[M(L_1)_2Cl_2].4H_2O$ (M = Co^{+2} and Ni^{+2}), $[M(L_1)_3][ClO_4]_2.H_2O$ (M = Co^{+2} and Ni^{+2}) and $[Cu(L_1)_2NO_2][ClO_4]$ [42, 43]. The X-ray structure of $[Co(L_1)_2Cl_2].4H_2O$ shows that cobalt atom has octahedral coordination environment and two Cl^- are in the trans position. The distance of Co-N from pyridine and Co-N from pyrazole are not same. This ligand also form octahedral complexes of the type $[M(L)_3](ClO_4)_2$ (M = Co(II) and Ni(II)).

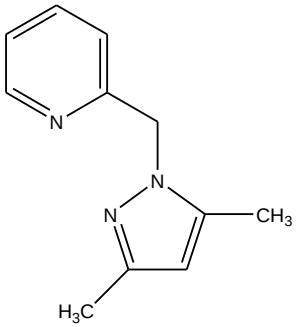

Fig.1. 2-((3,5-dimethyl-1*H*-pyrazol-1-yl) methyl)pyridine

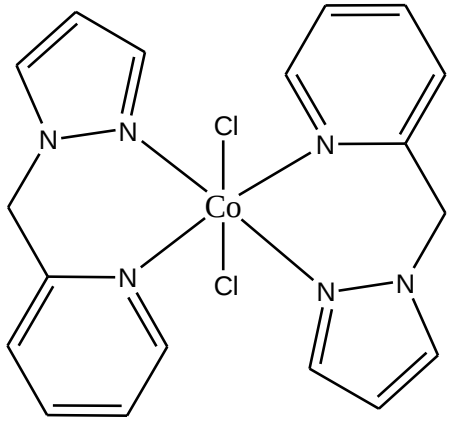

Fig.2. Structure of $[CoCl_2L_1]$

B. Two pyrazoles containing chelating ligand

In this type of ligand, two chelation sites are obtained from pyrazole nitrogen atoms. For example, bis(pyrazole-1-yl)methane and its derivatives [Fig.3 and Fig.4] has been used as ligands in the synthesis of complexes of the first transition series. The ligands are coordinated to a metal ion in a bidentate cyclic type and form a six-membered ring [44,45].

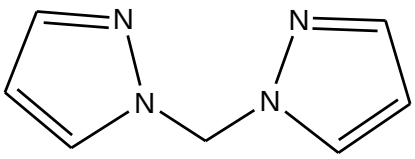

Fig. 3. Bis(pyrazol-1-yl)methane

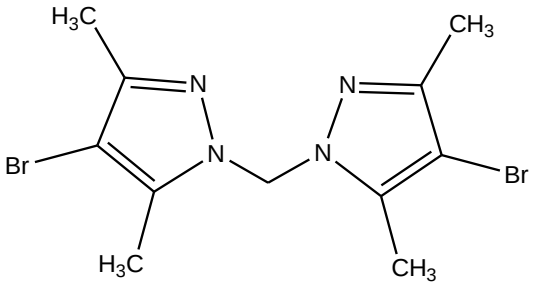

Fig.4. Bis(4-bromo-3,5-dimethylpyrazol-1-yl)methane

Another important bidentate pyrazole based ligand is 1,3-bis(3,5-dimethylpyrazol-1-yl) propane, where a propyl bridge connects two pyrazole rings [Fig. 5]. If a hydroxyl group is introduced on the central carbon of the propyl bridge, the resulting tridentate ligand 1,3-bis(3,5-dimethylpyrazol-1-yl)propan-2-ol ((Hdpzhp) leads to dinuclear species. In this bidentate ligand, the binding sites and the spacer groups play a very important role. These spacers connect the different coordination moieties at a desired distance from each other, thus regulating the steric factors. Copper complexes with the formula $[Cu_2(\mu$-dpzhp-$O,N,N')_2]X_2$ with X = $Cu(MeOH)Cl_3$, NO_3^-, and BF_4^- and $[Cu_2(\mu$-dpzhp-$O,N,N')(\mu$-$OH)Cl_2]$ have been synthesized and characterized. It shows the ligand is dinucleating and can act as an N_2O donor set with a bridging alkoxo group. The single-crystal X-ray structure of $[Cu_2(\mu$-dpzhp-$O,N,N')_2][Cu(MeOH)Cl_3]_2$ shows the copper ions in the dinuclear cation in distorted square-planar environments [46-48].

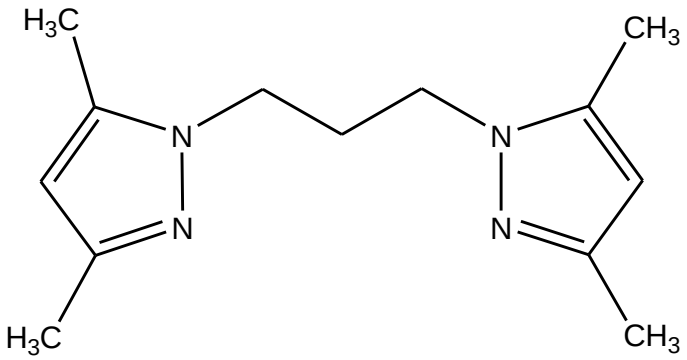

Fig. 5. 1,3-bis(3,5-dimethylpyrazol-1-yl)propane

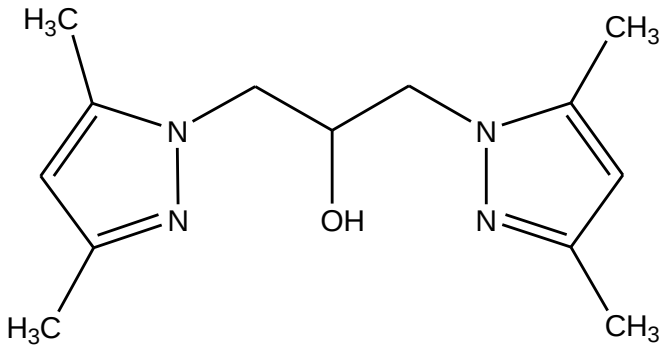

Fig. 6. 1,3-bis(3,5-dimethylpyrazol-1-yl)propan-2-ol

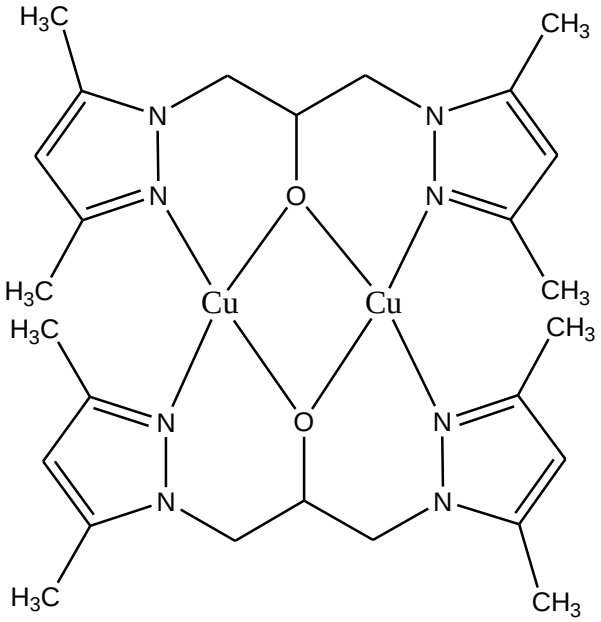

Fig. 7. Dinuclear copper(II) complex of 1,3-bis(3,5-dimethylpyrazol-1-yl)propan-2-ol

2. Pyrazole containing tridentate ligands and their complexes.

There are many pyrazole containing ligands which have tridentate chelation sites with the metal center. Majority of the pyrazole containing ligands have tridentate coordination sites and it is possible to understand the relationship between the bonding properties of pyridyl nitrogen and pyrazole nitrogen by incorporating a spacer between them. The introduction of methyl substituents in the 3,5 position of the pyrazole ring cause observation of the predominance of steric over electronic effect. There are two important

types' pyrazole containing tridentate ligands. They are (1).ligand containing two pyrazole and one amine, (2). ligand containing two pyrazoles and one pyridine.

A. **Two pyrazoles and one amine containing chelating ligand**

In this tridentate N_3-chelating ligand sites, two nitrogen chelation sites obtained from the pyrazol and one nitrogen chelation site from amine. Example of ligand having two pyrazoles and one amine is *N*,*N*-bis(3,5-dimethyl-l-pyrazol-ly-ethyl)aminoethane (aebd) and *N*,*N*-bis(l-pyrazolylethyl)aminoethane (aebp). Both the ligands form coordination compounds with copper(I) with the general formula [Cu(aebd)X] where X = Cl, Br, I and SCN. Here the ligand acts as bidentate ligand with two pyrazole groups coordinating with the metal copper atom [Fig. 8] [49].

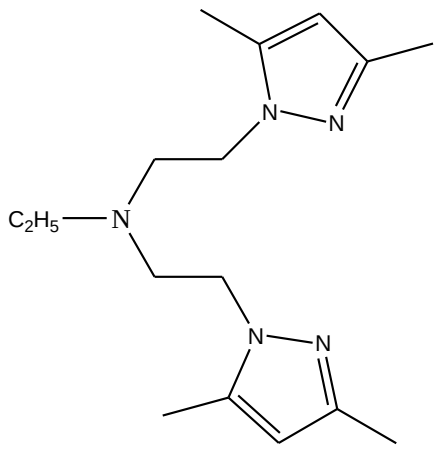

Fig.8. *N*,*N*-bis(l-pyrazoly-1yl-ethyl)aminoethane (aebp).

Sheu et al investigated the complexing properties of *N*,*N*-bis(pyrazol-1-ylmethyl) benzylamine (L_2) [Fig. 9], a newly prepared flexible ligand with iron(II), cobalt(II), nickel(II), copper(II) and zinc(II). The ligand reacted with metal ions to form $[Fe(L)Cl_3]$, $[Ni(L)(NCS)_2(CH_3OH)]$, $[M(L)X_2]$ (M = Co^{II}, Cu^{II} or Zn^{II}, X = Cl^-, Br^- and NCS^-) and most of the complexes have been structurally characterized. In $[Co(L_2)Cl_2]$ complex, the

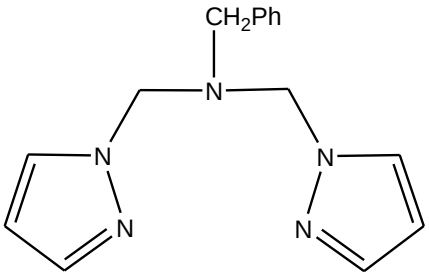

Fig. 9. *N*,*N*-bis(pyrazol-1-ylmethyl)benzylamine

cobalt(II) ion is surrounded by two pyrazolyl nitrogen atoms, an amine nitrogen and two chloride ions in a geometry which can be described as intermediate between tetrahedral and trigonal bipyramidal [Fig.10]. Similarly the geometry around cobalt(II) in $[Co(L_2)(NCS)_2]$ can also described as an intermediate between tetrahedral and trigonal bipyramidal. Here some of the angles between coordination bonds deviate from ideal tetrahedral angles [50].

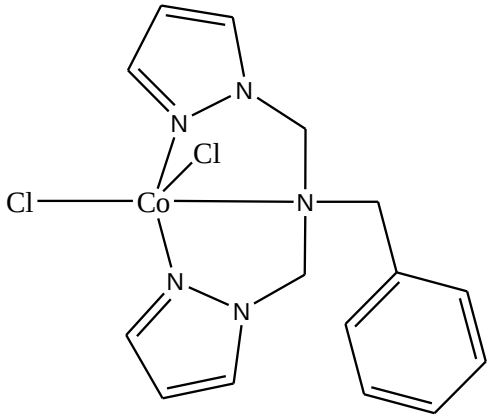

Fig. 10. Structure of $[Co(L_2)Cl_2]$

Blonk et al synthesized tridentate nitrogen containing *N*,*N*-bis(3,5-dimethylpyrazol-1-ylmethyl)aminobenzene (L_3) and synthesized compounds having general formula $[M(L_3)X_2]$ (M = Co(II), Cu(II) or Zn(II); X = Cl^- or Br^- and M = Co(II), X = NCS^- or NO_3^- and also $[Cu_2(L_3)(SCN)_3]$. The interesting point was that in some compounds e.g. M = Co(II) or Zn(II) and X = Cl^-, Br^- and M = Co(II), X = SCN^- or NO_3^-, the tridentate N_3-coordinate ligand acts as a bidentate ligand and in others (M = Cu(II); X = Cl^-, Br^- or

SCN^-) as a tridentate ligand [Fig.11]. In all compounds the anions are also bonded. Because of the flexible character of the ligand, the preference of the transition-metal ions for specific co-ordination geometries is reflected in the resulting co-ordination compounds. This was confirmed by the X-ray structure of $[Co(L_3)Cl_2]$ where cobalt(II) ion is surrounded by the two pyrazole nitrogens and the two chloride ions in a slightly

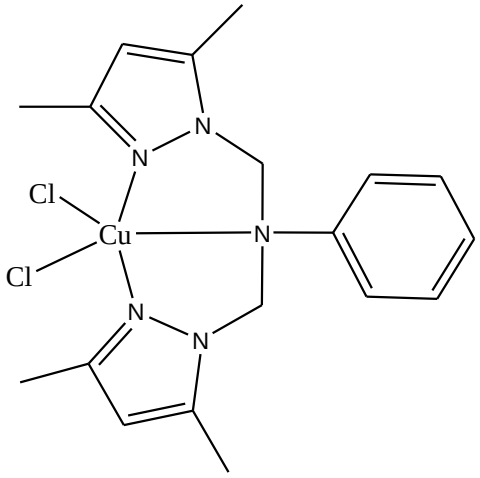

Fig. 11. Structure of $[Cu(L_3)Cl_2]$

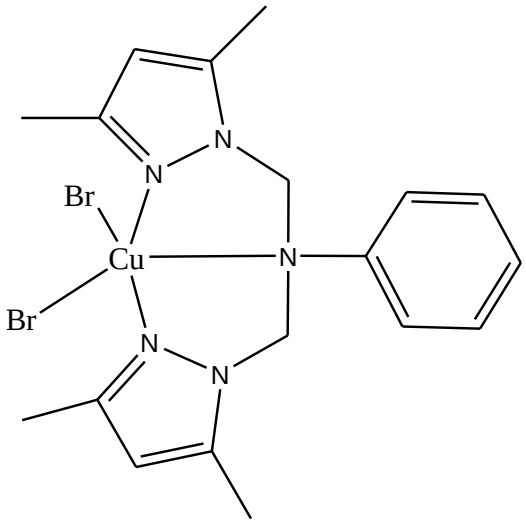

Fig. 12. Structure of $[Cu(L_3)Br_2]$

distorted tetrahedral configuration. Here ligand utilizes only two of the three potential donor sites for coordination, therefore, acting as bidentate ligand. Instead of coordinating, the lone pair on the nitrogen atom conjugates to the aromatic system of the phenyl ring. In $[Cu(L_3)Br_2]$, the copper(II) ion is surrounded by two pyrazole nitrogens and one aniline nitrogen atom and two Br^- ions in distorted trigonal bipyramidal geometry. Here, the ligand utilizes all its donor sites for coordination and acts as a tridentate ligand [Fig.12] [51].

Bis(1-pyrazolylmethyl)amine [Fig.13] is another amine and pyrazole containing tridentate N_3-coordinate ligand and it form mononuclear complexes with copper(II), cobalt(II) and zinc(II) ion of the type $[M(Cl)L]BF_4$ ($M = Co^{+2}, Cu^{+2}$) and the structure is of the complex is distorted tetrahedral. The metal(II) is bonded with three nitrogen atoms from ligand and one chloride ion.[52]

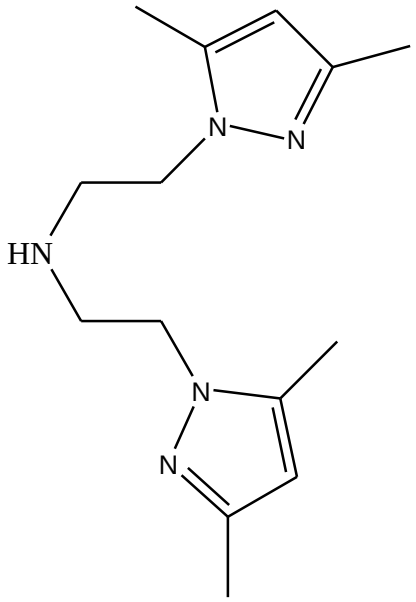

Fig.13. bis(2-(3,5-dimethyl-1-*H*-pyrazol-1-yl)ethyl)amine

B. Two pyrazoles and one pyridine containing tridentate chelating ligand

In this type of ligand, there are three coordination sites- two nitrogen from pyrazole and one nitrogen from pyridine. Example of tridentate N_3-coordinated ligand is 2,6-bis(3,5-dimethylpyrazol-1-ylpyridine) (L_4) [Fig.14] and it form complexes with different metal ions of this type $[M(L)_2]^{+2}$ (M = Fe, Ni and Ru). The X-ray structure of $[Ni(L_4)_2][ClO_4]_2$ revealed that the bonding geometry about the nickel atom is close to symmetrical octahedral. Interestingly, the Ni–N(pyridine) bond length is longer than the Ni–N(pyrazole) bond lengths. The pyrazole mean planes are inclined to the pyridine mean plane. The complex $[Fe(L_4)_2][ClO_4]_2 \cdot H_2O$ displays in the solid-state anomalous magnetic properties.

The ligand 2,6-bis(3,5-dimethylpyrazol-1-ylmethyl)pyridine) (L_4) also form mononuclear complexes of the type $[Cu(L_4)(N_3)_2]$ and $[Cu(L_3)(ONO)(OClO_3)]$ and crystal structure of the compounds shows it has trigonal bipyramidal geometry [Fig. 15] [53].

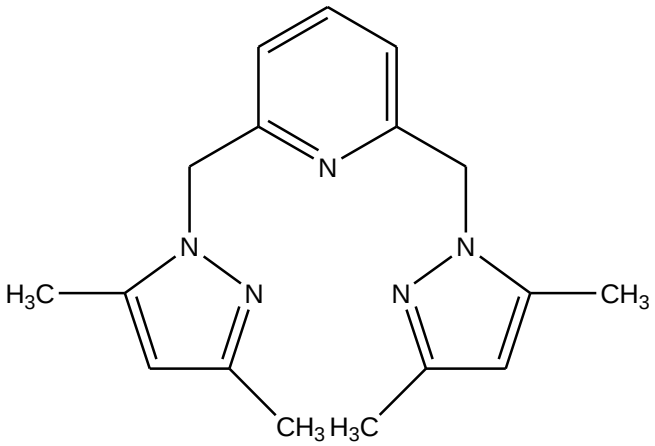

Fig. 14. 2,6-bis(3,5-dimethyl-pyrazol-1-ylmethyl)pyridine) (L_4)

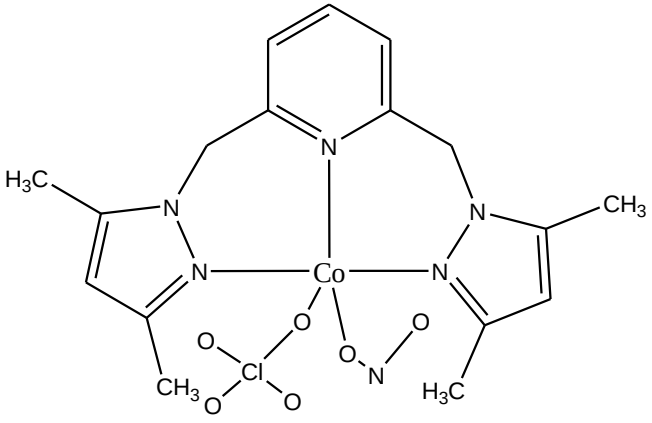

Fig.15. Structure of [Cu(L_4)(ONO)($OClO_3$]

3. Tetradentate Nitrogen containing of Pyrazole based chelating ligands

In the case of tetradentate nitrogen containing pyrazole based ligand, three donor sites can be incorporated in the ligand system from three pyrazolyl nitrogen and stability of the resulting complexes can be increased with the increasing chelate effect. Among the tetradentate N-derivatives of pyrazole based ligand, there are two important types of tetradentate ligands to be discussed here.

A. Three pyrazoles and one tertiary amine.

In this type of tetradentate N_4-chelating ligands, three donor sites are available from three pyrazolyl nitrogen and another one from tertiary amines [54,55] e.g. tris(3,5-dimethyl-1-pyrazolylmethyl)amine (L_5) form complexes of the types $M^{II}(L_5)X_2(H_2O)_n$, where M = Co, Ni and Cu and X = Cl^-, NCS^- and/or NO_3^- and n = 0 or 1, and with Zn^{+2} form $[Zn(L_5)(NCS)_2]$.

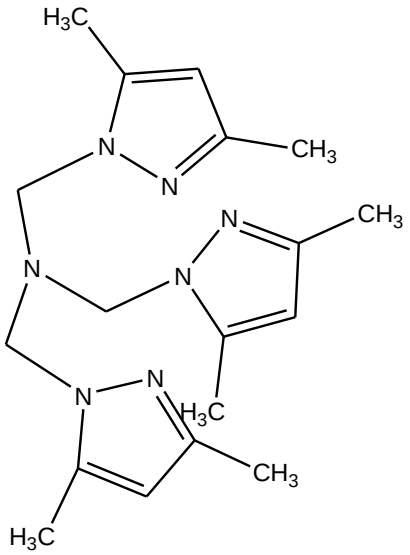

Fig. 16. Tris(3,5-dimethyl-1*H*-pyrazol-1-yl)methyl)amine

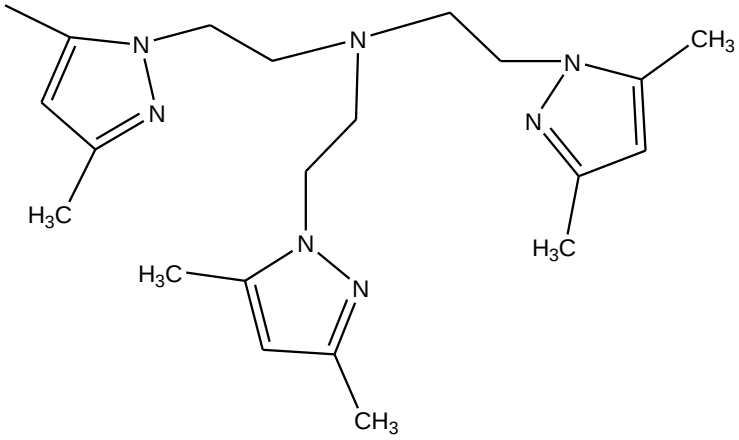

Fig.17. Tris(2-(3,5-dimethyl-1*H*-pyrazol-1-yl)ethyl)amine

B. **Two pyrazoles and two tertiary amines.**

In this type of ligand, two donor sites are available from pyrazolyl nitrogens and another two from tertiary amines e.g. *N*,*N*-dimethyl-*N*,*N*-bis(3,5-dimethyl-1H-pyrazol-1-yl) methyl)ethane-1,2-diamine (L_6) [Fig. 18] [56,57]. The ligand L_6 form complexes of the type $[M(L_6)X_2]$ (M = Mn, Fe, Co, Ni, Cu, Zn, Cd; X = NCS; M = Mn, Co, Ni, Zn, Cd; X= N_3; M = Mn, Cd; X = Cl, Br)

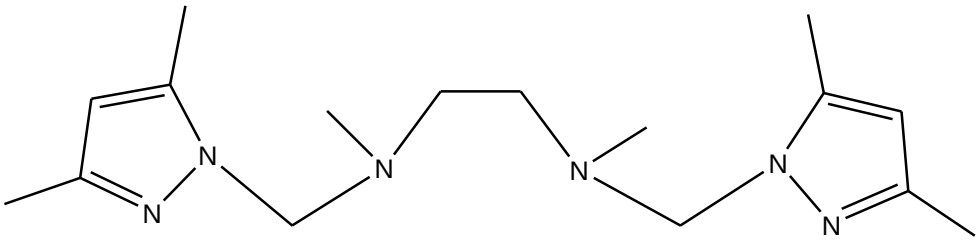

Fig. 18. *N*,*N*-dimethyl-*N*,*N*-bis(3,5-dimethyl-1H-pyrazol-1-yl)methyl)ethane-1,2-diamine

4. Multidentate Nitrogen containing Pyrazole based chelating ligands

There are variety of multidentate ligands with different chelation sites and these are of the following types.

A. Three pyrazoles, one secondary and one tertiary amine.

In this type of ligand, there are five nitrogen coordination sites incorporated three nitrogen donor sites from pyrazolyl group and one each from primary and secondary amine nitrogen atoms. For example, (N^1,N^1,N^2-tris((3,5-dimethyl-1-1*H*-pyrazol-1-yl) methyl)ehane-1,2-diamine) [58] [Fig 19] and form complex of the type $[M(L_7)(anion)_2{\cdot}(H_2O)_n]$where M = Co, Ni, Cu, and Zn, the anion is $ClO_4^-$and BF_4^- and x = 1–3.

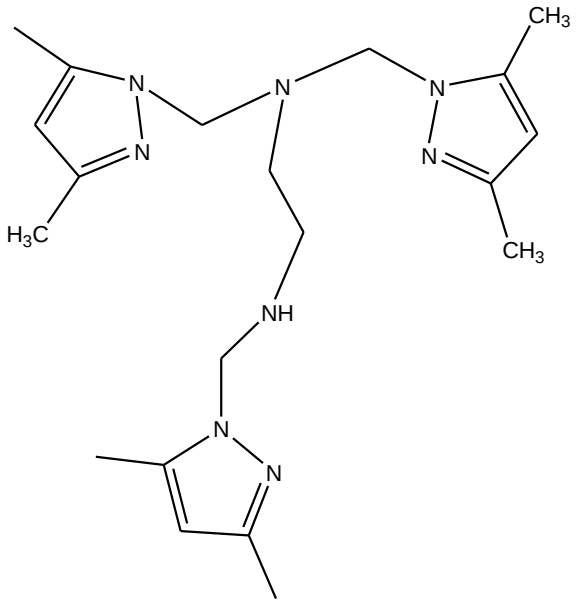

Fig. 19. N^1,N^1,N^2 –tris((3,5-dimethyl-1-1*H*-pyrazol-1-yl)methyl)ethane-1,2-diamine

B. Four pyrazoles and two tertiary amines.

In this N_6-coordination ligand, there are six nitrogen chelation sites-four nitrogen donor sites from pyrazolyl group and two from primary amine nitrogen atoms. For example, *N*,*N*,*N*,*N*-tetrakis(1*H*-pyrazol-1-yl)methyl)ethane-1,2-diamine (L_5) [59]. The ligand is hexadentate and crystal structure of $[Mn(L_5)(ClO_4)_2]$ shows that manganese(II) is coordinated with six nitrogen atom from ligand and one oxygen from perchlorate anion and form pentagonal bipyramidal structure.

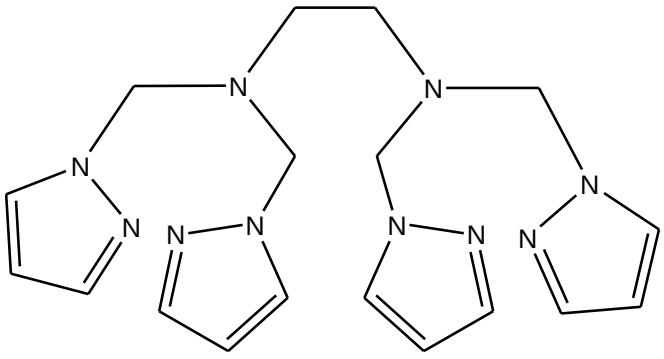

Fig. 20. *N*,*N*,*N*,*N*-tetrakis(1*H*-pyrazol-1-yl)methyl)ethane-1,2-diamine

C. Six pyrazoles and four tertiary amines.

In this ligand, there are ten nitrogen chelation sites-six nitrogen donor sites from pyrazolyl group and four from tertiary amine nitrogen atoms. For example, 1,1,4,7, 10,10-hexakis(3,5-dimethylpyrazol-1-ylmethyl)-1,4,7,10-tetraaza-decane (L_8) [60]. X-ray crystal structure of the cobalt(II) complex of the ligand show the general formula of the complex is $[Co_2(L_6)(H_2O)(CH_3OH)_4]$ and both the cobalt is octahedrally coordinated.

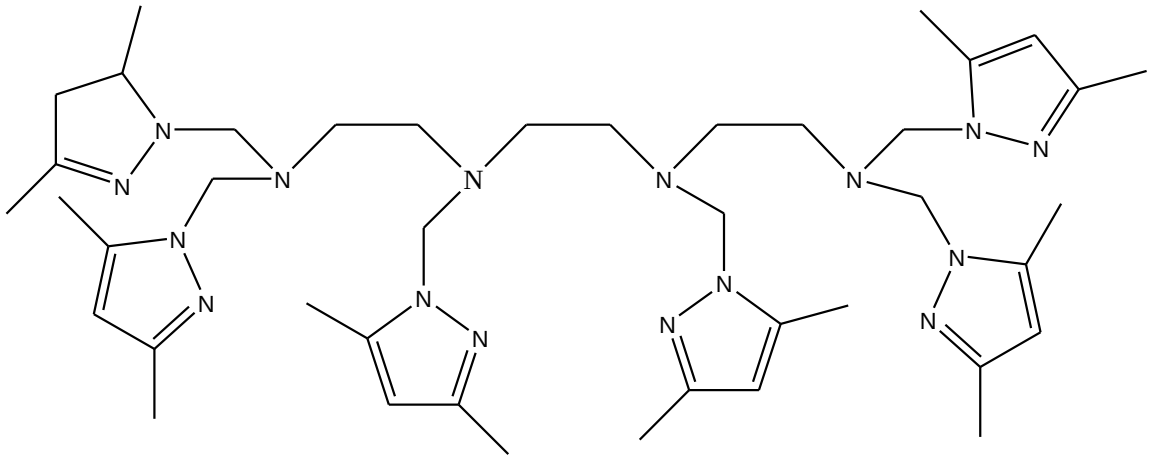

Fig.21. 1,1,4,7,10,10-hexakis(3,5-dimethylpyrazol-1-ylmethyl)-1,4,7,10-tetraaza decane

Apart from different coordinating ligand, polydentate pyrazolyl containing ligand shows different types of coordination.The flexibility of pyrazolic N-coordinating groups of the tridentate ligands could allow them to act as meridional or as facial ligands when coordinating to transition metal complexes. In case of polydentate ligands, they could coordinate in facial and meridional fashion as proposed in Scheme 1. [61].

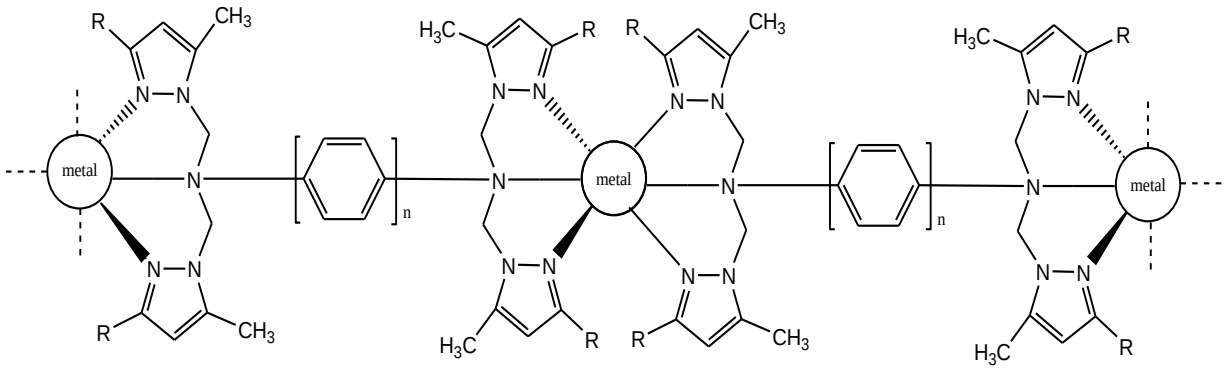

Scheme 1.Coordination behaviour of polydentate pyrazole containing ligand

.

In this survey we discussed (1) nitrogen containing pyrazole based chelating ligand and their complexes, (2) the geometries, nuclearities and reactivity properties of a particular compound can be controlled by the change in the coordination mode of chelating ligands in the coordination sphere of metal ions.

Application of pyrazole based ligand and their complexes

The chemistry of pyrazolyl containing multipodal ligand and their metal complexes have attracted considerable interest owing to the interesting coordination chemistry and for their biological and biochemical importance [62-64]. Pyrazole based new macrocyclic ligands in are used in oxygen transfer biochemistry and for the formation of three dimensional structures around the active sites of complex formation [65]. For example, the pyrazole containing copper complexes are of particular interesting bioinorganic chemistry as they can be used as model for the active sites in copper protein like hemocyanin and tyrocinage. These compounds are of great important for building polynuclear complexes as well as for the discovery of new catalyst precursor [66]. Another important area of research with pyrazole based ligand into polynuclear transition metal complexes is molecular magnetism [67], and to study the correlation of the structural and magnetic properties of these complexes. Pyrazole ligand and their complexes have application in antipyretics and antirheumatics and also in herbicides and fungicides [68].

In recent times, pyrazoles and related N-containing heterocyclic compounds have been given attention because these complexes have wide application in the field of analytical [69], pharmacological [70] and agrochemical [71]. Pyrazoles and their complexes with metals are analgesic and antiinflammatory agents besides having antitumor activity. Some mixed chelate copper-based drugs have exhibited greater antineoplastic potency than cisplatin *in vitro* and *in vivo* studies of a variety of tumor cell lines [72]. Pyrazol-thioketone derivatives have antimicrobial activity and O-Hydroxyphenylopyrazoles are used as UV stabilizers. They inhibit growth of staphylococcus aureus, staphylococcus typhii, candida albicans and mycobacterium tuberculosis [73]. The pyrazole containing heterocyclic compounds have been proven to be useful as cytotoxic agents.

Present work.

So from the above discussion, it is necessary to design appropriate multidentate ligand where besides the binding sites, the spacer groups between them play a very important role and thus regulating the steric factor and electronic environment of the complexes. Pyrazole containing chelating ligands form a variety of coordination complexes with a number of metal ions, providing varying coordination geometry and nuclearity. But no tetradentate N_4-coordinating ligand with both pyridine and pyrazole is reported so far.

Work embodied in this thesis is devoted primarily to study the coordination behaviour of pyridylpyrazole ligand and its complexation with different metal ions such as copper(II), nickel(II), cobalt(II), zinc(II) and cadmium(II). The ligand which I have used to explore chemistry of metal complexes is *N*,*N*-bis(3,5-dimethylpyrazol-1-ylmethyl)aminomethylpyridine (Fig. 22) and it was synthesized by condensing 2-aminomethylpyridine and *N*-(hydroxymethyl)-3,5-dimethylpyrazole. It has been used to explore the co-ordination chemistry of transition metal ions like Cu(II), Co(II), Ni(II), Zn(II) and Cd(II). In each case the compounds are structurally established by spectroscopic studies (IR, UV-Vis, and NMR) and in some cases the confirmation of structure has been established by X-ray diffraction study. Electrochemical properties of the compounds are established by cyclic voltammetry studies.

Many pyrazole containing bridging complexes have been synthesized and characterized. But pyrazole containing pseudohalide (N_3^-, NCS^-, NCO^-) bridge complexes are very limited and magnetic properties of these complexes are not well studied. So, synthesis, characterization, structure and magnetic properties of the metal complexes with new pyridine and pyrazole containing ligand will be interesting. Our main part of the work is to synthesis and characterization of psuedohalides (N_3^-, NCS^- and NCO^-) containing metal complexes of copper(II), nickel(II), cobalt(II) zinc(II) and cadmium(II) with the ligand (L). The tendency lies on the versatile coordination modes of this pseudohalides which can act as a bridging ligand and its ability to mediate different kinds of interactions based on its coordination mode and angle.

A variety of binuclear azido and cyanate bridged complexes with structures have been reported, in which azido and cyanato ligand exhibits diverse bridging modes ranging from μ-1,1 [end-on] and μ-1,3 [end-to-end] depending upon the steric and electronic

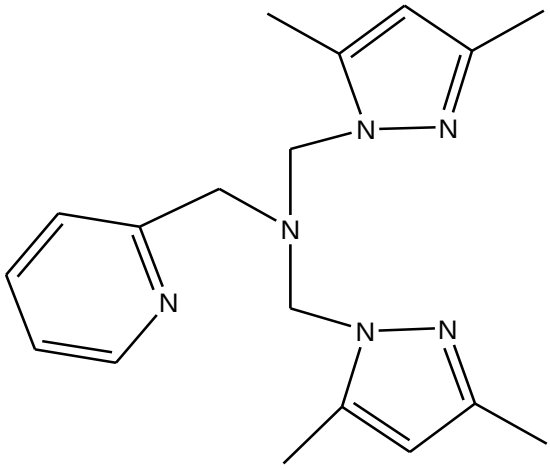

Fig.22. *N*,*N*-bis(3,5-dimethylpyrazol-1-ylmethyl)aminomethylpyridine

demands of the co-ligands. Here, we report the synthesis, characterization, structure and magnetic properties of many new binuclear complexes, of the type namely $[M_2(L)_2(Y)_2](X)_2$, where M = Cu(II) and Ni(II), Y = N_3^-, NCO^- , X = ClO_4^-, PF_6^-, BF_4^- ; M= Zn(II) and Cd(II), Y = NCO^-, X = PF_6^- and L = *N*,*N*-bis(3,5-dimethylpyrazol-1-ylmethyl)aminomethylpyridine. All NCS^- and $SeCN^-$ containing complexes are mononuclear.

We have also synthesized and characterized mononuclear complexes of copper(II), nickel(II) and cobalt(II) with this N_4-coordinate ligand. Mononuclear copper(II) complexes of the type $[Cu(L)(CH_3COO)]X$ (X = PF_6^- and BF_4^-), cobalt(II) complexes of

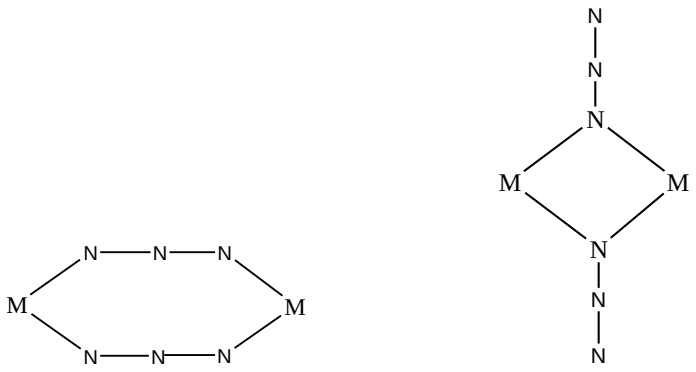

a **b**

Scheme 2. Bridging mode of azide ligands (a) end-to-end (b) end-on

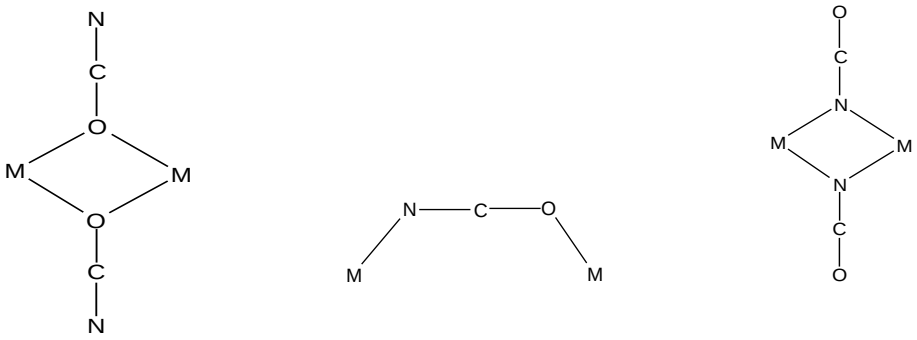

Scheme 3. Bridging mode of cyanate ligand

the type [Co(L)(Cl)]Y (Y = PF_6^-, BF_4^- and ClO_4^-) and binuclear copper (II) complexes [Cu(L')(Cl)-(μ-Cl)-Cu(L')(pz)]$(Z)_2$ (Z = PF_6^- and ClO_4^-), L' = N-(3,5-dimethylpyrazol-1-ylmethyl)aminomethylpyridine).

The ligand and representative complexes were screened *in vitro* for their cytotoxic activity against the human lymphocytic cell line (HL 60). Metal complexes were explored for their cytotoxic activity in HL 60 cells cultured *in vitro*. HL 60 cells were grown according to standard methods and cells were exposed to various concentrations (10 μg/mL, 20 μg/mL, 100 μg/mL and 200 μg/mL) of ligand, salt and metal complexes. After 96 hours of culture the cells were analyzed for toxicity of these compounds using standard MTT test, and showed that both ligand and salts are toxic but after complex formation, cytotoxic activity alter the original activity of the salt or ligand and amongst the various complexes, thiocyanate and selenocyanate containing complexes were found to be most toxic.

Physical Measurements

(i) **FT-IR spectra:** The IR spectrums were recorded on a Perkin-Elmer FT-IR spectrometer RX1 spectrum using KBr pellets.

(ii) **Elemental analysis:** The elemental analyses were carried out on Perkin Elmer IA 2400 series elemental analyzer.

(iii) **UV-Vis spectra:** . UV-Vis spectra (900 - 190 nm) were recorded on a Perkin-Elmer spectrophotometer model Lambda 35 in acetonitrile solution.

(iv) **Conductance measurements:** The solution conductivity was measured using Systronics 304 digital conductivity meter with a solution concentration of 10^{-3} M.

(v) **Room Temperature magnetic susceptibility measurement**

Room temperature magnetic susceptibilitiesof powder samples were measured using Faraday magnetic balance equipped with a Mettler UMX 5 balance, with a field strength of 0.8 Tesla using $Hg[Co(SCN)_4]$ as the reference.

(vi) **Variable temperature Magnetic measurements:**

The magnetic susceptibility of a powder sample was carried out in the magnetochemistry Service of Universitat de Barcelona, on polycrystalline samples with a DSM5 Quantum Design SQUID magnetometer working in the 2-300 K range. The magnetic field was 0.1 T between 300-30 K and 0.03 T between 30-2 K to avoid saturation effects. The contribution of the sample holder was determined separately in the same temperature range and magnetic field. The diamagnetic corrections were evaluated from Pascal's constants.

(vii) **Single crystal X-ray diffraction study:** Instrumental details are given in each chapter wherever structures are reported.

Reference:

1 F.Blau, *Ber, Dtsch. Chem. Ges*., 1888,27,1077

2 W.R. McWhinnie, J.D. Miller, Adv. Inorg. Chem. Radiochem. 1969,12, 135.

3 L.A. Summers, Adv. Heterocycl. Chem.1984,35, 281.

4 S. Trofimenko, J. Am. Chem. Soc.1966,88, 1842.

5 S. Trofimenko, Prog. Inorg. Chem. 1986,34,115.

6 R. N. Mukherjee, Coord. Chem. Rev., 2000, 203, 151

7 S. Trofimenko, Chem. Rev. 1993,93, 943.

8 N. Kitajima, W.B. Tolman, Prog. Inorg. Chem. 1995, 43, 419.

9 S. Trofimenko, J. Am. Chem. Soc. 1970, 92, 5118.

10 K. Niedenzu, S. Trofimenko, Top. Curr. Chem. 1986, 131, 1.

11 E.C. Constable, P.J. Steel, Coord. Chem. Rev. 1989, 93, 205

12 W.L. Driessen, Recl. Trav. Chim. Pays-Bas 1982, 101, 441.

13 W.L. Driessen, W.G.R. Wiesmeijer, M. Schipper-Zablotskaja, R.A.G. de Graaff, J. Reedijk, Inorg. Chim. Acta 1989, 162, 233

14 E. Bouwman, W.L. Driessen, J. Reedijk, Inorg. Chem. 1985, 24, 4730.

15 F.B. Hulsbergen, W.L. Driessen, J. Reedijk, G.C. Verschoor, Inorg. Chem. 1984, 23, 3588

16 F. Paap, W.L. Driessen, J. Reedijk, Inorg. Chim. Acta 1985, 104, 55.

17 F. Paap, W.L. Driessen, J. Reedijk, Polyhedron 1986, 5, 1815.

18 W.G. Haanstra, W.L. Driessen, R.A.G. de Graaff, G.C. Sebregts, J. Suriano, J. Reedijk, U.Turpeinen, R. Hamalainen, J.S. Wood, Inorg. Chim. Acta 1991,189, 243

19 K. Locher, W.L. Driessen, J. Reedijk, Inorg. Chim. Acta 1987, 127, 135

20 W.G. Haanstra, W.L. Driessen, M. van Roon, A.L.E. Stoffels, J. Reedijk, J. Chem. Soc. Dalton Trans. 1992, 481

21 S. Mahapatra, N. Gupta, R. Mukherjee, J. Chem. Soc. Dalton Trans. 1991, 2911.

22 F.B. Hulsbergen, W.L. Driessen, J. Reedijk, G.C. Verschoor, Inorg. Chem. 1984, 23, 3588.

23 F. Paap, W.L. Driessen, R.A.G. de Graaff, J. Reedijk, Polyhedron 1988, 7, 2575.

24 G. Tabbı`, W.L. Driessen, J. Reedijk, R.P. Bonomo, N. Veldman, A.L. Spek,

Inorg. Chem. 1997, 36, 1168

25 G.J. van Driel, W.L. Driessen, J. Reedijk, Inorg. Chem. 1985, 24, 2919.

26 S. Mahapatra, D. Bhuniya, R. Mukherjee, Polyhedron 1992, 11, 2045.

27 S. Mahapatra, T.K. Lal, R. Mukherjee, Polyhedron 1993, 12, 1477.

28 S. Mahapatra, R. Mukherjee, Indian J. Chem. 1993, 32A, 64.

29 S. Mahapatra, R. Mukherjee, J. Chem. Soc. Dalton Trans. 1992, 2337.

30 S. Mahapatra, R. Mukherjee, Ind. J. Chem. 1993, 32A, 428.

31 S. Mahapatra, R. Mukherjee, Polyhedron 1993, 12, 1603.

32 S. Mahapatra, R.J. Butcher, R. Mukherjee, J. Chem. Soc. Dalton Trans. 1993, 3723.

33 F. Paap, A. Erdonmez, W.L. Driessen, J. Reedijk, Acta Crystallogr. C42 1986, 783.

34 F. Paap, W.L. Driessen, J. Reedijk, M. Dartmann, B. Krebs, Inorg. Chim. Acta 1986, 121, 185.

35 W.G. Haanstra, W.A.J.W. van der Donk, W.L. Driessen, J. Reedijk, J.S. Wood, M.G.B. Drew, J.Chem. Soc. Dalton Trans. 1990, 3123.

36 W.G. Haanstra, M.F. Cabral, J.D.O. Cabral, W.L. Driessen, J. Reedijk, Inorg. Chem. 1992, 31, 3150.

37 W.G. Haanstra, W.A.J.W. van der Donk, W.L. Driessen, J. Reedijk, M.G.B. Drew, J.S. Wood, Inorg. Chim. Acta 1990, 176, 299.

38. W.G. Haanstra, M.F. Cabral, J.D.O. Cabral, W.L. Driessen, J. Reedijk, Inorg. Chem. 1992, 31, 3150.

39. W.G. Haanstra, W.A.J.W. van der Donk, W.L. Driessen, J. Reedijk, M.G.B. Drew, J.S. Wood, Inorg. Chim. Acta 1990, 176, 299

40. T.K. Lal, J.F. Richardson, M.S. Mashuta, R.M. Buchanan, R. Mukherjee, Polyhedron 1997, 16, 4331.

41 Z. Shirin, R. Mukherjee, J.F. Richardson, R.M. Buchanan, J. Chem. Soc. Dalton Trans. 1994, 465.

42 D.A. House, P.J. Steel, A.A. Watson, Aust. J. Chem. 1986, 39, 1525.

43. T.K. Lal, R. Mukherjee, Polyhedron 1997, 16, 3577.

44 L-1, 19. Julia, S., Sala, P., Mazo, J., et al., *J. Heterocycl. Chem.*,1982, 19, 1141.

45 L-2, E. V. Lider, O. L. Krivenko, E. V. Peresypkina, A. I. Smolentsev, Yu. G. Shvedenkov,S. F. Vasilevskii, L. G. Lavrenova Russian Journal of Coordination Chemistry, 2007, 33, 12, 896–907.

46 Y. Ni, S.W. Li, K.B. Yu, W.Z. Zheng, L.F. Zhang, J. S. Uni. (Nat. Sci.) 1999, 22, 707.

47 B. Kozlevc ar, P. Gamez, R. de Gelder, W.L. Driessen, J. Reedijk, Eur. J. Inorg. Chem. 2003, 47.

48 A. Otero, J. Fernandez-Baeza, A. Antinolo, F. Carrillo- Hermosilla, J. Tejeda, E. Diez-Barra, A. Lara-Sanchez, L. Sanchez-Barba, I. Lopez-Solera, M.R. Ribeiro, J.M. Campos, Organometallics 2001, 20, 2428.

49 Boussalah N, Touzani R, Bouabdallah I, Ghalem S, El Kadiri S ,Inter. J. Acad. Res. 2009, 2: 137-143

50 S.-C. Sheu, M.-J. Tien, M.-C. Cheng, T.-I. Ho, S.-M. Peng, Y.-C. Lin, J. Chem. Soc. Dalton Trans. 1995, 3503.

51 H.L. Blonk, W.L. Driessen, J. Reedijk, J. Chem. Soc. Dalton Trans. 1985, 1699.

52 Bouwman E, Drissen WL, Reedjik J Coor. Chem. Rev.1990, 104:143-172

53 S. Mahapatra, N. Gupta, R. Mukherjee, J. Chem. Soc. Dalton Trans. 1991, 2911.

54 F. Mani, G. Scapacci, Inorg. Chim. Acta 1980, 38, 151.

55 G.J. van Driel, W.L. Driessen, J. Reedijk, Inorg. Chem. 1985, 24, 2919.

56 F. Paap, W.L. Driessen, J. Reedijk, Inorg. Chim. Acta 1985, 104, 55.

57 F. Paap, W.L. Driessen, J. Reedijk, Polyhedron 1986, 5, 1815.

58 E. Bouwman, W.L. Driessen, J. Reedijk, Inorg. Chem. 1985, 24, 4730.

59 F.B. Hulsbergen, W.L. Driessen, J. Reedijk, G.C. Verschoor, Inorg. Chem. 1984, 23, 3588.

60 F. Paap, W.L. Driessen, R.A.G. de Graaff, J. Reedijk, Polyhedron 1988, 7, 2575.

61 Maria Daoudi, Najib Ben Larbi, Abdelali Kerbal, Brahim Bennani, Jean-Pierre Launay, Jacques Bonvoisin, Taibi Ben hadda and Pierre H. Dixeuf, Tetrahedron 2006, 62, 3123-3127.

62 M.R. Malachowski, H.B. Huynh, L.J. Tomlinson, R.S. Kelly, Dalton Trans. 1995, 31.

63 (a) Solomon, E. I.; Baldwin, M. J.; Lowery, M. D. *Chem. Rev.* 1992, *92*, 521. (b) Solomon, E. I.; Hemming, B. L.; Root, D. E. In *Bioinorganic Chemistry* of *Copper;* Karlin, K. D., and Tyeklk, Z.,Eds.; Chapman & Hall: London, 1993.

64 Noms, G. E.; Anderson, B. F.; Baker, E. N. J. *J. Am. Chem. SOC.* 1986, *108*, 2784.

65 Volbeda, A.; Hol, W. G. J. *J. Mol. Biol.* 1989, *209*, 249. 1979,*81*, 87. Shemngton, D. C. *Eur. Polym. J.* 1992, *28*, 747.

66 M.C. Linder, Biochemistry of Copper, Plenum Press, New York, 1991.

67 I.A. Koval, K. van der Schilden, A.M. Schuitema, P. Gamez, C. Belle, J.-L. Pierre, M. Lueken, B. Krebs, O. Roubeau, J. Reedijk, Inorg. Chem. 2006, 44, 4372.

68 T. Wang, Z. Guo, Curr. Med. Chem. 2006, 13, 525.

69 Y.H. Sung, C. Rospigliosi, D. Eliezer, Biochim. Biophys. Acta2006, 5, 1764.

70 H. Hayashi, M. Yano, Y. Fujita, S. Wakusawa, Med. Mol. Morphol. 2006, 39, 121.

71 M.L. Schlief, T. West, A.M. Craig, D.M. Holtzman, J.D. Gitlin, Proc. Natl. Acad. Sci. U.S.A. 2006, 103, 14919.

72 T. Fujimori, S. Yamada, H. Yasui, H. Sakurai, Y. In, T. Ishida, J. Biol. Inorg. Chem. 2005, 10, 831.

73 Y. Zheng, Y. Yi, Y. Wang, W. Zhang, M. Du, Bioorg. Med. Chem. Lett. 2006, 16, 4127.

Chapter II

Synthesis and Characterization of Pyridylpyrazole Ligand and some mononuclear Copper(II), Nickel(II) and Cobalt(II) and Binuclear Copper(II) complexes with Pyridylpyrazole ligand.

Chapter II

Abstract

A new tetradentate N_4-coordinated ligand *N*,*N*-bis(3,5-dimethylpyrazol-1-ylmethyl)amino- methylpyridine and some mononuclear complexes of the type $[Cu(L)(CH_3COO)]X.H_2O$ (X = PF_6^- (**1**) and BF_4^- (**2**)), $[Co(L)Cl]Y.{}^1/_2CH_3OH$ (Y = BF_4^-(**3**), PF_6^- **(4)** and ClO_4^- (**5**)), $[Ni(L)Cl_2]$ (**6**) and dinuclear copper(II) complexes $[L'(Cl)Cu\text{-}(\mu\text{-}Cl)\text{-}Cu(pz)L'](Z)_2$ (Z = PF_6^- (**7**) and ClO_4^- (**8**) (L = *N*,*N*-bis(3,5-dimethylpyrazol-1-ylmethyl)aminomethylpyridine, L' = N-(3,5-dimethyl pyrazol-1-ylmethyl)aminomethylpyridine have been synthesized and characterized by elemental analysis and physico-chemical method. Crystal structures of two mononuclear complexes $[Cu(L)(CH_3COO)]PF_6.H_2O$ (**1**), $[Co(L)Cl]BF_4.{}^1/_2CH_3OH$ (**3**) and binuclear copper(II) complex $[L'(Cl)Cu\text{-}(\mu\text{-}Cl)\text{-}Cu(pz)L'](PF_6)_2$ (**7**) have been solved by single crystal X-ray diffraction studies and it shows that Cu(II) atoms in complexes **1** and **7** have square pyramidal geometry and Complex **3** has trigonal bipyramidal geometry.

1. Introduction

Pyrazole containing multipodal ligand and their metal complexes are of great interest in research due to their biological activity. Pyrazole based ligands have been proposed as model compounds for active sites in metalloproteins and metalloenzymes [1-8]. Pyrazole based ligands form variety of coordination complexes with large number of metal ions and their compounds are also of great importance for building polynuclear complexes [9-10].

Anion tripodal ligands poly(pyrazole)borate was introduced by Trofimenko in 1966 and its transition metal complexes have wide application in bioinorganic and organometalic chemistry. A number of review articles have been published in the literature [9-14]. The ease of synthesis of various pyrazole and their incorporation of pyrazole group in the new ligand help to control electronic and steric properties of the metal complexes [15-20].

As our interest on pyrazole containing ligand and their transition metal complexes, we have synthesized a new ligand *N*,*N*-bis(3,5-dimethylpyrazol-1-ylmethyl)aminomethylpyridine (L) where both six-membered heterocyclic like pyridine and five membered pyrazole are present in a single ligand and form tetradentate N_4-coordinate ligand. In this chapter, we describe the synthesis and characterization of ligand *N*,*N*-bis(3,5-dimethylpyrazol-1-ylmethyl)amino methylpyridine (L) and some mononuclear complexes of the type $[Cu(L)(CH_3COO)]X.H_2O$ (X = PF_6^- (**1**) and BF_4^- (**2**)), $[Co(L)Cl]Y.^1/_2CH_3OH$ (Y = BF_4^- (**3**), PF_6^- **(4)** and ClO_4^- (**5**)), $[Ni(L)Cl_2]$ (**6**) and binuclear copper(II) complexes $[Cu(Cl)L'\text{-}(\mu\text{-}Cl)\text{-}Cu(pz)(L')](Z)_2$, (Z = PF_6^- (**7**) and ClO_4^- (**8**)), where L = *N*,*N*-bis(3,5-dimethylpyrazol-1-ylmethyl)aminomethylpyridine and L' = *N*-(3,5-dimethylpyrazol-1-ylmethyl)aminomethylpyridine. Crystal Structure of the complexes $[Cu(L)(CH_3COO)]PF_6.H_2O$ (**1**), $[Co(L)Cl]BF_4.^1/_2CH_3OH$ (**3**) and $[Cu(Cl)L'\text{-}(\mu\text{-}Cl)\text{-}Cu(pz)(L')](PF_6)_2$ (**7**) have been solved by single crystal X-ray diffraction studies.

2. Experimental

2.1. Materials and methods

All chemicals and solvents were of analytical grade reagents. 2-(aminomethyl)pyridine (Aldrich), hydrazine hydrate, acetylacetone, paraformaldehyde, $Cu(CH_3COO)_2.H_2O$, $CuCl_2.2H_2O$, $CoCl_2.6H_2O$, and $NiCl_2.6H_2O$ (Loba, India), sodium perchlorate monohydrate, ammonium hexafluorophosphate (Aldrich) and ammonium tetrafluoroborate (Aldrich) were of reagent grade and used as received. *N*-(hydroxymethyl)-3,5-dimethylpyrazole was synthesized as per published procedure [21]. Solvents used in this study were purified following the standard procedures.

2.2. Synthesis of compounds

2.2.1. Synthesis of *N*,*N*-bis(3,5-dimethylpyrazol-1-ylmethyl)aminomethylpyridine (L)

A solution of *N*-(hydroxymethyl)-3,5-dimethylpyrazole (1.26 g, 10.0 mmol) in acetonitrile was added to a solution of 2-aminomethylpyridine (0.540 g, 5 mmol) in acetonitrile (20 mL). This solution was stirred for three days in a closed vessel at room temperature. The resulting solution was then dried over anhydrous $MgSO_4$ and the organic solvent was removed on a vacuum rotary evaporator. A light yellow viscous liquid was obtained. Yield. 2.6g (80%) Microanalysis; Found: C, 66.6; H, 7.4; N, 25.8%; Calc. for $C_{18}H_{24}N_6$: C, 66.7; H, 7.4; N, 25.9%. IR (neat), cm^{-1}: ν(C=C) + ν(C=N)/pyrazole ring, 1,591 s, 1,556 vs. ^{1}H NMR (400 MHz, $CDCl_3$, 20 °C), δ/ppm: 2.03 (s, 6H, CH_3/pz ring), 2.21 (s, 6H, CH_3/pz ring), 3.88 (s, 2H, pyridine-CH_2N), 4.98 (s, 4H, CH_2), 5.78 (s, 2H, CH/pz ring), 7.12 (m, 1H, C^5H/py ring), 7.18 (d, J_{HH} = 8 Hz, 1H, C^3H/py ring), 7.57 (ddd, J_{HH} = 7.6, 1.6, 1.6 Hz, C^4H/py ring), 8.50 (d, J_{HH} = 5.2 Hz, 1H, C^6H/py ring).

2.2.2. Synthesis of $[Cu(L)(CH_3COO)]PF_6.H_2O$ (**1**)

A methanol solution (10 ml) of the ligand L (0.162 g, 0.5 mmol) was added drop wise to a methanol solution of $Cu(CH_3COO)_2.H_2O$ (0.1 g, 0.5 mmol) with constant stirring. After 10 min, NH_4PF_6 (0.162 gm, 1 mmol) in little amount of water was added to the mixture.

The colour of the solution was changed to deep green immediately and stirring was continued for 2 h. The solution was filtered and the filtrate was kept for slow evaporation. It was possible to obtain diffraction quality crystal after 5 days. Yield. 0.153 g. (50%). Found: C = 39.72, H = 4.55, N = 12.82 %. Anal calc. for $CuC_{19}H_{29}N_6O_3PF_6$; C = 39.38 ; H = 4.76; N = 13.78 %. IR (KBr disk): cm^{-1}; ν(C=C) + ν(C=N)/pyrazole ring, 1604, 1555 vs, ν(PF_6^{-1}), 844 vs. UV-Vis spectra: λ_{max}(nm)(ε_{max}/$mol^{-1}cm^{-1}$): 630 (64); 380 (6900) . $\Lambda_M(CH_3CN)$ ($\Omega^{-1}cm^2mol^{-1}$): 118, μ_{eff} = 1.78 BM.

2.2.3. Synthesis of $[Cu(L)(CH_3COO)]BF_4.H_2O$ (**2**)

This complex was prepared by following the same procedure as for complex **1** except NH_4BF_4 was used instead of NH_4PF_6. Yield. 0.132 g. (50%). Found: C = 40.78, H = 4.75, N = 14.27 %. Anal calc. for $CuC_{20}H_{28}N_6O_3PF_6$; C = 44.98; H = 5.06; N = 15.75 %.. IR (KBr disk): cm^{-1}; ν(C=C)+ν(C=N)/pyrazole ring, 1604, 1555 vs, ν(PF_6^{-1}), 844 vs. UV-Vis spectra: λ_{max}(nm)(ε_{max}/$mol^{-1}cm^{-1}$): 634 (64); 381 (7000). $\Lambda_M(CH_3CN)$ ($\Omega^{-1}cm^2mol^{-1}$): 120. μ_{eff} = 1.79 BM.

2.2.4. Synthesis of $[Co(L)Cl]BF_4.½\ CH_3OH$ (**3**)

A methanol solution (10 ml) of ligand L (0.162 g, 0.5 mmol) was added drop wise to methanol solution (10 ml) of $CoCl_2.6H_2O$ (0.120 g, 0.5 mmol) with stirring. After 10 min, NH_4BF_4 (0.104 g, 1.0 mmol) in little amount of water was added dropwise. The mixture was stirred for another 2 h. Filtered the solution and the solution was kept for slow evaporation. It was possible to obtain diffraction quality crystal from the filtrate after five days. Yield. 0.140 g. (50%). Anal calc. for $C_{18.5}H_{26}BClCoF_4N_6O_{0.5}$; C = 42.65; H = 5.00; N = 16.14%. Found: C = 38.62, H = 4.62, N = 15.00%. IR (KBr pellet), cm^{-1}: ν(C=C) + ν(C=N)/pyrazole ring, 1604 s, 1555 vs; $\nu_{asmy}(BF_4^-)$, 1091 vs;. UV-Vis spectra: λ_{max}(nm)(ε_{max}/$mol^{-1}cm^{-1}$): 604 (192); 506 (235), 293(7,250). $\Lambda_M(CH_3CN)$ ($\Omega^{-1}cm^2mol^{-1}$): 115, μ_{eff} = 3.88 BM.

2.2.5. Synthesis of $[Co(L)Cl]PF_6$. (**4**)

This complex was prepared by following the same procedure as for complex **3** with the exception NH_4BF_4 was used instead of NH_4PF_6. . Yield. 0.130 g. (50%). Anal calc. for $CoC_{18}H_{24}N_6ClPF_6$; C = 38.20; H = 4.27; N = 14.93%. Found: C = 42.40, H = 5.36, N =

22.15%. IR (KBr pellet), cm^{-1}: ν(C=C) + ν(C=N)/pyrazole ring, 1604 s, 1555 vs; $\nu_{asmy}(BF_4^-)$, 1091 vs;. UV-Vis spectra: λ_{max} (nm)(ε_{max}/$mol^{-1}cm^{-1}$): 604 (192), 506 (235), 296(7,259). $\Lambda_M(CH_3CN)$ ($\Omega^{-1}cm^2mol^{-1}$): 118, μ_{eff} = 3.88 BM.

2.2.6. Synthesis of [Co(L)Cl]ClO_4 (**5**)

This complex was prepared by following the same procedure as for complex 3 with the exception $NaClO_4.H_2O$ was used instead of NH_4PF_6. . Yield. 0.143 g. (50%). Anal calc. for $CoC_{18}H_{24}N_6Cl_2O_4$; C = 41.79; H = 4.63; N = 16.21%. Found: C = 42.10, H = 4.76, N = 1615%. IR (KBr pellet), cm^{-1}; ν(C=C) + ν(C=N)/pyrazole ring, 1604 s, 1555 vs; $\nu_{asmy}(ClO_4^-)$, 1091 vs;. 625; UV-Vis spectra: λ_{max} (nm)(ε_{max}/$mol^{-1}cm^{-1}$): 605 (186); 504 (230), 295(7,257). $\Lambda_M(CH_3CN)$ ($\Omega^{-1}cm^2mol^{-1}$): 118. μ_{eff} = 3.88 BM.

2.2.6. Synthesis of [Ni(L)Cl_2] (**6**)

A methanol solution (10 ml) of ligand L (0.324 g, 1 mmol) was added to methanol solution of $NiCl_2.6H_2O$ (0.237 g, 1 mmol) with constant stirring. After 10 min, NH_4BF_4 (0.104 g, 1.0 mmol) in little amount of water was added into it with stirring and stirring was continued for 3 h. Filtered the solution and filtrate was kept to evaporate slowly. Yield. 0.270 g (60 %). Found: C = 42.78 ; H = 18.46 ; N = 18.62%; Anal calc for $NiC_{18}H_{24}Cl_2N_6$; C = 47.68 ; H = 5.30 ; N = 18.54% ; IR (KBr pellet), cm^{-1}: ν(C=C) + ν(C=N)/pyrazole ring, 1613 s, 1554 vs; $\nu(PF_6^-)$, 844 vs;. UV-Vis spectra: λ_{max}(nm) (ε_{max} /$mol^{-1}cm^{-1}$): 535 (15), 290 (7000). $\Lambda_M(CH_3CN)$ ($\Omega^{-1}cm^2mol^{-1}$): 8 μ_{eff} = 2.88 BM

2.2.7. Synthesis of [CuL'(pz)-(μ-Cl)-CuClL'](Y)$_2$ (Y = PF_6^- (**7**) or ClO_4^- (**8**))

To a methanol solution (10 ml) of $CuCl_2.2H_2O$ (0.085 g, 0.5 mmol), ligand L (0.162 g, 0.5 mmol) in methanol (10 ml) was added drop wise with constant stirring. Finally, NH_4PF_6/$NaClO_4$ (1.0 mmol) in minimum quantity of water was added into the mixture. The colour of the solution was changed to deep green immediately and stirring was continued for 2 h. The solution was filtered and the filtrate was left to evaporate slowly and it was possible to obtain diffraction quality blue crystal after five days. Yield. 50%.

Anal calc. For (**7**) $C_{29}H_{38}Cl_2Cu_2F_{12}N_{10}P_2$; C = 34.30; H = 3.75; N = 13.80%. Found: C = 34.20, H = 3.80, N = 13.75%. IR (KBr pellet), cm^{-1}: ν(C=N)/pyrazole ring, 1613 s, 1553

vs; ν(PF_6^-), 842; ν(>NH), 3141 s, 3262 s; UV-Vis spectra: λ_{max}(nm)(ε_{max} /$mol^{-1}cm^{-1}$): 688 (201), 301 (2177); μ_{eff} = 1.78 BM.

Anal calc. For (**8**) $C_{29}H_{38}Cl_4Cu_2N_{10}O_8$; C = 40.85; H = 4.46; N = 16.13%. Found: C = 34.20, H = 3.80, N = 13.75%. IR (KBr pellet), cm^{-1}: ν(C=C)+ν(C=N)/pyrazole ring, 1613 s, 1553 vs; ν(ClO_4^-), 1102; ν(O–Cl–O), 627 s, ν(>NH), 3141 s, 3262 s; UV-Vis spectra: λ_{max}(nm)(ε_{max} /$mol^{-1}cm^{-1}$): 688 (195), 301 (2167) ; μ_{eff} = 1.79 BM.

2.3. Physical Measurements

The infrared spectrum was recorded on a Perkin-Elmer FT-IR spectrometer RX1 spectrum using KBr pellets. The elemental analysis was carried out using a Perkin-Elmer IA 2400 series elemental analyzer. UV-Vis spectra (900 - 190 nm) were recorded on a Perkin-Elmer spectrophotometer model Lambda 35 in acetonitrile solution. ^{1}H NMR spectra was recorded on Bruker NMR AV400 spectrometer and solution conductivity was measured on Equip-Tronics conductivity meter (model no. EQ-660A) using CH_3CN solvent.

2.4. X-ray Crystallography

2.4.1.X-ray crystal data and refinement

The crystallographic data, details of data collection and some important features of the refinement for the compound **1,** 3 and **7** are given in Table 1 and selected bond lengths and angles are given in Table 2. Blue crystals of suitable size of complex **1, 3** and **7** were obtained by slow evaporation of methanol solution. Crystals of **1**, **3** and **7** were selected and mounted. Data were collected with Mo-K_α radiation (λ = 0.71073Å) at 293 K ,110 K and 293 K for complex **1**, **3** and **7** respectively, on a Bruker SMART APEX diffractometer equipped with CCD area detector. The data interpretation were processed with SAINT software [22] and empirical absorption correction was applied with SADABS [23] software programs. Both structures were solved by direct methods using SHELXTL [24] and refined by the full-matrix least-square based on F^2 technique using SHELXL-97 [25] program package. All non-hydrogen atoms were refined

anisotropically. The positions of the hydrogen atoms positions were calculated from the difference Fourier map or Stereo Chemically fixed Complex **3.**

2. Results and discussion

3.1. General Characterization

The tetradentate N_4-coordinated ligand *N*,*N*-bis(3,5-dimethylpyrazol-1-ylmethyl)aminomethyl- pyridine (L) [Fig. 1] was synthesized as viscous liquid with high yield (80%) and characterized by microanalysis, IR (Fig.2), ^{1}H NMR (Fig.3), ^{13}C NMR(Fig.4) studies. Mononuclear complexes of the types $[Cu(L)(CH_3COO)](X)$ (X = PF_6^- and BF_4^-), $[Ni(L)Cl_2]$, $[Co(L)Cl](Y).\ ^1/_2(CH_3OH)$ (Y = BF_4^-, PF_6^- and ClO_4^-) (L = *N*,*N*-bis(3,5-dimethylpyrazol-1-ylmethyl)amino- methylpyridine) and binuclear copper(II) complexes $[L'(Cl)Cu\text{-}(\mu\text{-}Cl)\text{- }Cu(pz)L'](Z)_2$ (Z = PF_6^- and ClO_4^-) (where L' = *N*-(3,5-dimethylpyrazol-1-ylmethyl)aminomethylpyridine) have been synthesized with good yield (>50%) through one-pot reaction of metal salt like acetate/chloride, L and ammonium hexafluorophosphate / tetrafluoroborate in 1:1:1 mole ratio in methanol and characterized by microanalysis and physico-chemical methods. There was no change of structure when excess hexafluorophosphate / tetrafluoroborate were added and mononuclear complex was always formed. We tried to prepare binuclear bridged metal complexes of Co(II), Ni(II) and Cu(II) by the addition of 4,4'-bipyridyl during the reaction, but mononuclear complexes were always formed. In the case of copper chloride, we obtained chloride bridged binuclear copper(II) complex with modified ligand structure [scheme 1]. In the case of nickel complex, we always obtain $[Ni(L)Cl_2]$ even after addition of excess PF_6^-/BF_4^- ions. The ESI-MS spectral measurement of the **6** shows an intense peak (100%) at m/z 417 $(C_{18}H_{24}N_6ClNi)^+$ indicating the integrity of the complexes in solution [Fig. 5]. For the mononuclear complexes, ligand L has utilized all its four coordination sites for the formation of complexes but for binuclear copper(II) complex, N_4-coordinated L transformed into N_3-coordinated *N*-(3,5-dimethylpyrazol-1-ylmethyl) aminomethylpyridine (L') ligand during reaction and this was confirmed by single crystal X-ray diffraction studies.

Table 1. Crystal data and structure refinement for the complexes

	[Cu(L)(CH_3COO)]PF_6.H_2O	[Co(L)Cl]BF_4.$^1/_2$(CH_3OH)	Complex **7**
Empirical formula	C_{20} H_{29} Cu_1 F_6 N_6 O_3P_1	C_{37} H_{52} B_2 Cl_2 Co_2 F_8 N_{12} O	$C_{29}H_{38}Cl_2Cu_2F_{12}N_{10}P_2$
Formula weight	609.995	1043.29	1014.61
Temperature (K)	293(2) K	110(2)	293(2)
Wavelength (Å)	0.71073 A	0.71073	0.71073
Crystal system	Triclinic,	Monoclinic	Triclinic
Space group	*P-1*	$P_{21/c}$	*P-1*
a (Å)	8.748(5) A	13.2938(9)	12.587(3
b (Å)	10.440(5)	12.8524(9)	13.921(3)
c (Å)	15.063(5)	26.3516(17)	14.818(3)
α(°)	81.692(5	90	104.902(3)
β(°)	80.524(5)	91.8830(10)	107.505(3)
γ(°)	78.826(5	90	109.019(3)
Volume ($Å^3$)	1322.2(11)	4499.9(5)	2151.8(8)
Z	2	4	2
Density (Mg/m^3)	1.532	1.540	1.566
Absorption coefficient (mm^{-1})	0.962	0.936	0.945
F(000)	626	2144	1024
Crystal size (mm)	0.35 x 0.31 x 0.29	0.65 x 0.40 x 0.32	0.36 x 0.24 x 0.11
Theta range for data collection (°)	2.93 to 29.19	1.53 to 26.00	1.68 to 28.33
Index ranges	-10<=h<=11, -13<=k<=14, -19<=l<=19	-14≤h≤16, -15≤k≤14 -32≤l≤26	-16 ≤h≤16, -18 ≤k≤18, -19 ≤l≤18
Reflections collected	11299	23429	17608
Independent reflections	5970 [R(int) = 0.0698]	8832 [R(int) = 0.0258]	9578 [R(int) = 0.0430]
Absorption correction	Semi-empirical from equivalents	Semi-empirical from equivalents	Semi-empirical from equivalents
Max. and min. transmission	1.00000 and 0.84480	0.7539 and 0.5814	0.8726 and 0.6570
Refinement method	Full-matrix least-squares on F^2	Full-matrix least-squares on F^2	Full-matrix least-squares on F^2
Data / restraints / parameters	5970 / 0 / 337	8832 / 0 / 577	9578 / 0 / 528
Goodness-of-fit on F^2	1.044	1.071	0.968
Final R indices [I>2sigma(I)]	*R1* = 0.0682, w*R2* = 0.1771	*R1* = 0.0596, wR2 = 0.1502	*R1* = 0.0724, wR2 = 0.1855
R indices (all data)	*R1* = 0.1053, wR2 = 0.2111	*R1* = 0.0679, wR2 = 0.1552	*R1* = 0.1330, wR2 = 0.2198
Largest diff. peak and hole (eA^{-3})	1.126 and -0.560	1.194 and -0.866	0.931 and -0.345

This type of transformation of ligand structure is already reported in the literature with pyrazole containing ligand [27-29]. All complexes are stable at room temperature

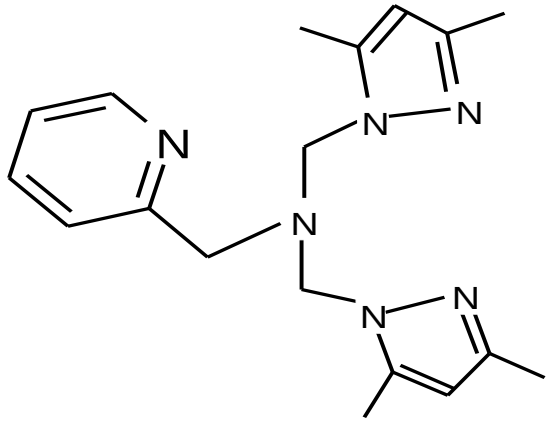

Fig.1. *N*,*N*-bis(3,5-dimethylpyrazol-1-ylmethyl)aminomethylpyridine (L)

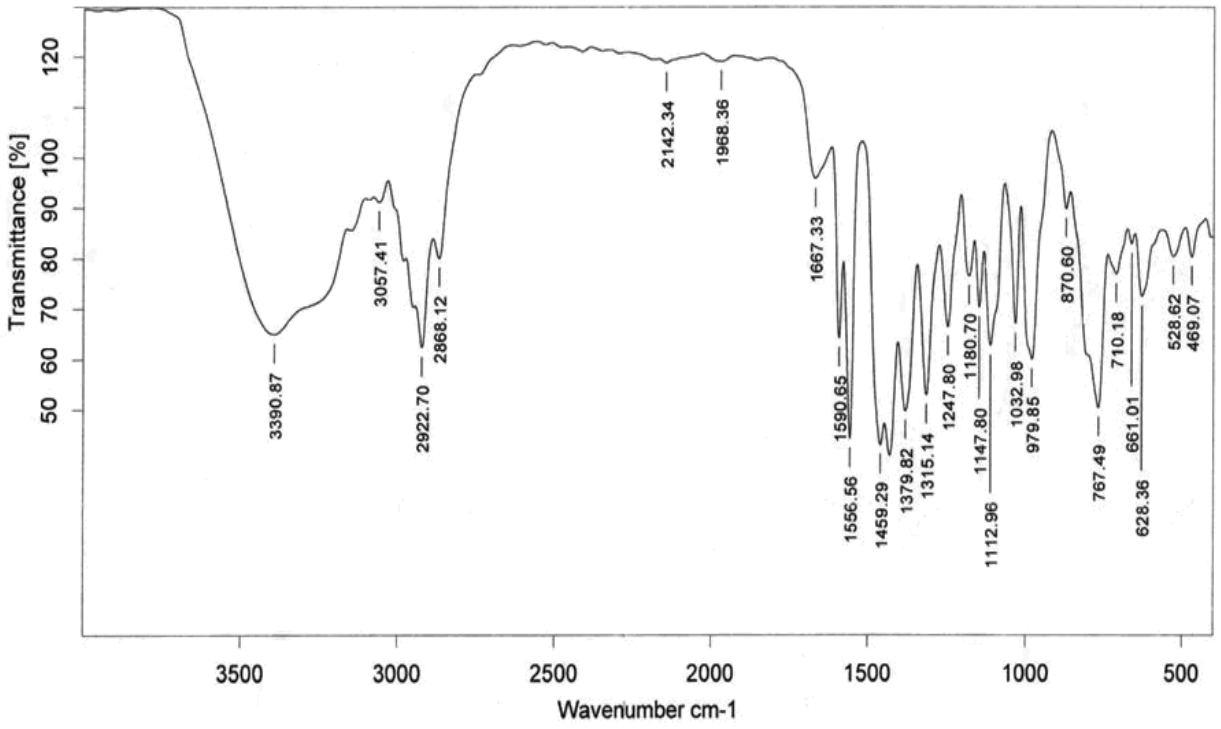

Fig.2. IR spectra of ligand *N*,*N*-bis(3,5-dimethylpyrazol-1-ylmethyl)aminomethylpyridine (L)

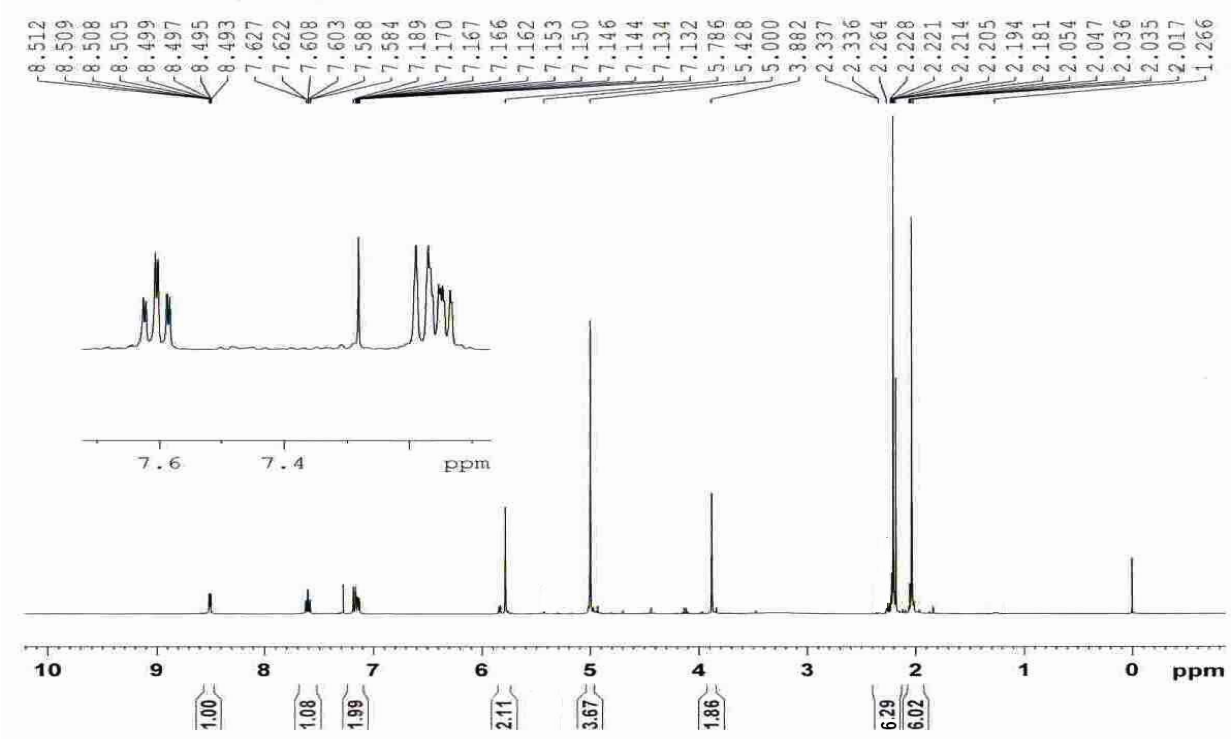

Fig.3. [1]H NMR spectra of *N*,*N*-bis(3,5-dimethylpyrazol-1-ylmethyl)aminomethylpyridine (L)

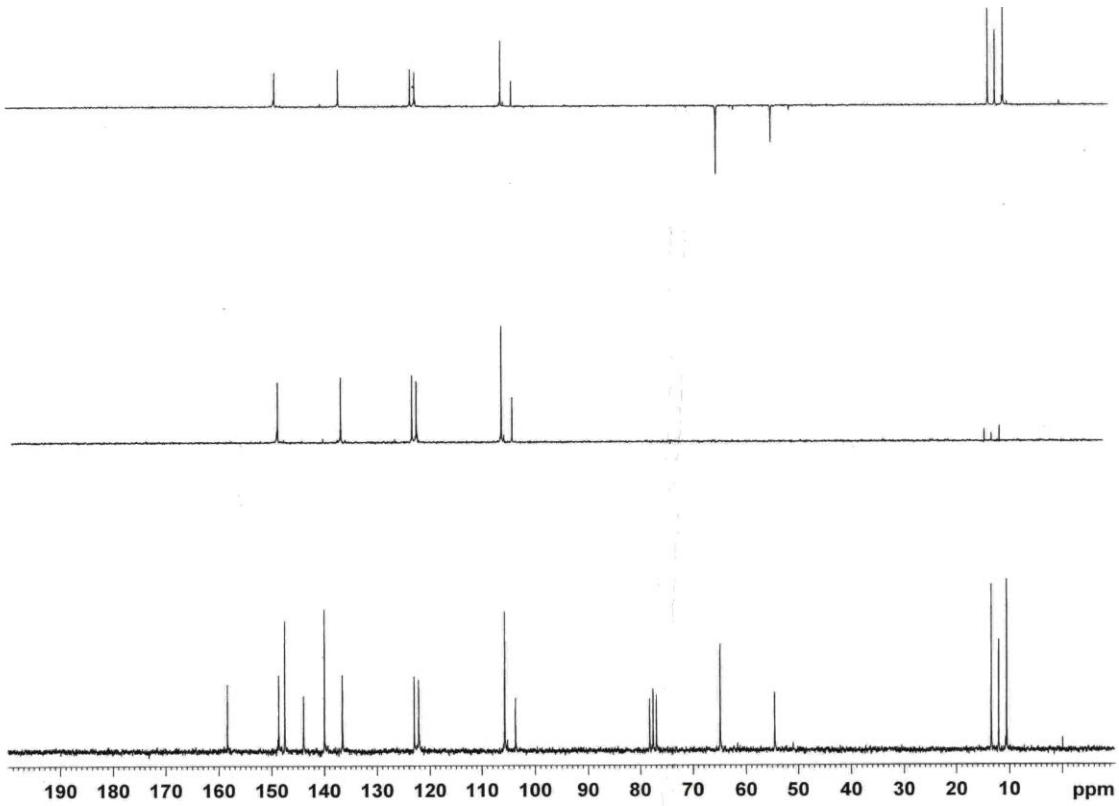

Fig. 4. [13]C- NMR spectra of *N*,*N*-bis(3,5-dimethylpyrazol-1-ylmethyl)aminomethylpyridine (L)

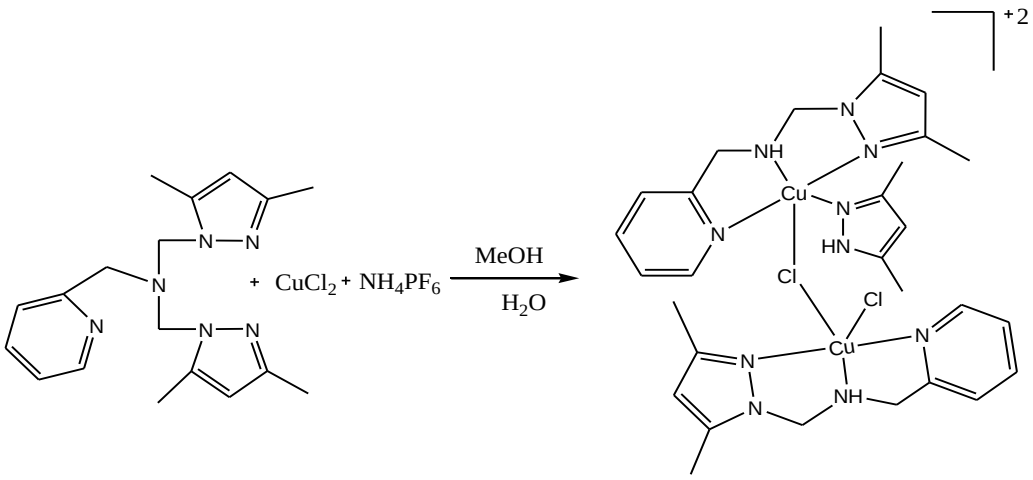

Scheme 1. Synthesis of [L'(Cl)Cu-(μ-Cl)-Cu(pz)L'](PF$_6$)$_2$

and soluble in common organic solvents like dichloromethane, methanol, acetonitrile etc. Conductivity measurements in CH_3CN solution show 1:1 electrolyte for complexes **1**, **2**, **3**, **4** and **5** and 1:2 electrolyte for complex **7** and **8**. Mononuclear complexes **1** and **3** have square bipyramidal geometry. In complex **7,** two square planner copper atoms are joined through chloride bridge and coordination environment of two copper atoms is different. In one side copper atom has [L'CuCl] and another side it has [Cu L'(pz)] environment.

3.2. IR spectra

The IR spectra of the complexes [**1-8]** as well as free ligand [Fig. 2] show strong bands in the region of 1615-1550 cm^{-1}, confirming the coordination of 3,5-dimethylpyrazole to the metals. The complexes **1**, **4** and **6** also have characteristics bands at ca 844 cm^{-1} for $\nu(PF_6^-)$ and at ca 1091 cm^{-1} for $\nu(BF_4^-)$ for complex **2** and **3**. For complex **7** and **8**, there are two bands in the region of 3141 and 3262 cm^{-1}for ν(>NH) for coordinated 3,5-dimethylpyrazole and L' generated from ligand L during reaction. All other bands obtained for the ligand are also present in the complexes. The IR spectra of the nickel complex also shows the characterized bands for ν(C=C) + ν(C=N) at 1613, 1554 cm^{-1} which suggest the coordination of ligand with the nickel complex [30]. IR spectra of complexes [Cu(L)(CH_3COO)]PF_6 and [L'(Cl)Cu-(μ-Cl)-Cu(pz)L'](PF$_6$)$_2$ are given in Fig. 6 and 7.

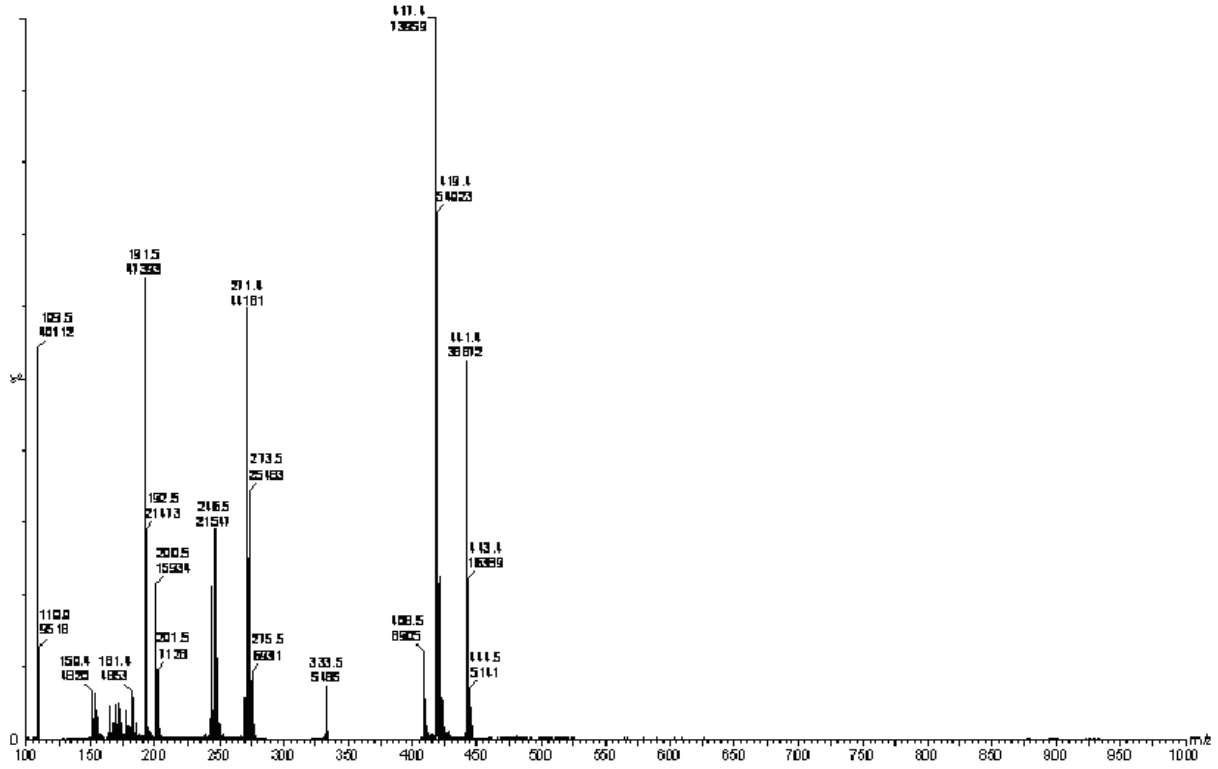

Fig. 5. Mass spectra(ESI) of [$NiLCl_2$]

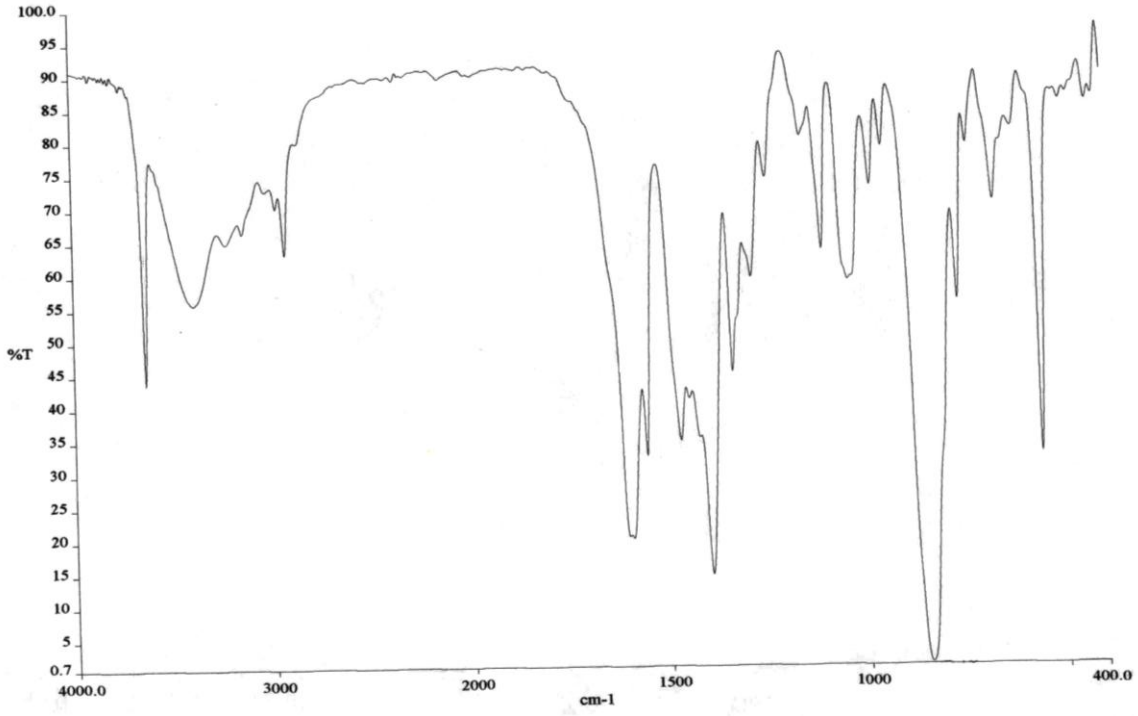

Fig.6. IR spectra of [$Cu(L)(CH_3COO)]PF_6.H_2O$

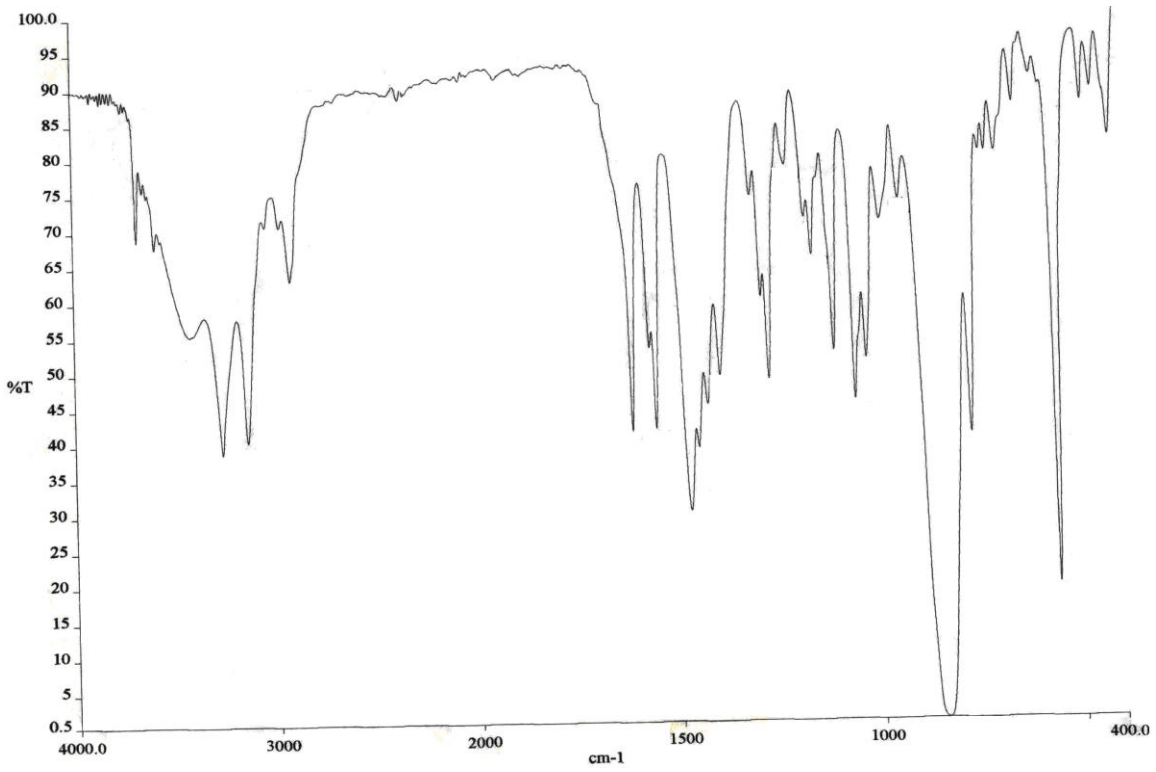

Fig. 7. IR Spectra of [L'(Cl)Cu-(μ-Cl)-Cu(pz)L'](PF$_6$)$_2$

3.3. Description of crystal structure of complexes

3.3.1. Crystal structure of [Cu(L)(CH$_3$COO)]PF$_6$.H$_2$O **(1)**.

Crystal structure of cationic part of complex **1** in the asymmetric unit with atom numbering scheme is shown in Fig. 8. Selected bond lengths and angles related to metal coordination sphere for the structure **1** are given in Table 2. The copper atom has five coordination with distorted square pyramidal geometry. The coordination environment around Cu(II) has been observed with a tetradentate supporting ligand L along with terminal acetate ligand. In the equatorial plane, three nitrogen atoms N1, N2, N3 from ligand L and O1 from acetate ligand and N4 from pyrazole ring in the axial position. The bond length in the equatorial plane Cu1-N1, Cu-N2, Cu-N3 and Cu1-O1 are 2.008(3), 2.097(4), 2.335(4), 1.906(3) (Å) respectively and they are nearly equal to each other. The axial Cu1-N4 distance is 1.998(3) (Å).

3.3.2. Description of crystal structure of complex $[Co(L)Cl]BF_4$. ½ CH_3OH **(3).**

Crystal structure of cationic part of one molecule of complex **3** in the asymmetric unit with atom numbering scheme is shown in Fig. 9. For complex **3**, there are two $[Co(L)Cl]^+$ units and one methanol molecule in the unit cell. The cobalt atom has five coordination with distorted trigonal bipyramidal geometry. The coordination environment around Co(II) has been observed with a tetradentate supporting ligand L along with terminal chloride ion. In the trigonal plane, there are three nitrogen atoms-N2 and N4 from ligand L and terminal Cl1 atom and N1 and N6 from ligand in the axial position. The bond distances of equatorial plane Co1-Cl, Co1-N2 and Co1-N6 are 2.2743, 2.273 and 2.044 and Å, respectively and the axial distances Co1-N1 and Co1-N4 are 2.064 and 2.065 Å, respectively. The bond angles of N(6)-Co(1)-N(1), N(6)-Co(1)-N(4), N(1)-Co(1)-N(4), N(4)-Co(1)-Cl(1) and N(2)-Co(1)-Cl(1) are 117.17(11), 110.91(12), 115.92(11), 106.43(9) and 175.81°, respectively.

3.3.3. Description of structure of binuclear copper(II) complex [CuL'(pz)-(μ-Cl)-CuClL'](PF$_6$)$_2$

Crystal structure of cationic part of complex **7** with atom numbering scheme is shown in Fig. 10. The structure of the complex reveals that two square planer copper atoms are bonded with bridging chloride ion. Both the copper atoms have five coordination with distorted square pyramidal geometry but the coordination environment is little different around Cu1 and Cu2. The ligand L' coordinate meridionally to the Cu(II) atoms like other chloride bridged binuclear complexes [1] and two monodentate ligands are bonded with different Cu atom i.e. Cl(1) is bonded with Cu(1) and pyrazole nitrogen N9 is bonded with Cu(2). The ligand L' has three potential nitrogen donor atoms: the nitrogen atoms of the pyrazole ring, the secondary amino group and pyridine ring. Square pyramidal environment around Cu1 has been observed with three nitrogen atoms from tridentate supporting ligand L' along with bridging chloride ion Cl2
and one terminal chloride ion Cl1. The equatorial Cu1-Cl1 (2.263 Å) distance is much smaller than axial Cu1-Cl2 (2.635 Å) distance. Cu2 is bonded with three nitrogen atoms

from ligand L', one nitrogen atom N9 from 3,5-dimethylpyrazole and from bridging chlorine atom Cl2. The equatorial Cu1-Cl1 (2.262 Å) bond distance is comparable to those of the similar reported complexes but this distance higher than Cu1-N1 (2.012 Å), Cu1-N2 (2.013 Å) and Cu1-N4 (2.007 Å). For Cu2, the entire equatorial bond distances i.e. Cu2-N5 (2.007 Å), Cu2-N6 (2.023 Å), Cu2-N9 (1.982 Å), Cu2-N8 (2.002 Å) are nearly same but smaller than Cu2-Cl2 (2.524 Å). The Cu1-Cl2-Cu2 angle (125.70°) is low and differs widely than the other reported complexes with angle ranges from 136.90° in $[Cu_2(bzpy)_2Cl_3]ClO_4.0.5H_2O$ [35] to 180° in $[\{(pmtpm)Cu(Cl)\}_2$ (μ-Cl)](ClO_4) [1]. The Cu1---- Cu2 distance is 4.591 Å.

3.3. Electronic spectra

The electronic spectra of the complexes were measured in CH_3CN solution. Very similar bands appear in both the copper complexes **1** and **2.** It shows one strong absorption bands obtained at 668 nm with molar extinction coefficient 201 l $cm^{-1}mol^{-1}$. This may be attributed to the d-d transition and generally obtained in typical square planner complexes [26] [Fig.11]. For cobalt complexes **3** and **4**, two strong bands obtained at ca. 604 and 509 nm with molar extinction coefficient 190 and 230 l $cm^{-1}mol^{-1}$, respectively and this may be attributed to d-d transitions. For nickel complex **6**, it shows weak absorption band at 539 nm and for binuclear copper (II) complex, a strong absorption band obtained at ca. 630 nm due to d-d transition. For all complexes, spectral band obtained at less than 400 nm are due to intraligand charge transfer transition.

3.4. Magnetic susceptibility

Room temperature magnetic susceptibility μ_{eff} of the complexes **1**, **2**, **6** and **7** show one-electron paramagnetism (μ_{eff} ~ 1.78 BM) which is close to one electron paramagnetism of copper(II) ions and three electron paramagnetism (μ_{eff} ~3.90BM) for cobalt(II) complexes **3** and **4**. For nickel complex **6**, two electron paramagnetism with μ_{eff} ~.2.87 BM obtained. This indicates **1** and **2** as well as **3** and **4** have same geometry. Variable temperature magnetic study of the complexes were not studied for complexes **7** and **8** as the distance between Cu2-Cl2 (2.635 Å) and Cu1----Cu2 distance (4.591 Å) are very high and therefore, it will be either very weak or no interaction among the two copper centers.

Table 2. Bond lengths (Å) and bond angles (˚) of Complex **1**, **3** and **7**

Bond lengths		Bond angles	
		Complex **1**	
Cu1-N1	2.008(3)	N2-Cu1-N6	80.05(15)
Cu1-N2	2.097(4)	N1-Cu1-N6	85.16(14)
Cu1-N4	1.998(3)	N4-Cu1-N6	105.72(15)
Cu1-N3	2.335(4)	O1-Cu1-N6	99.58(15)
Cu1-O1	1.906(3)	N1-Cu1-N2	82.27(13)
		N4-Cu1-N2	81.50(14)
		O1-Cu1-N2	178.85(12)
		O1-Cu1-N4	99.65(15)
		Complex **3**	
Co(1)-N(6)	2.044(3)	N(6)-Co(1)-N(1)	117.17(11)
Co(1)-N(4)	2.064(3)	N(6)-Co(1)-N(4)	110.91(12)
Co(1)-N(2)	2.273(3)	N(1)-Co(1)-N(4)	115.92(11)
Co(1)-N(1)	2.064(3)	N(6)-Co(1)-N(2)	76.74(10)
Co(1)-N(4)	2.065(3)	N(1)-Co(1)-N(2)	76.47(11)
Co(1)-N(2)	2.273(3)	N(4)-Co(1)-N(2)	76.09(11
Co(1)-N(6)	2.044(3)	N(6)-Co(1)-Cl(1)	105.11(8)
Co(1)-Cl(1)	2.2743(10)	N(1)-Co(1)-Cl(1)	99.36(9)
		N(4)-Co(1)-Cl(1)	106.43(9)
		N(2)-Co(1)-Cl(1)	175.81(8)
		Complex **7**	
Cu(1)-N(4)	2.007(4)	Cu(2)-Cl(2)-Cu(1)	125.70(6)
Cu(1)-N(1)	2.012(5)	N(4)-Cu(1)-N(1)	162.3(2)
Cu(1)-N(2)	2.013(5)	N(4)-Cu(1)-N(2)	81.0(2)
Cu(2)-N(9)	1.982(4)	N(1)-Cu(1)-N(2)	81.7(2)
Cu(2)-N(5)	2.007(4)	N(4)-Cu(1)-Cl(1)	100.11(14)
Cu(2)-N(8)	2.002(4)	N(4)-Cu(1)-Cl(1)	100.11(14)
Cu(2)-N(6)	2.023(4)	Cl(1)-Cu(1)-Cl(2)	99.22(5)
Cu(1)-Cl(1)	2.2625(16)	N(9)-Cu(2)-N(8)	98.73(19)
Cu(1)-Cl(2)	2.6352(15)	N(9)-Cu(2)-Cl(2)	91.20(15)
Cu(2)-Cl(2)	2.5240(16)	N(9)-Cu(2)-N(6)	171.2(2)

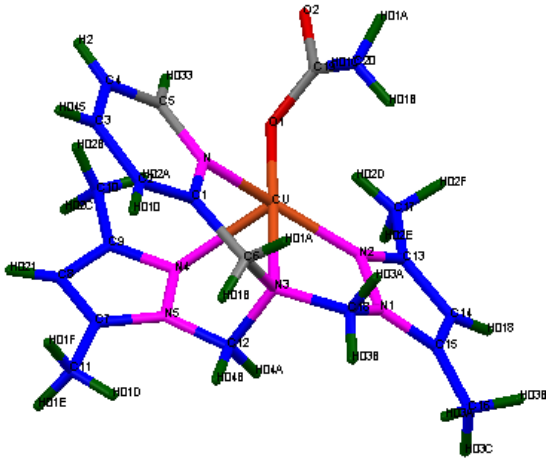

Fig.8.ORTEP diagram of the cationic part of $[Cu(L)(CH_3COO)]PF_6.H_2O$ with atom numbering scheme

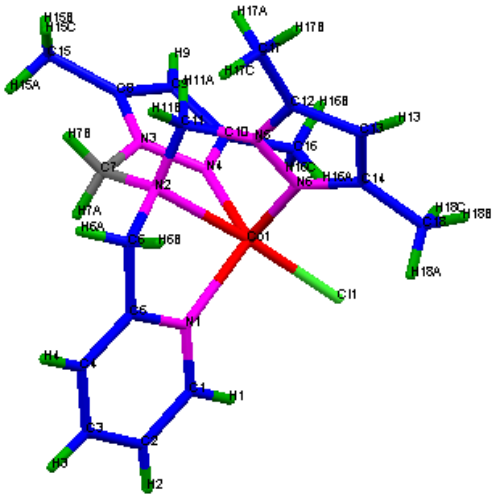

Fig.9. ORTEP diagram of the cationic part of $[Co(L)Cl]BF_4.{}^1/_2(CH_3OH)$ with atom numbering scheme

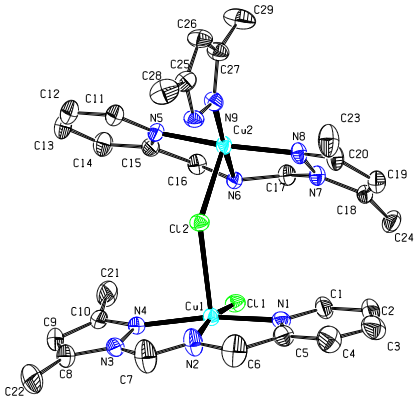

Fig.10. ORTEP diagram of the cationic part of $[Cu(Cl)L'\text{-}(\mu\text{-}Cl)\text{-}Cu(pz)lL'](PF_6)_2$ with atom numbering scheme

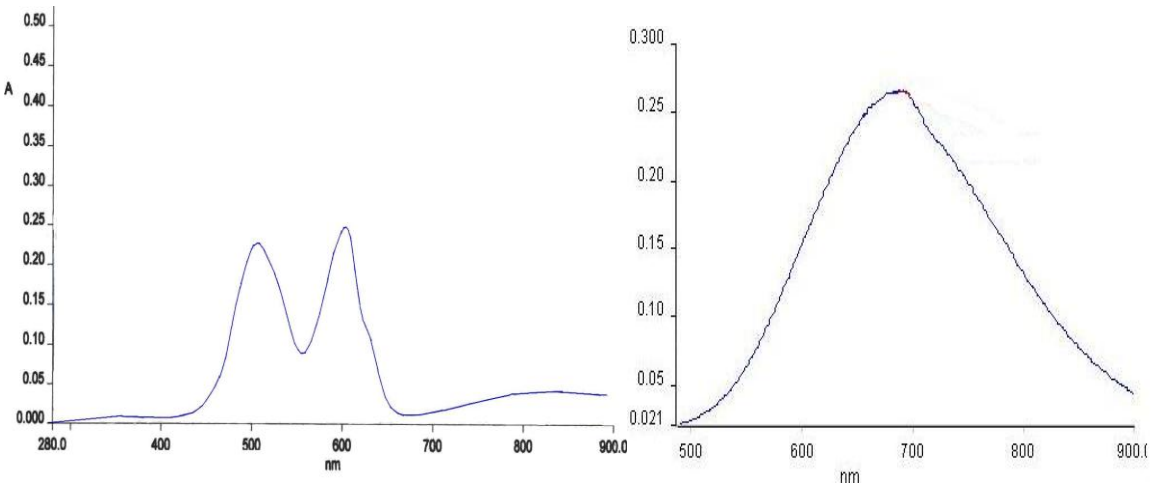

(a) (b)

Fig.11. Visible Spectra of (a). $[Co(L)(Cl)]BF_4$ and (b)$Cu(Cl)L'$-(μ-Cl)-$Cu(pz)L'](PF_6)_2$ in CH_3CN (1×10^{-3}M).

Similar long Cu-N bond (2.637 Å) and Cu-O (2.777 Å) distances were also observed in binuclear azido and cyanate bridged complexes, respectively, with this ligand [32, 34] and in both cases they were either no or very weak magnetic interaction between two copper centers [27, 28].

3.5. Cyclic Voltammetry

The cyclic voltammetry (CV) of the complexes **7** and **8** was recorded in CH_3CN solution (containing 0.1 M tetraethylammoniumfluoroborate as supporting electrolyte) at room temperature using platinum electrode, Ag/Ag^+ and a platinum wire as a working, reference and auxiliary electrode, respectively. It shows a reduction process corresponding to Cu(II)/Cu(I) with ΔE_p value is ~ 240 mV at a scan rate 300 mV^{-1}, indicating quasi-reversible one electron transfer for complexes **6** and **7**. For other complexes no such characteristic electron transfer were observed [Fig. 11].

4. Conclusion

In summary, we have synthesized and characterized new ligand *N*,*N*-bis(3,5dimethyl-1-ylmethyl) aminomethylpyridine (L) and its mononuclear copper(II) complexes $[Cu(L)(CH_3COO)](X)$, (X = PF_6^- and BF_4^-), cobalt(II) complexes [Co(L)(Cl)](Y)

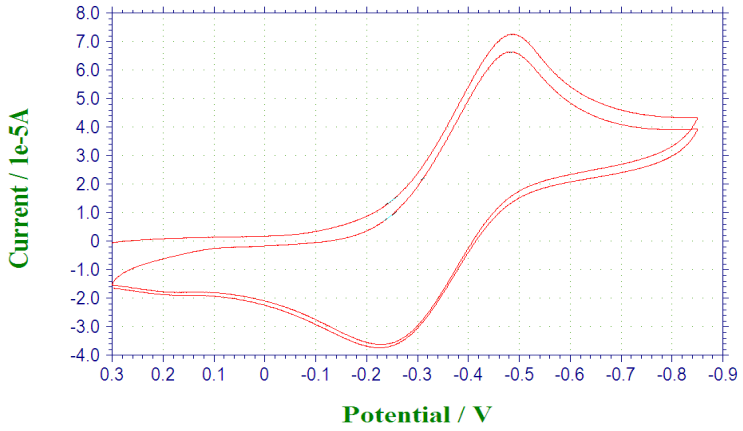

Fig.11. Cyclic Voltammograms of $[Cu(Cl)L'\text{-}(\mu\text{-}Cl)\text{-}Cu(pz)L'](PF_6)_2$ in CH_3CN of 0.1 M TEAF (scan rate 300 mV/s), using platinum working electrode.

(Y = PF_6^-, BF_4^- and ClO_4^-), nickel(II) complex $[Ni(L)Cl_2]$ and binuclear copper(II) complexes $[Cu(L')(pz)\text{-}(\mu\text{-}Cl)\text{-}Cu(Cl)L'](Z)_2$ (Z = PF_6^- and ClO_4^-) and these were characterized by microanalysis, ^1H N.M.R. and physico-chemical method. Crystal structure of the complexes $[Cu(L)(CH_3COO)]PF_6.H_2O$, $[Co(Cl)(L)]BF_4.1/2CH_3OH$ and $[CuL'(pz)\text{-}(\mu\text{-}Cl)\text{-}CuClL'](PF_6)_2$ have been solved by single crystal X-ray diffraction study. It shows complexes **1** and **7** have five coordination with square pyramidal geometry and complex **3** has trigonal bipyramidal structure. Tridentate N_3-coordinated ligand *N*-(3,5-dimethylpyrazol-1-ylmethyl)aminomethylpyridine (L') and 3,5-dimethyl pyrazole were obtained from tetradentate N_4-coordinated ligand *N*,*N*-bis(3,5-dimethylpyrazol-1-ylmethyl)aminomethylpyridine (L) during reaction of $CuCl_2.2H_2O$, ligand L and $PF_6^{'}/ClO_4^{'}$ in presence of methanol. Coordination environment around each copper atoms in the binuclear copper(II) complex are not same.

Supplementary materials

Crystallographic data for the structural analysis have been deposited with the Cambridge Crystallographic data Center, CCDC 835974, CCDC 819410, CCDC 815050 for complexes 1, 3 and 7, respectively. Copies of this information may be obtained free of charge from the Director, 12 Union Road, Cambridge, CB2 1EZ, UK; (fax: +44-1223-336033; e.mail: deposit@ccdc.cam.ac.uk or www.http://www.ccdc.ac.uk).

References

1 Sridhar R, Perumal PT, Etti S, Shanmugam G, Ponnuswamy MN, Prabavathy V, Mathivanna RN Bioorg. Med. Chem. Lett., 2004, 14:6035.

2 Jain AK, Moore SM, Yamaguchi K, Eling TE, Back SJ J. Pharmacol. Exp. Ther., 2004, 311:885.

3 Haanstra WG, Donk WAJWV, Drissen WL, Reedijk J, Wood JS, Drew MGB J. Chem. Soc., Dalton Trans, 1990, 3123.

4 Sorrell TN, Vankai VA, Garrity ML Inorg. Chem., 1991, 30, 207.

5 Bouwman E, Driessen WL, Reedijk J Inorg. Chem,, 1985, 24, 4730.

6 Blonk HL, Driesen WL, Reedijk J, J. Chem. Soc., Dalton Trans, 1985, 1699.

7 Veldhuis JBJ, Drissen WL, Reedijk J, J. Chem. Soc., Dalton Trans, 1986, 537.

8 K. D. Karlin, Z. Tyeklar, Bioinorganic Chemistry of Copper, Chapman and Hall, New (1993).

9 R. N. Mukherjee, Coord. Chem. Rev. 2000, 203, 151

10 T. Rachid, R. Abdelkrim, El K. Sghir Int. Jour. Phy. Sci. 2009, 4(13), 906

11 S. Trofimenko, Chem. Rev., 1993, 93, 943.

12 S. Trofimenko, Prog. Inorg. Chem.. 1995, 43, 419.

13 J. Reedijk, in: G. Wilkinson, R.D. Gillard, J.A. McCleverty (Eds.), Comprehensive Coordination Chemistry, vol. 2, Pergamon, Oxford, 1987, p. 73.

14 E.C. Constable, P.J. Steel, Coord. Chem. Rev., 1989, 93, 205.

15 Hulsbergen FB, Driessen WL, Reedijk J, Verschoor GC Inorg Chem, 1984, 23, 3588.

16 S. -C. Sheu, M.-J. Tien, M.-C. Cheng, T.-I. Ho, T-I, S.-M. Peng, Y.-C Lin, J. Chem. Soc., Dalton Trans. 1995, 3503.

17 B, Barszcz, T. Glowiak, J. Jezierska, A. Tomkiewicz Polyhedron , 2004, 23,1309.

18 A .Kovacs, D. Nemesok, G. Pokol, K.M. Szecsenyi, V.M. Leovac, Z.K. Jacimovic, I.R. Evans, J.A.K.Howard, Z.D. Tomic, G .Giester New. J. Chem., 2005, 29, 833.

19 R. N. Mukherjee, R. Gupta, T. K. Lal, R. Mukherjee, Polyhedron, 2002, 21, 1245.

20 J. G. Haasnoot, W. L. Driessen, J. Reedijk, Inorg. Chem., 1984, 23, 2803.

21 W. L. Driessen Recl. Trav. Chim. Pays-Bas , 1982, 101, 441

22 Sheldrick GM (1995) SAINT 5.1 ed. Siemens Industrial Automation Inc, Madison WI.

23 SADABS (1997) empirical absorption correction program. University of Go¨ttingen, Go¨ttingen, Germany

24 Sheldrick GM (1997) SHELXTL reference manual: version 5.1. Bruker AXS, Madison, WI

25 Sheldrick GM, SHELXL-97: program for crystal structure refinement. University of Go¨ttingen: Go¨ttingen

26 S. Roy, P. Mitra, A. K. Patra, Inorg. Chim. Acta., 2011, 370, 247

27 S. Bhattacharyya, T. J. R. Weakley, M. Chaudhury, Inorg. Chem., 1999, 38, 633

28 S. Bhattacharyya, T. J. R. Weakley, M. Chaudhury, Inorg. Chem., 1999, 38, 5453

29 B. Barszcz, T. Glowiak, J. Jezierska, A. Tomkiewicz, Polyhedron, 2004, 23, 1309

30 K. Nakamoto Infrared and Raman Spectra of Inorganic AND Coordination compounds. Part B. Application in Coordination, Organometallic and Bioinorganic Chemistry, John Wiley & Sons Inc., New York (1997).

31 S. Bhattacharyya, S. B. Kumar, S. K. Dutta, E.R.T. Tiekink, m. Chaudhury, Inorg. Chem., 1996, 35, 1967.

32 Z. Mahendrasihn,. S B. Kumar, E Suresh, J. Ribas, Trans. Met. Chem., 2010, 35, 757

33 Zala M., E. Suresh, S.B. Kumar, J. Coord. Chem., 2011, 64, 483.

34 Mahendrasinh, Zala.; Ankita, S.;. Kumar, S. B.; Escuer, A.; Suresh, E. (Inorg. Chim. Acta-2011 in press).

CHAPTER III

Syntheses, Characterization and Structure of Thiocyanate and Selenocyanate Complexes of Copper(II), Nickel(II) and Cobalt(II) with Pyridylpyrazole based ligand

Chapter III

Abstract

Mononuclear NCS^- containing complexes, $[M(NCS)_2L]$ (L = *N*,*N*-bis(3,5-dimethyl pyrazol-1-ylmethyl)aminomethylpyridine), $[CuL(NCS)]X$ (X = PF_6^- and ClO_4^-), $[Cu(NCS)_2L']$ (L'= *N*-(3,5-dimethylpyrazol-1-ylmethyl)aminomethylpyridine), and $NCSe^-$ containing complexes $[ML(NCSe)(H_2O)]ClO_4$ (M = Ni^{+2}, Co^{+2}) have been synthesized and characterized by elemental analysis, spectroscopic, and physico-chemical methods. Structural studies of $[Cu(NCS)_2L']$ show copper has five coordination with distorted trigonal bipyramidal geometry with two equatorial NCS^- and $[CuL(NCS)]PF_6$ show copper is five coordinate with square pyramidal geometry. $[M(NCS)_2L]$ and $[ML(NCSe)(H_2O)]ClO_4$ (M = Ni^{+2} and Co^{+2}) are expected to be octahedral.

1. Introduction

Pseudohalide-containing transition metal complexes can form mono-, di-, and polynuclear complexes using different blocking ligands and they have potential applications as magnetic materials. Pseudohalides can bind to metal ions end-to-end or end-on, generally forming polyatomic molecules. Among the psuedohalides, azido bridged complexes are most studied; thiocyanate-bridged complexes are fewer and they are not widely used as magnetic materials [1–4].

Metal complexes of nitrogen-containing heterocyclic ligands have biological activity. Metal complexes of pyrazole-based ligands have been used as models for the active sites of metalloenzymes [5–8]. As our interest was in the synthesis of new transition metal complexes with biologically active pyrazole-based ligands, we were interested to study complexing properties of N_4-coordinated *N,N*-bis(3,5-dimethylpyrazol-1-ylmethyl) aminomethylpyridine. Recently, we reported synthesis, structure, and magnetic properties of N_3^- and NCO^- bridged binuclear complexes of Ni(II) and Cu(II) with the ligand [9].

There are some reports on tridentate pyrazole and pseudohalide-containing complexes of Cu(II), Ni(II), and Co(II) [10–14], but tetradentate N_4-containing pseudohalide complexes are limited [15]. In continuation of our research on pseudohalide-containing polynuclear complexes with L, we report here the syntheses, spectroscopic characterization, and crystal structure of mononuclear complexes $[M(NCS)_2L]$, $[CuL(NCS)]X$ (X = PF_6^- and ClO_4^-), $[Cu(NCS)_2L']$ and $[ML(NCSe)(H_2O)]ClO_4$, where L = *N,N*-bis(3,5-dimethylpyrazol-1-ylmethyl)aminomethylpyridine, L′ = *N*-(3,5-dimethylpyrazol-1ylmethyl)aminomethylpyridine, M = Ni^{+2} and Co^{+2}. The ligand L′ is transformed from L during reaction. The crystal structure of $[CuL(NCS)]PF_6$ and $[Cu(NCS)_2L']$ are reported.

2. Experimental

2.1. Materials and methods

Chemicals and solvents were of analytical grade. 2-(aminomethyl)pyridine (Aldrich), hydrazine hydrate (GR, Loba, India), acetylacetone (GR, Loba, India), paraformaldehyde (GR, Loba, India), copper carbonate and nickel carbonate (Loba, India), potassium thiocyanate (Qualigens, India), and potassium selenocyanate (99%) (Aldrich) were used as received. 3,5-dimethyl-1-ylthiocarboxamide pyrazole (L") [16] and *N*,*N*-bis(3,5-dimethylpyrazol-1-ylmethyl)aminomethylpyridine (L) [9] were synthesized by published procedures. Solvents were purified following the standard procedures.

2.2. Synthesis of compounds

2.2.1. Synthesis of $[Cu(NCS)_2L']$ **(1).**

A solution of L (0.324 g, 1 mmol) in methanol (10 mL) was added to a solution of $Cu(NO_3)_2.3H_2O$ (0.242 g, 1 mmol) in methanol (10 mL). The color changed to deep blue immediately. To this solution, potassium thiocyanate (0.192 g, 2 mmol) in methanol was added dropwise with stirring. After 3 h, the mixture was filtered off and the solution was left for slow evaporation. Blue crystals were obtained after five days. Found (%): C, 42.50; H, 4.05; and N, 21.28. Anal. Calcd for $C_{14}H_{16}CuN_6S_2$ (%): C, 42.43; H, 4.04; and N, 21.21; Yield, 0.158 g (40%). IR (KBr pellet) cm^{-1}; ν(>NH), 3129; ν(NCS^{-1}), 2091 vs; ν(C=C)+ν(C=N)/pyrazole ring, 1607 s, 1559 vs. UV-Vis spectra: λ_{max}(nm) (ε_{max}($mol^{-1}cm^{-1}$)): 700 (65), 390 (6213), 382 (6534), 370 (14,880). $\Lambda_M(CH_3CN)$ ($\Omega^{-1}cm^2mol^{-1}$); 10. μ_{eff} =1.80 BM.

2.2.2. Synthesis of $[Ni(NCS)_2L]$ **(2).**

A methanol solution (10 mL) in L (0.324 g, 1 mmol) was added dropwise to a solution of $Ni(NO_3)_2.6H_2O$ (0.290 g, 1 mmol) in methanol (10 mL). To this solution, potassium thiocyanate (0.192 g, 2 mmol) in methanol (10 mL) was added dropwise. After 2 h, sky blue compound was filtered off, washed with methanol, and dried in vacuum. Yield: 0.250 g (50%). Found (%): C, 48.46; H, 4.87; and N, 22.64; Anal. Calcd for $C_{20}H_{24}NiN_8S_2$ (%): C, 48.10; H, 4.81; and N, 22.45; MS (EI): m/z 440 (100%) $(C_{19}H_{24}N_7SNi)^+$. IR (KBr pellet) cm^{-1}; ν(NCS^-), 2091, ν(C=C)+ν(C=N)/ pyrazole ring,

1607 s, 1550 vs. UV-Vis spectra: λ_{max}(nm) (ε_{max}(mol^{-1}cm^{-1})): 535 (sh, 15), 350 (sh), 270 (24,560). Λ_M(CH_3CN) (Ω^{-1}cm$_2$mol^{-1}); 10. μ_{eff} = 2.88 BM.

2.2.3. Synthesis of [Co(NCS)$_2$L] **(3).**

A solution of L (0.324 g, 1 mmol) in methanol (10 mL) was added to a solution of $Co(NO_3)_2.6H_2O$ (0.291 g, 1 mmol) in methanol (10 mL). The colour changed to bluish violet immediately. To this solution, potassium thiocyanate (0.192 g, 2 mmol) in methanol was added dropwise with stirring. After 2 h, the mixture was filtered and the solution was left for slow evaporation. Light purple powder was obtained after slow evaporation. Found (%): C, 48.15; H, 4.85; and N, 22.28. Anal. Calcd for $C_{20}H_{24}CoN_8S_2$ (%): C, 48.10; H, 4.81; and N, 22.44; Yield: 0.300 g (60%). MS (EI): m/z 441(100%) $[C_{19}H_{24}N_7SCo]^+$. IR (KBr pellet) cm^{-1}; ν(NCS$^-$), 2081 vs, ν(C=C)+ ν(C=N)/pyrazole ring, 1603 s, 1555 vs. UV-Vis spectra: λ_{max}(nm) (ε_{max}(mol^{-1}cm^{-1})) 750 (sh), 580 (285), 490 (123), 325 (17,425), 285 (29,710). Λ_M(CH_3CN) (Ω^{-1}cm^{2}mol^{-1}); 8. μ_{eff} =3.89 BM.

2.2.4. Synthesis of [Ni(NCSe)L(H_2O)]ClO_4 **(4).**

A solution of L (0.324 g, 1 mmol) in methanol (10 mL) was added to a solution of $Ni(ClO_4)_2.6H_2O$ (0.365 g, 1 mmol) in methanol (10 mL) in the dark. After 10 min, potassium selenocyanate (0.192 g, 2 mmol) in methanol was added dropwise with stirring. After 1 h, the light blue precipitate was filtered off, washed with methanol, and dried. Yield: 0.330 g (55%). Found (%): C, 38.02; H, 4.19; and N, 16.45. Anal. Calcd. for $NiC_{19}H_{26}N_7SeClO_5$ (%): C, 37.66; H, 4.29; N, 16.19. MS (EI): m/z 488 $(C_{19}H_{24}N_7SeNi)^+$. IR (KBr pellet), cm^{-1}: ν(OH$^-$), 3437 s, br; ν(NCSe^{-1}), 2091 vs; ν(C=C)+ν(C=N)/pyrazole ring, 1608 s, 1559 vs; ν_{asmy}(Cl–O), 1086 vs; δ(O–Cl–O), 627 s. UV-Vis spectra λ_{max}(nm) (ε_{max}(mol^{-1}cm^{-1})) 600 (sh), 535 (15), 270 (21,350). Λ_M(CH_3CN) (Ω^{-1}cm^{2}mol^{-1}); 118. μ_{eff}=2.89 BM.

2.2.5. Synthesis of [Co(NCSe)(L)(H_2O)]ClO_4 **(5).**

A solution of L (0.324 g, 1 mmol) in methanol (10 mL) was added to a solution of $Co(ClO_4)_2.6H_2O$ (0.365 g, 1 mmol) in methanol (10 mL) in the dark. After 10 min, potassium selenocyanate (0.288 g, 2 mmol) in methanol (15 mL) was added dropwise

with constant stirring. After 1 h, the mixture was filtered and the solution was left for slow evaporation. Brownish compound was obtained after a few days. Yield: 0.360 g (60%). Found (%): C, 37.98; H, 4.25; and N, 16.50. Anal. Calcd for $CoC_{19}H_{26}N_7SeClO_5$ (%): C, 37.66; H, 4.29; and N, 16.19. MS (EI): m/z (100%) 489 $(C_{19}H_{24}N_7SeCo)^+$. IR (KBr pellet), cm^{-1}: ν(OH^-), 3427 s, br; ν($NCSe^{-1}$), 2107 vs; ν(C=C)+ν(C=N)/pyrazole ring, 1604 s, 1556 vs; ν_{asmy}(Cl–O), 1102 vs; δ(O–Cl–O), 628 s. UV-Vis spectra: λ_{max}(nm) (ε_{max}($mol^{-1}cm^{-1}$)) 700 (sh), 576 (281), 484 (183), 346 (20,426), 287 (30,244). $\Lambda_M(CH_3CN)$ ($\Omega^{-1}cm^2mol^{-1}$); 116. μ_{eff}= 3.90 BM.

2.2.6. Synthesis of $[Cu(NCS)L]PF_6$ (**6**).

A solution of ligand L (0.324 g, 1 mmol) in methanol (10 ml) was added drop wise to a solution of $Cu(CH_3COO)_2$. H_2O (0.250 g, 1 mmol) in methanol (10 ml) with stirring. The colour of the solution changed to deep blue immediately. To this solution, 3,5-dimethyl-1-ylthiocarboxamide pyrazole (L") (0.156 g, 1 mmol) in methanol was added drop wise with stirring. After 20 min, NH_4PF_6 (0.163 g, 1 mmol) in minimum amount of water was added into it and stirring was continued for 3 hr. The mixture was filtered off and the solution was left for slow evaporation. Found (%): C, 37.78; H, 4.25; N, 16.15. Anal Calc for $C_{19}H_{24}CuN_7SPF_6$ (%): C, 38.61; H, 4.06; N, 16.59; Yield 0.158 g (40%). IR (KBr pellet) cm^{-1}; ν(NCS^{-1}), 2043 vs; ν(C=N)/ pyrazole ring, 1604 s 1556 vs, ν(PF_6^-), 844 vs. UV-Vis spectra: λ_{max}/nm (ε_{max}/$mol^{-1}cm^{-1}$). 669 (160), 390 (6 213), 382 (6534), 370 (14 880). Λ_M ($\Omega^{-1}cm^2\,mol^{-1}$) = 118; μ_{eff} = 1.80 BM.

2.2.7. Synthesis of $[Cu(NCS)L]ClO_4$ (**7**).

This complex was synthesized by following the same procedure as that of $[Cu(NCS)L]\ PF_6$ except $Cu(ClO_4)_2.6H_2O$ was used instead of $Cu(CH_3COO)_2.H_2O$. Analytical data for $[Cu(NCS)L]ClO_4$; Found (%): C, 41.42; H, 4.35; N, 18.12. Anal Calc for $C_{19}H_{24}CuN_7SClO_4$ (%): C, 41.83; H, 4.40; N, 17.98; Yield 0.140 g (51%). IR (KBr pellet) cm^{-1}; ν(NCS^{-1}), 2042 vs; ν(C=N)/ pyrazole ring, 1604 s 1556 vs, ν(ClO_4^-), 1091 vs. UV-Vis spectra: λ_{max}/nm (ε_{max}/$mol^{-1}cm^{-1}$). 668 (164), 390 (6 213), 382 (6 534), 370 (14 880). Λ_M ($\Omega^{-1}cm^2\,mol^{-1}$) = 116 μ_{eff} = 1.79 BM.

2.3**.** *Physical measurements*

Infrared spectra were recorded on a Perkin Elmer FT-IR spectrometer RX1 using KBr pellets. The elemental analysis was carried out using a Perkin Elmer IA 2400 series elemental analyzer. UV-Vis spectra (900–190 nm) were recorded on a Perkin Elmer spectrophotometer model Lambda 35 in acetonitrile. Room temperature magnetic susceptibilities of powder samples were measured using a Faraday magnetic balance equipped with a Mettler UMX 5 balance, OMEGA temperature controller with a field strength of 0.8 Tesla using $Hg[Co(SCN)_4]$ as the reference. $M(ClO_4)_2.6H_2O$ (M = Cu^{+2}, Ni^{+2}, and Co^{+2}) were prepared on the treatment of metal carbonate with dilute $HClO_4$ acid and followed by slow evaporation of the solution.

2.4. X-ray crystallography crystal data and refinement.

Crystallographic data and details of data collection for **1** and **6** are given in Table 1. Single crystals of suitable size of **1** and **6** were obtained by slow evaporation of methanol. A deep blue crystal was mounted on glass fiber with epoxy resin. Data were collected with Mo-Kα radiation (λ=0.71073Å) at 293 K on a Bruker SMART APEX diffractometer equipped with a CCD area detector. Of the 17,510 and 9200 reflections, 3420 and 5235 with $I > 2\alpha(I)$ were used for structure solutions for complex **1** and **6,** respectively. The data were processed with SAINT [17] and empirical absorption correction was applied with SADABS [18] programs. The structure was solved by direct methods using SHELXTL [19] and the refinement was based on $|F|^2$ by full-matrix least-squares using SHELXL-97 [20]. All non-hydrogen atoms were refined with anisotropic displacement parameter. Hydrogen positions were calculated from the difference Fourier map.

3. Results and discussion

3.1. General characterization

The tetradentate *N*,*N*-bis(3,5-dimethylpyrazol-1-ylmethyl)aminomethylpyridine (L) was

Table 1. Crystal data and structure refinement for Complex **1** and Complex **6**

Molecular Formula	$C_{14}H_{16}CuN_6S_2$	$C_{19}H_{24}CuF_6N_7PS$
Formula weight	395.99	591.02
Temperature (K)	293(2)	293(2)
Wavelength (Å)	0.71073	0.71073
Crystal system	Orthorhombic	Triclinic
Space group	*Pbca*	*P-1*
Unit cell dimensions		
a (Å)	16.375(3)	10.136(4)
b (Å)	14.173(3)	11.858(5)
c (Å)	14.954(3)	12.070(5)
α (°)	90	113.829(6)
β (°)	90	108.829(6)
γ (°)	90	94.952(6)
Volume $Å^3$	3470.6 (12)	1216.1(8)
Z	8	2
Density calculated(mg/m^3)	1.516	1.614
F(000)	1624	602
Absorption coefficient (mm^{-1})	1.506	1.119
Crystal size (mm^3)	0.58 x 0.37 x 0.33	0.43 x 0.24 x 0.11
θ range for data collection (°)	2.34 to 26.00 deg	2.01 to 28.00
Index ranges	$-18\leq h\leq 20$, $-17\leq k\leq 14$, $18\leq l\leq 18$	$-12\leq h\leq 13$, $-15\leq k\leq 15$, $-15\leq l\leq 15$
Reflections collected	17510	9200
Independent reflections	3420 [R(int) = 0.0352]	5235 [R(int) = 0.0366]
Absorption correction	Semi-empirical form Equivalents	Semi-empirical from equivalents
Max. and min. transmission	0.6364 and 0.4754	0.8868 and 0.6448
Refinement method	Full-matrix least-squares on F^2	Full-matrix least-squares on F^2
Data / restraints / parameters	3420/0/206	5235 / 0 / 320
Goodness-of-fit on F^2	1.174	1.104
Final *R* indices [$I>2\sigma(I)$]	$R_1 = 0.0885$, $wR_2 = 0.2441$	$R_1 = 0.0625$, $wR_2 = 0.1757$
R indices (all data)	$R_1 = 0.1201$, $wR_2 = 0.2635$	$R_1 = 0.0933$, $wR_2 = 0.2061$
Largest diff. peak and hole (e $Å^{-3}$)	0.932 and -0.354	1.035 and -0.474

synthesized and characterized as per published procedure [9]. Mononuclear complexes $[M(NCS)_2L]$ (M = Ni^{+2} and Co^{+2}) and $[Cu(NCS)_2L']$ were obtained in good yield (~50%) through one-pot reaction of metal salt (nitrate/perchlorate/acetate), L and sodium thiocyanate in 1 : 1 : 2 mole ratio in methanol. Complexes containing NCS^- were mononuclear even on changing starting metal salts during the preparation of complexes. Similar NCS^- containing mononuclear complexes are reported [10–15]. The tetradentate N_4–L is transformed into tridentate N_3-coordinated L′ with Cu^{+2}, NCS^- and L under reaction condition for the formation of five-coordinate copper (scheme 1). Isolation of 3,5-dimethylpyrazole from reaction leading to **1** suggests that Cu^{+2} promotes the cleavage of C–N single bond of L in the presence of methanol. Such change of ligand and consequent change of geometries during complexation are already reported [21–23]. When complexation with Cu(II) is carried out in solvents other than alcohol, we obtained product with unknown composition. For Ni(II) and Co(II) complexes, L is expected to

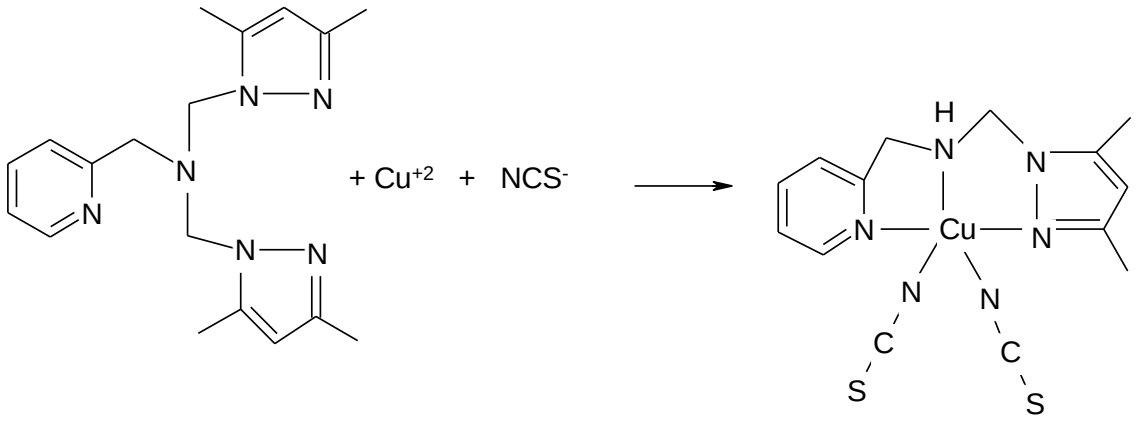

Scheme 1. Synthesis of $[Cu(NCS)_2L']$

utilize all four potential N_4-donor sites plus two nitrogen donor sites from NCS^- to form octahedral complexes. Diffraction quality crystals for structural studies were obtained only for copper complex by slow evaporation of the solution; we were unsuccessful with nickel and cobalt complexes. All complexes (**1**–**3**) are moderately soluble in acetonitrile, alcohol, and DMF but insoluble in dichloromethane, acetone, etc. Conductance measurements show that all the complexes are nonelectrolytes indicating both NCS^- are coordinated. The complexes gave satisfactory microanalytical data. The crystal structure

of $[Cu(NCS)_2L']$ shows two equatorial NCS^- attached to copper. Due to the unavailability of X-ray quality single crystals, the structures of **2** and **3** could not be solved. The ESI-MS spectral measurement showed an intense peak (100%) at m/z 443 $(C_{19}H_{24}N_7SNi)^+$ for nickel complex **2** [Fig. 1] and at m/z 441 $(C_{19}H_{24}N_7SCo)^+$ for complex **3** indicating the integrity of the complexes in solution. So, based on spectroscopic and other physicochemical data, we expect that both Ni(II) and Co(II) complexes are octahedral with two equatorial NCS^- ions.

The mononuclear selenocyanate complexes were synthesized in good yield (>50%) through one-pot reaction of metal perchlorate, L, and sodium selenocyanate in 1 : 1 : 2 mole ratio in methanol. For copper, we obtained gummy product with unknown composition. Complexes **4** and **5** gave satisfactory microanalysis confirming their composition. The ESI–MS spectral measurement showed an intense peak (100%) at m/z 488 $(C_{19}H_{24}N_7SeNi)^+$ for complex **4** [Fig. 2] and at m/z 489 $(C_{19}H_{24}N_7SeCo)^+$ indicating the integrity of the complexes in solution. The complexes are moderately soluble in acetonitrile but insoluble in dichloromethane, acetone, etc. Conductivity in CH_3CN shows that **4** and **5** are 1 : 1 electrolytes indicating the presence of ClO_4^- as counter anion. Due to unavailability of diffraction quality crystals, crystal structures of **4** and **5** could not be solved. On the basis of spectral, magnetic, and microanalytical data, we expect that both Ni(II) and Co(II) selenocyanate complexes are octahedral.

$[Cu(NCS)L](X)$ ($X = PF_6^-$ or ClO_4^-)

The complexes $[Cu(NCS)L](X)$ ($X = PF_6^-$ or ClO_4^-) are obtained in good yield by the reaction between copper salt, ligand L, another L" and counter anions ClO_4^- or PF_6^- in presence of methanol. Here, NCS^- was obtained from ligand L" during reaction with the elimination of 3,5-dimethylpyrazole according to the scheme 2. This was confirmed by ^1H NMR study of the isolated 3,5-dimethylpyrazole. When the same reaction is carried out in CH_3CN, gummy product with unknown composition was obtained. Crystal structure of $[Cu(NCS)L](PF_6)$ has been solved by X-ray diffraction study and it shows that it has square pyramidal structure. The important point is that same ligand L on reaction with $Cu(ClO_4)_2.6H_2O$ and NCS^{-1} in presence of methanol produce

$[Cu(NCS)_2L']$ where L' = *N*-(3,5-dimethylpyrazol-1-ylmethyl)aminomethylpyridine. Here not only two NCS^{-1} were coordinated but ligand L has been transformed into L'. The

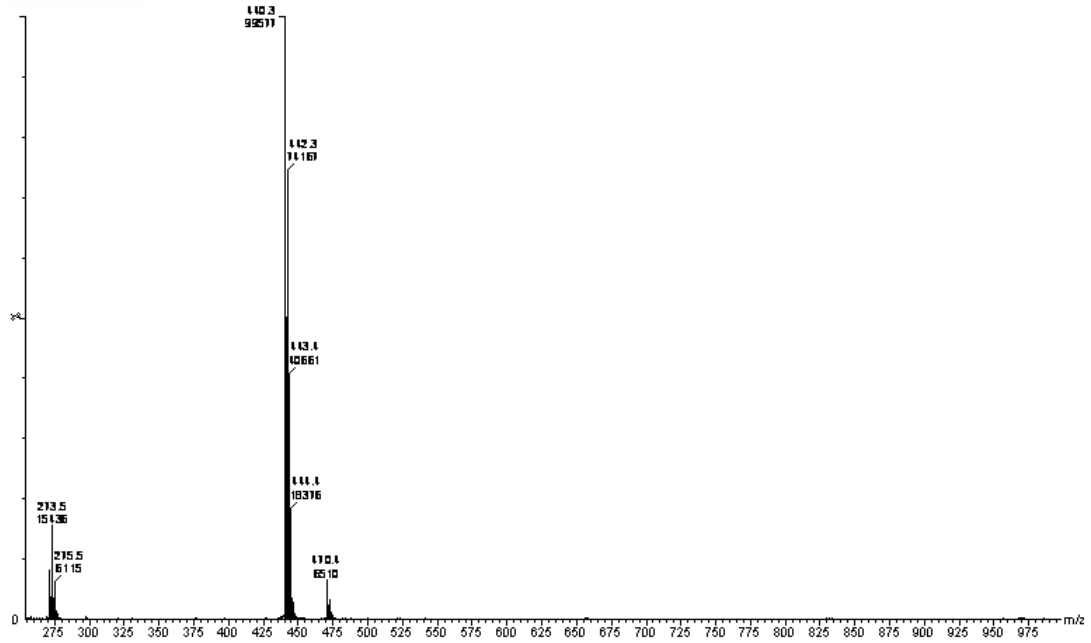

Fig. 1. Mass spectra (ESI) of $[Ni(NCS)_2L]$

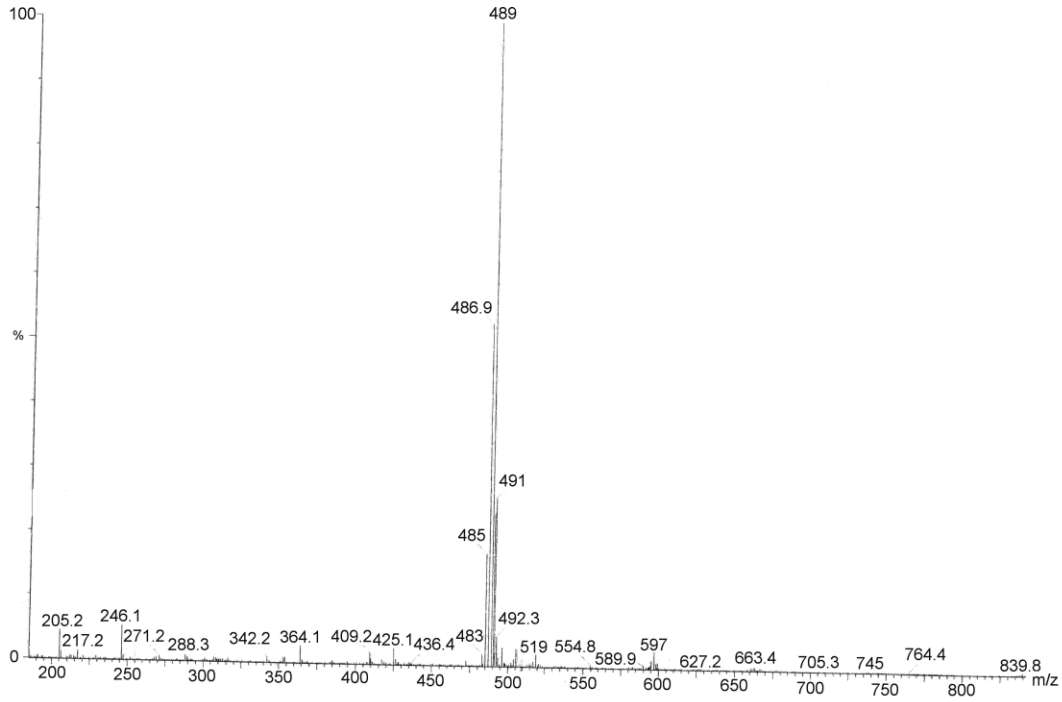

Fig. 2. Mass spectra (ESI) of $[CoL(NCSe)(H_2O)]ClO_4$

actual mechanism for the formation of $[Cu(NCS)L]^+$ is not known but after addition of L" in the reaction mixture of Cu^{+2}, ligand L and counter anion in presence of methanol, the blue colour of Cu^{+2} is transformed into yellow-grey colour insoluble product with unknown composition and finally light blue compound obtained with stirring for few hrs. In both cases copper is five coordinated and prefers to form five coordinated either trigonal bipyramidal or square pyramidal complex due to steric hindrance of the ligand. Complexes are soluble in acetonitrile, dichloromethane and other common organic solvents. Conductivity in CH_3CN show that both complexes 1 and 2 are 1:1 electrolyte indicating the presence of counter anion in both the complexes

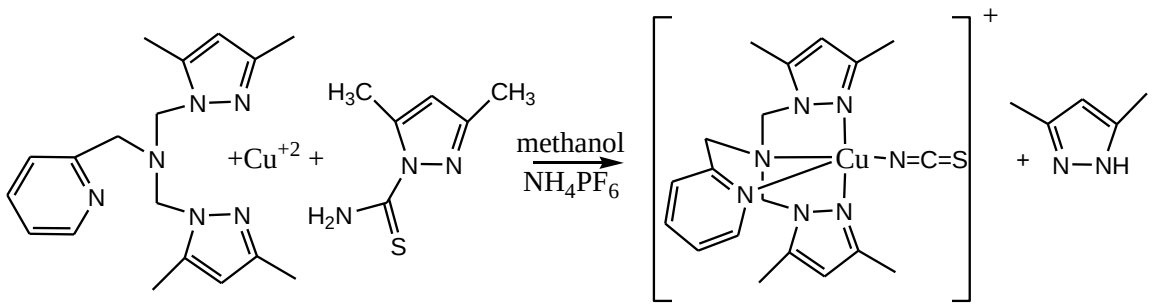

Scheme 2. Synthesis of $[Cu(L)(NCS)]^+$

3.2. IR spectra

The IR spectrum of the free ligand and **1–5** show two strong bands at 1604–1556 cm^{-1} due to pyrazole ν(C=N) + ν(C=C) vibrations indicating coordination of pyrazole to the metal. One strong band at ca 2085 cm^{-1} for NCS^- containing complexes **1–3** and at 2077 cm^{-1} for $NCSe^-$ containing complexes **4** and **5** indicate bonding of NCS^- and $NCSe^-$. Position and nature of NCS^- spectral bands for **1–3** are the same type indicating cis NCS^- for cobalt and nickel complexes like the Cu(II) complex [Fig.3 and 4]. For **1**, one band at 3129 cm^{-1} due to ν(>NH) is absent in other complexes indicating the transformation of ligand of **1**. Two strong bands at 1102 and 628 cm^{-1} indicate the presence of ClO_4^- as

counter anion and one broad brand at ~3437 cm^{-1} is due to ν(OH^-) from water present in **4** and **5** [24]. For complex **6**, one strong band appears at 844 cm^{-1}indicating the presence of. PF_6^- and another two bands appear at 1091 for ν(ClO_4^-) and at 625 for δ(O-Cl-O) indicating the presence of ClO_4^- as counter anion for complex **7**. All other bands of the ligand are also present in the complexes.

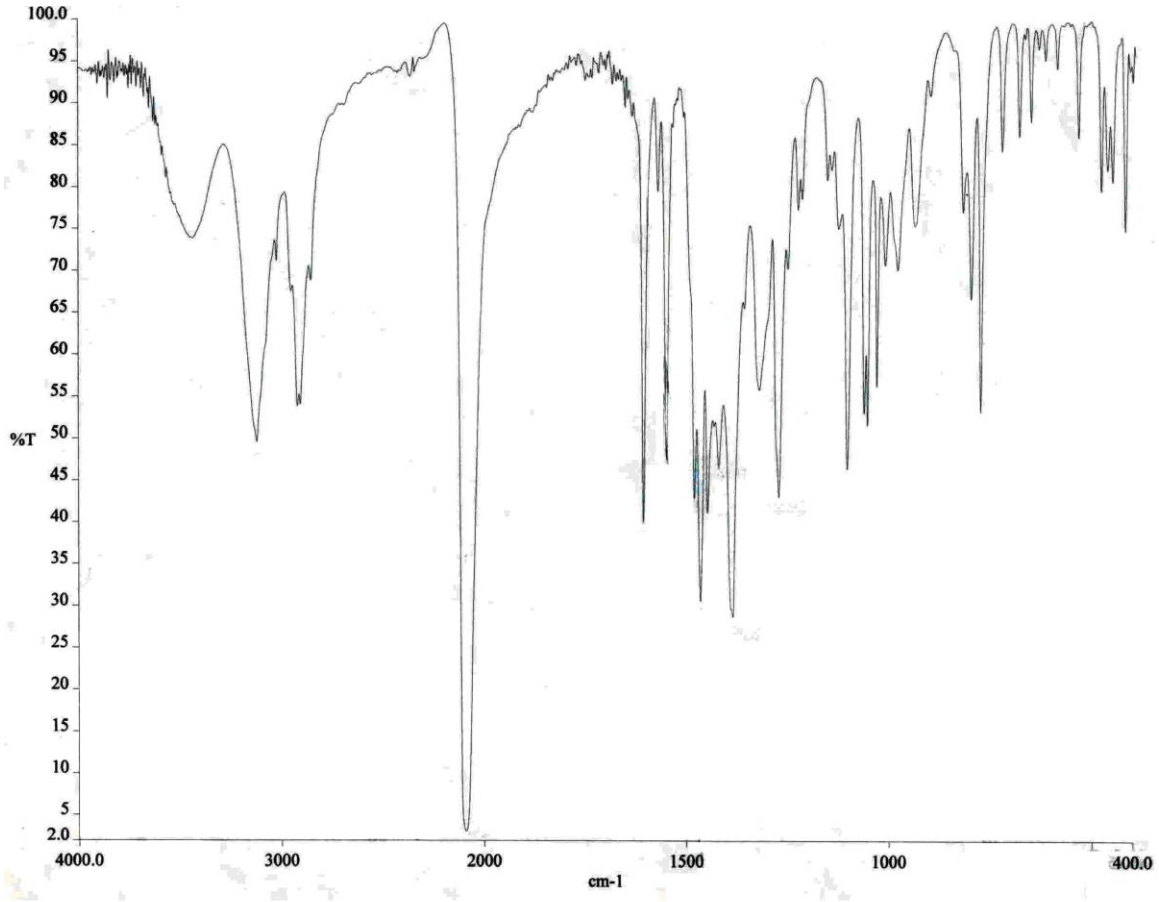

Fig. 3. IR spectra of [$Cu(NCS)_2L'$]

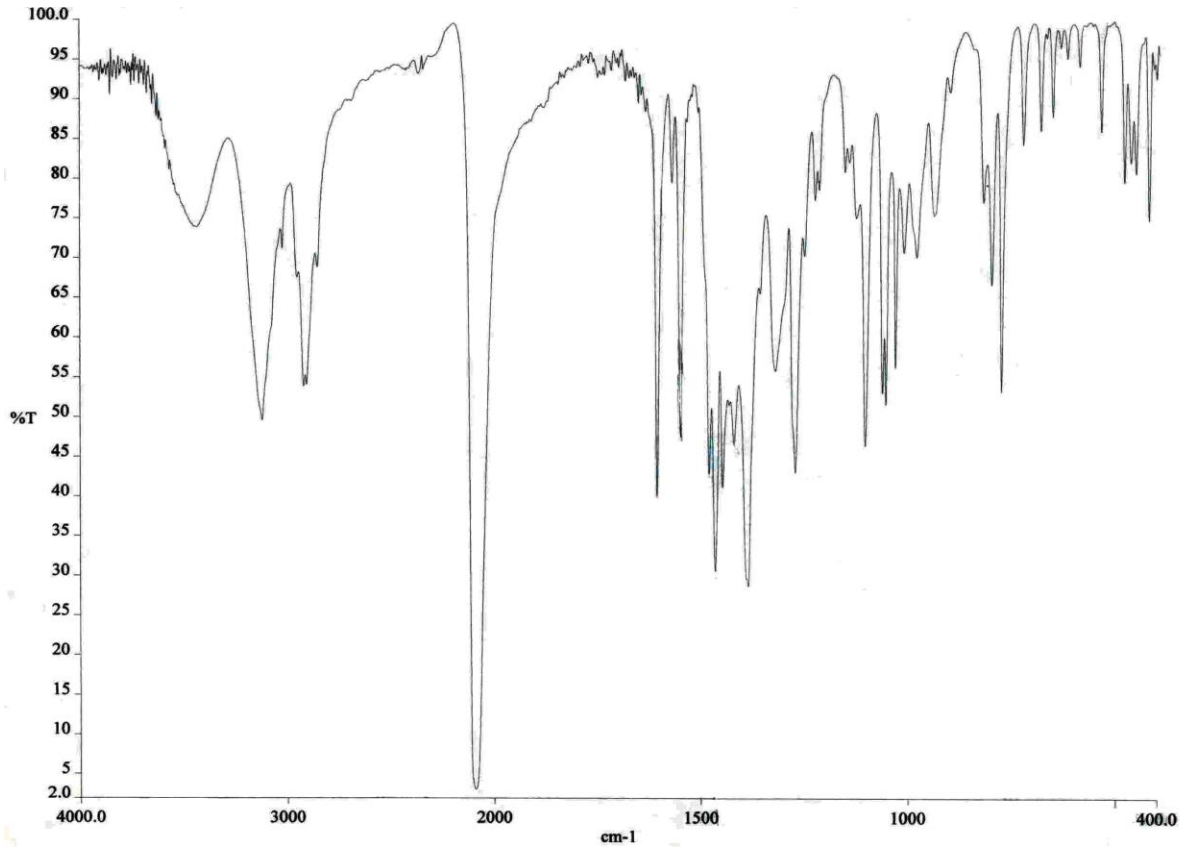

Fig. 4. IR spectra of $[CoL(SeCN)(H_2O)]ClO_4$

3.3 Description of crystal structure of $[Cu(NCS)_2L']$.

The molecular structure of the complex and the atom-labeling scheme are shown in Fig. 5. Selected bond lengths and angles related to the metal coordination sphere for the structure are given in Table 2. The structure shows that two equatorial NCS^- ions are bonded to copper through nitrogen. Ligand *N*-(3,5-dimethylpyrazol-1-ylmethyl) aminomethylpyridine (L′) is tridentate and bonded through pyridine nitrogen (N1), secondary amine nitrogen (N2), and a pyrazole nitrogen (N4). Copper atom is five coordinate with distorted trigonal bipyramidal geometry with CuN_5 coordination environment being bond to three nitrogen from L′ and N5 and N6 from two NCS^-. The Cu–N2, Cu–N1 and Cu–N4 bond distances are 1.992, 1.999, and 1.981Å, respectively, while Cu–N5 (2.096Å) and Cu–N6 (2.012Å) from two NCS^- are approximately equal to each other. N6–C14–S2 of 177.9° is linear compared to N5– C13–S1 of 162.4°.

3.2. Description of crystal structure of complex $[Cu(NCS)L]PF_6$.

The molecular structure of the complex and the atom-labeling scheme is shown in Fig. 6. Selected bond lengths and angles related to metal coordination sphere for the structure are given in Table 2. The structure shows that the NCS^- ion is bonded to copper atom through nitrogen atoms. The ligand *N*,*N*-(3,5-dimethylpyrazol-1-ylmethyl)aminomethyl-pyridine (L) is tetradentate and has utilized all potential donor atoms-pyridine nitrogen (N1), tertiary nitrogen atom (N2), and two pyrazole nitrogen atoms (N4 and N6) for complex formation. Copper atom is five coordinate with distorted square pyramidal geometry CuN_5 environment being bond to four nitrogen atoms- pyridine nitrogen (N1), tertiary nitrogen atom N2, one pyrazole nitrogen atom N4 and N7 from NCS^- in the square plane and another pyrazole nitrogen atom N6 in the apical position. The bond distances in the square plane copper-nitrogen atoms are of Cu-N1, Cu-N2, Cu-N4 and Cu-N7 are 2.005, 2.062(3), 1.995(4) and 1.933(4) Å, respectively and are almost equal to each other. The apical Cu-N6 bond distance (2.468 Å) is longer than equatorial bond length. The bond angle N(7)-C(19)-S(1) is 176.6(4) which is almost linear but C(19)-N(7)-Cu(1) angle is 147.3(4) which means NCS^- is little away from the plane.

3.3. Electronic spectral analysis and magnetic susceptibility

The electronic spectra of the complexes were measured in CH_3CN. Very similar bands appear in both NCS^- and $NCSe^-$ complexes. Electronic spectral bands at higher wavelength (800–400 nm) are attributed to d–d transitions or metal-to-ligand charge transfer and spectral bands below 400 nm are due to intraligand charge transfer. Electronic spectra of complexes **1**, **6** and **7** in acetonitrile solution at room temperature exhibited a band 700, 669 and 668 nm, respectively which may be attributed to d-d transition [Fig7]. Similarily, for complexes **2** and **4**, weak spectral band appear at 535 nm and for complexes **3** and **5**, a weak band at 700 and 585 nm, respectively and a strong band at ~580 nm either due to d-d or metal to ligand charge transfer transition. Room temperature magnetic susceptibilities show one electron paramagnetism for **1, 6** and **7** [μ_{eff} ~1.80 BM], two electron paramagnetism for **2** and **4** [μ_{eff} ~2.88 BM], and three

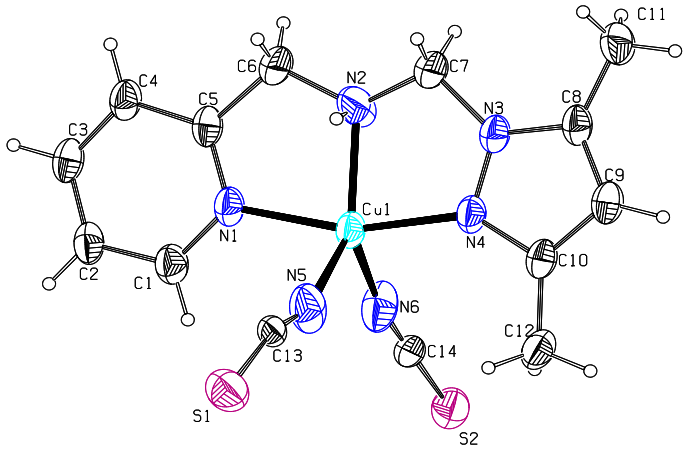

Fig.5. ORTEP diagram of complex [Cu(NCS)$_2$L′] with atom numbering scheme

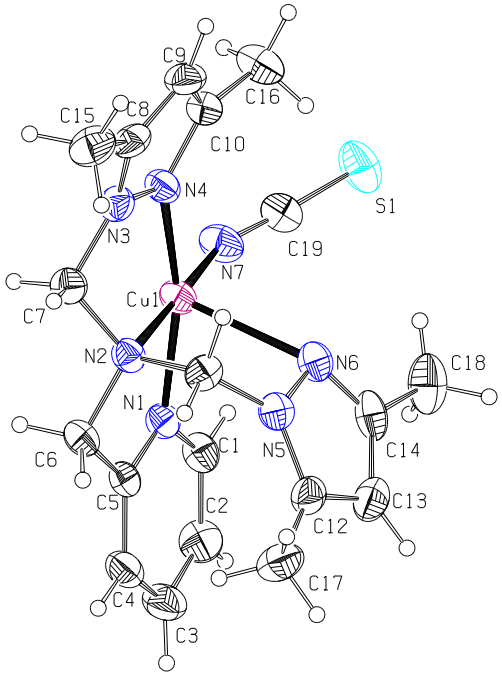

Fig. 6. ORTEP diagram of complex [Cu(NCS)(L)]PF_6 with atom numbering scheme

Table 2. Bond length (Å) and bond angles (˚) of complex **1** and complex **6**

Complex 1

Bond length		Bond angles	
Cu(1)-N(4)	1.981(6)	N(4)-Cu(1)-N(2)	80.5(3)
Cu(1)-N(2)	1.992(10)	N(4)-Cu(1)-N(1)	161.8(3)
Cu(1)-N(1)	1.999(6)	N(2)-Cu(1)-N(1)	81.3(3)
Cu(1)-N(6)	2.012(10)	N(4)-Cu(1)-N(6)	97.0(3)
Cu(1)-N(5)	2.096(10)	N(2)-Cu(1)-N(6)	126.4(5)
		N(1)-Cu(1)-N(6)	95.2(3)
		N(4)-Cu(1)-N(5)	97.3(3)
		N(6)-Cu(1)-N(5)	104.5(5)

Complex 2

Cu(1)-N(7)	1.933(4)	N(7)-Cu(1)-N(1)	96.78(16)
Cu(1)-N(4)	1.995(4)	N(4)-Cu(1)-N(1)	162.17(14)
Cu(1)-N(1)	2.005(4)	N(7)-Cu(1)-N(2)	178.31(15)
Cu(1)-N(2)	2.062(3)	N(4)-Cu(1)-N(2)	81.80(14)
Cu(1)-N(6)	2.468(4)	N(1)-Cu(1)-N(2)	82.28(14)
N(7)-Cu(1)-N(4)	98.93(16)	N(7)-Cu(1)-N(6)	102.20(16)
		N(4)-Cu(1)-N(6)	102.18(14)
		N(1)-Cu(1)-N(6)	82.58(13)
		N(2)-Cu(1)-N(6)	79.09(13)

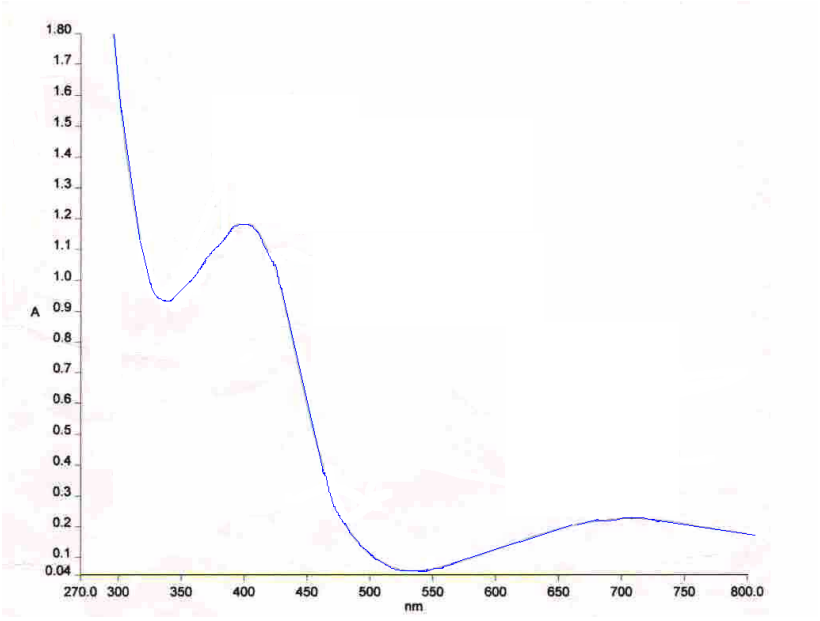

Fig. 7. Visible Spectra of $[Cu(NCS)_2L']$ in CH_3CN solution

electron paramagnetism for 3 and 5 [μ_{eff} ~3.90 BM]. This indicates that 2 and 4 and 3 and 5 have the same geometries.

4. Conclusion

Four mononuclear NCS^- complexes of the type $[M(NCS)_2L]$ (M = Ni^{+2}, Co^{+2}) (L= *N*,*N*-bis(3,5- dimethylpyrazol-1-ylmethyl)aminomethylpyridine), [CuL(NCS)]X (X = PF_6^- and ClO_4^-), $[Cu(NCS)_2L']$ (L′ = *N*-(3,5-dimethylpyrazol-1-ylmethyl)aminomethylpyridine), and two $NCSe^-$ containing complexes, $[ML(NCSe)(H_2O)](ClO_4)$ are reported. Compared to azido complexes, all NCS^- coordinated complexes are mononuclear. Crystal structure of $[Cu(NCS)_2L']$ shows that it has distorted trigonal bipyramidal geometry and $[CuL(NCS)]PF_6$ shows that copper has square pyramidal geometry.

Supplementary material

Crystallographic data for the structural analysis have been deposited with CCDC no. 784906 and 835975 for complexes **1** and **6,** respectively. Copies of this information can be obtained from The Director, CCDC, 12 Union Road, Cambridge, CB2 IEZ, UK (Email; deposit@ccdc.cam.ac.uk or www.http://www.ccdc.ac.uk).

References

1 J .Ribas, A. Escuer, M. Monfort, R. Vicente, R. Cortes, L. Lezama, R. Rojo. Coord. Chem. Rev., 1999, 1027, 193–195.

2 O. Kahn. Molecular Magnetism, VCH, New York 1993.

3 C.G. Pierpont, D.N. Hendrickson, D.M. Duggan, F. Wagner, E.K. Barefield. Inorg. Chem., 1975, 14, 604.

4 P. Chaudhuri, R. Wagner, S. Khanra, T. Weyhermuller. J. Chem. Soc., Dalton Trans., 2006, 4962 .

5 K.D. Karlin, Z. Tyeklar, Bioinorganic Chemistry of Copper, Chapman & Hall, New York 1993.

6 Z. Tyekla´ r, R.R. Jacobson, N. Wei, N.N. Murthy, J. Zubieta, K.D. Karlin. J. Am. Chem. Soc., 1984, 106, 2677.

7 W.G. Haanstra, W.A.J.W. van der Donk, W.L. Driessen, J. Reedijk, J.S. Wood, M.G.B. Draw. J. Chem. Soc., Dalton Trans., 1990, 3123.

8 N. Kitajima, T. Koda, S. Hashimoto, T. Kitagawa, Y. Morooka. J. Am. Chem. Soc., 1991, 113, 5664.

9 Z. Mahendrasinh, S.B. Kumar, E. Suresh, J. Ribas. Transition Met. Chem., 2010, 35, 757 .

10 R. Gupta, T.K. Lal, R. Mukherjee. Polyhedron, 2002, 21, 1245.

11 J.G. Haasnoot, W.L. Drissen, J. Reedijk. Inorg. Chem., 1984, 23, 2803.

12 T.L. Lal, R. Gupta, S. Mahapatra, R. Mukherjee. Polyhedron, 1999, 18, 1743.

13 R. Gupta, R. Mukherjee. Polyhedron, 2001, 20, 2545.

14 S.-C. Sheu, M.-J. Tien, M.-C. Cheng, T.-I. Ho, S.-M. Peng, Y.-C. Lin. J. Chem Soc., Dalton Trans., 1995, 3503.

15 U. Mukhopadhyay, I. Bernal, S.S. Massoud, F.A. Mautner. Inorg. Chim. Acta., 2004, 357, 3673.

16 A.Kovics, D. Nemcsok, G. Pokol, K, M. Szecenyi, V. M. Leovac, Z. K. Jacimovic, I. R. Evans, J. A. K. Howard, Z. D. Tomic, G. Giester, New J. Chem., 2005, 29, 833

17 G.M. Sheldrick. SAINT, 5.1 ed. Siemens Industrial Automation Inc., Madison, WI (1995).

18 G.M. Sheldrick. SADABS, Empirical Absorption Correction Program, University of Go¨ ttingen, Go¨ ttingen, Germany (1997).

19 G.M. Sheldrick. SHELXTL Reference Manual (Version 5.1), Bruker AXS, Madison, WI (1997).

20 G.M. Sheldrick. SHELXL-97: Program for Crystal Structure Refinement, University of Go¨ ttingen, Go¨ ttingen (1997).

21 S. Bhattacharyya, T.J.R. Weakley, M. Chaudhury. Inorg. Chem., 1999, 38, 633.

22 S. Bhattacharyya, T.J.R. Weakley, M. Chaudhury. Inorg. Chem., 1999, 38, 5453.

23 B. Barszcz, T. Glowiak, J. Jezierska, A. Tomkiewicz. Polyhedron, 2004, 23, 1309.

24 K. Nakamoto. Infrared and Raman Spectra of Inorganic and Coordination Compounds. Part B, Application in Coordination, Organometallic, and Bioinorganic Chemistry, John Wiley & Sons Inc., New York (1997).

Chapter IVA

Syntheses, Characterization, Structure and Magnetic Properties of Azido-Bridged Nickel(II) and Copper(II) complexes with Pyridylpyrazole ligand

Chapter IVA

Abstract

Two new binuclear azido bridged nickel(II) complexes, $[Ni_2(L)_2(N_3)_2](X)_2.2EtOH$ (X = ClO_4^-(**1**) and PF_6^- (**2**)) and three azido bridged copper(II) complexes, $[Cu_2(L)_2(N_3)_2](Y)_2$ (Y = ClO_4^- (**3**), PF_6^- (**4**) and BF_4^- (**5**)) have been synthesized and characterized by physico-chemical and spectroscopic methods. The crystal structures of $[Ni_2(L)_2(N_3)_2](ClO_4)_2.2EtOH$(**1**) and $[Cu_2L_2(N_3)_2](ClO_4)_2$ (**3**) complexes are reported. Each metal atom in the complexes has a MN_6 coordination environment with distorted octahedral geometry. Variable-temperature magnetic susceptibility measurements for Nickel(II) complex (**1**) show typical antiferromagnetic behavior with *J* value -84.5 ± 1.3 cm^{-1}, whereas Copper(II) (**3**) complex has no magnetic interactions.

.

1. Introduction

An important property of pseudohalide-bridged binuclear transition metal complexes is the appearance of exchange interactions between the two metal centers. Among the binuclear complexes, azido-bridged complexes have been extensively studied. This is because of the fact that azide ion (N_3^-) is a versatile bridging ligand [1] that can coordinate to metal ions either in the end-to-end (μ-1,3) or in the end-on (μ-1,1) modes [2–23] (Scheme 1). Among the azido-bridged Ni(II) complexes, it has been observed that μ-1,3-coordination gives antiferromagnetic (AF) coupling, whereas μ-1,1 coordination gives ferromagnetic (F) coupling. In the case of binuclear Ni(II) systems with double (μ-1,3) bridges, it has been observed in the literature that there is wide difference in the *J* values, from -47.5 to -90 cm^{-1} [24].

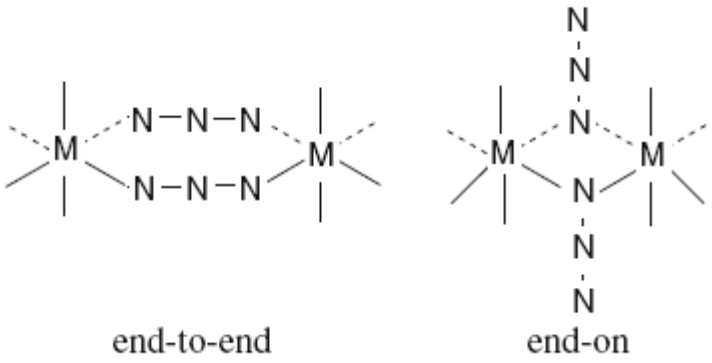

Scheme **1.** Bridging mode of metal-azide ions

As our interest was in new polynuclear complexes, we were interested in metal complexes containing pyrazole based ligands. This is because pyrazole-type ligands can have biological activity [25, 26] and their compounds serve as models for active sites in metalloproteins [27, 28]. The chemistry of pyrazole-containing mononuclear complexes toward several first row transition elements has been discussed in the literature [29–35]. Here, we report the synthesis, characterization, structure and magnetic properties of five new binuclear complexes, namely $[Ni_2(L)_2(N_3)_2](X)_2.2EtOH$ (X = ClO_4^- (**1**) and PF_6^- (**2**)) and $[Cu_2(L)_2(N_3)_2](Y)_2$ (Y = ClO_4^- (**3**), PF_6^- (**4**) and BF_4^- (**5**)), where L is *N*,*N*-bis(3,5-

dimethylpyrazol-1-ylmethyl)aminomethylpyridine), a newly synthesized and characterized tetradentate N_4-coordinating ligand.

2. Experimental

2.1. Materials and methods

The chemicals and solvents were of analytical grade and purchased from commercial sources. 2-(aminomethyl)pyridine (Aldrich), acetylacetone (GR, Loba, India), paraformaldehyde (GR, Loba, India), hydrazine hydrate (GR, Loba, India), sodium azide (Qualigens, India), $Cu(ClO_4)_2$. $6H_2O$ (Aldrich), $Ni(ClO_4)_2.6H_2O$ (Aldrich), NH_4PF_6 (99%, Aldrich), NH_4BF_4 (99%, Aldrich),CH_3CN (AR, Merck) were of reagent grade and used as received. *N*-(hydroxymethyl)-3,5-dimethylpyrazole was synthesized according to the reported method [36].

2.2 Synthesis of compounds

2.2.1 Synthesis of *N*,*N*-bis(3,5-dimethylpyrazol-1-ylmethyl) aminomethylpyridine (L)

The tetradentate *N*,*N*-bis(3,5-dimethylpyrazol-1-ylmethyl)aminomethylpyridine (L) ligand was synthesized and characterized procedure described in chapter II.

2.2.2**.** Synthesis of $[Ni_2(L)_2(N_3)_2](ClO_4)_2.2EtOH$ (1**)**

A solution of ligand L (0.65 g, 2 mmol) in ethanol (10 ml) was added to a stirred solution of $Ni(ClO_4)_2.6H_2O$ (0.73 g, 2 mmol) in ethanol (15 ml). After 10 min, a solution of sodium azide (0.26 g, 4 mmol) in ethanol (15 ml) was added slowly to the mixture. The mixture was stirred for 2 h, then the solution was filtered, and the filtrate was left to evaporate slowly. It was possible to obtain diffraction quality crystal after seven days. Yield 0.57 g. (50%) (based on Ni). Microanalysis; Found: C = 42.4, H = 5.4, N = 22.2%. Calc. for $Ni_2C_{40}H_{60}Cl_2N_{18}O_{10}$; C= 42.1; H = 5.3; N = 22.1%. IR (KBr pellet), cm^{-1}: $\nu_{asym}(N_3^-)$, 2,107, 2,057 vs; ν (C=C) + ν (C=N)/pyrazole ring, 1,604 s, 1,555 vs; ν_{asmy}(Cl–O), 1,091 vs; δ (O–Cl–O), 625 s.

2.2.3. Synthesis of $[Ni_2(L)_2(N_3)_2](PF_6)_2$ **(2)**

A solution of ligand L (0.65 g, 2 mmol) in ethanol (10 ml) was added to a stirred solution of $Ni(CH_3COO)_2.2H_2O$ (0.498 g, 2 mmol) in ethanol (15 ml). After 10 min, a solution of sodium azide (0.26 g, 4 mmol) in ethanol (15 ml) was added slowly to the mixture. After 10 min, ammonium hexaflourophosphate (0.326 g, 4 mmol) in little amount of water was added. The mixture was stirred for 2 h, then the solution was filtered and the filtrate was left to evaporate slowly. It was possible to obtain diffraction quality crystal after seven days. Yield 0.58 g. (51%) (based on Ni). Microanalysis; Found: C = 38.12, H = 4.3, N = 22.43%. Calc. for $Ni_2C_{36}H_{48}N_{18}P_2F_{12}$; C = 37.91; H = 4.21; N = 22.11%. IR (KBr pellet), cm^{-1}: ν (N_3^-), 2,073 vs; ν (C=C) + ν (C=N)/pyrazole ring, 1,609 s, 1,557 vs; ν(PF_6^-) 844 s.

2.2.4. Synthesis of $[Cu_2(L)_2(N_3)_2](ClO_4)_2$ **(3)**

A solution of ligand L (0.65 g, 2 mmol) in ethanol (10 ml) was added to a stirred solution of $Cu(ClO_4)_2.6H_2O$ (0.73 g, 2 mmol) in ethanol (15 ml). After 10 min, a solution of sodium azide (0.26 g, 4 mmol) in ethanol (15 ml) was added slowly to the mixture. The mixture was stirred for 2 h, then the solution was filtered, and the filtrate was left to evaporate slowly. It was possible to obtain diffraction quality crystal after seven days. Yield 0.53 g (50%) (based on Cu). Microanalysis; Found: C = 40.9, H = 4.6, N = 23.7%. Calc. For $Cu_2C_{36}H_{48}Cl_2N_{18}O_8$; C = 40.8; H = 4.5; N = 23.8%. IR (KBr pellet), cm^{-1}: ν (N_3^-), 2,073 vs; ν (C=C) + ν (C=N)/ pyrazole ring, 1,609 s, 1,557 vs; ν_{asmy}(Cl–O), 1,094 vs; δ(O–Cl–O), 625 s. UV–Vis (CH_3CN), λmax/nm (ε_{max}/mol^{-1} cm^{-1}): 655 (58), 424 (5,426), 279 (27,910).

2.2.5. Synthesis of $[Cu_2(L)_2(N_3)_2](PF_6)_2$ **(4)**

Complex (**4**) was prepared by the same procedure as for complex (**2**) with the exception of $Cu(CH_3COO)_2.H_2O$ was used instead of $Ni(CH_3COO)_2.2H_2O$. Yield 0.575 g. (50%) (based on Cu). Microanalyses; Found: C = 37.42, H = 4.23, N = 18.86%. Calc. For $Cu_2C_{36}H_{48}N_{18}P_2F_{12}$; C = 37.59; H = 4.17; N = 18.79%. IR (KBr pellet), cm^{-1}: ν (N_3^-), 2,073 vs; ν (C=C) + ν (C=N)/ pyrazole ring, 1,609 s, 1,557 vs; ν(PF_6^-) 843 s. UV–Vis (CH_3CN), λmax/nm (ε_{max}/mol^{-1} cm^{-1}): 657 (60), 420 (5,400), 279 (27,890).

2.2.6. Synthesis of $[Cu_2(L)_2(N_3)_2](BF_4)_2$ **(5)**

A solution of ligand L (0.65 g, 2 mmol) in ethanol (10 ml) was added to a stirred solution of $Cu(CH_3COO)_2.2H_2O$ (0.396 g, 2 mmol) in ethanol (15 ml). After 10 min, a solution of sodium azide (0.26 g, 4 mmol) in ethanol (15 ml) was added slowly to the mixture. After 10 min, ammonium tetrafluoroborate (0.208 g, 4 mmol) in little amount of water added slowly to the mixture. The mixture was stirred for 2 h, then the solution was filtered, and the filtrate was left to evaporate slowly. Yield 0.515 g. (50%) (based on Cu). Microanalysis; Found: C = 40.47, H = 4.87, N = 23.61%. Calc. For $Cu_2C_{36}H_{48}N_{18}B_2F_8$; C = 40.48; H = 4.80; N = 23.38%. IR (KBr pellet), cm^{-1}: $\nu(N_3^-)$, 2,073 vs; ν(C=C) + ν(C=N)/ pyrazole ring, 1,609 s, 1,557 vs; $\nu(BF_4^-)$, 1095 s. UV–Vis (CH_3CN), λ_{max}/nm (ε_{max}/mol^{-1} cm^{-1}): 650 (50), 421 (5,326), 279 (27,810).

2.3. Physical measurements

Elemental analyses were carried out using a Perkin-Elmer IA 2400 series elemental analyzer. IR spectra (400–4,000 cm^{-1}) were recorded on a Perkin-Elmer FT-IR spectrometer model RX1 using KBr pellets. UV–Vis spectra (190–900 nm) were recorded on a Perkin-Elmer spectrophotometer model Lambda 35 in acetonitrile solution. Cyclic voltammetry studies were carried out using a CH instrument model 600C. The cell system consisted of three electrodes: Pt rod as working electrode and Pt wire and Ag/AgCl as counter and reference electrodes, respectively. Approximately 0.1 M tetraethyl ammonium tetrafluoroborate was used as supporting electrolyte. ^1H NMR spectra were recorded on a Bruker AV-400 NMR instrument in $CDCl_3$ and ESR spectra were recorded on a Varian model E-112 ESR spectrometer in frozen acetonitrile solution. The magnetic susceptibility of a powder sample was carried out in the ‘‘Servei de Magnetoquimica (Universitat de Barcelona)’’ on polycrystalline samples (30 mg) with a Quantum Design SQUID MPMS-XL magnetometer working in the 2–300 K range. The magnetic field was 0.1 T. The contribution of the sample holder was determined separately in the same temperature range and magnetic field. The diamagnetic corrections were evaluated from Pascal’s constants.

2.4. Crystal data collection and refinement

The crystallographic data and details of data collection for compounds (**1**) and (**3**) are given in Table 1. Crystals of suitable size were selected from the mother liquor and immersed in partone oil, then mounted on the tip of a glass fiber and cemented using epoxy resin. Intensity data for both the crystals were collected using Mo-Kα X-ray (λ = 0.71073 Å) radiation on a Bruker SMART APEX diffractometer equipped with CCD area detector at 293 K. The data integration and reduction were processed with SAINT software [37]. An empirical absorption correction was applied to the collected reflections with SADABS software programs [38]. The structure was solved by direct methods using SHELXTL [39] and refined on F^2 by the full-matrix least-squares technique using the SHELXL-97 program package [40]. All non-hydrogen atoms were refined anisotropically till convergence was reached. Hydrogen atoms attached to the ligand moiety were either located from the difference Fourier map or stereochemically fixed.

3. Results and discussion

3.1. Synthesis

The ligand *N*,*N*-bis(3,5-dimethylpyrazol-1-ylmethyl)aminomethylpyridine (L) was synthesized as a viscous yellow liquid by the condensation reaction between 2 (aminomethyl) pyridine and *N*-(hydroxymethyl)-3,5-dimethylpyrazole in acetonitrile and characterized by physico-chemical and spectroscopic methods. The ligand possesses four potential donor sites, specifically two nitrogen donor atoms from the pyrazole rings, one nitrogen from the tertiary amine and one from the pyridine. The binuclear complexes were readily obtained in good yield by the reaction of L with the appropriate metal perchlorate hexahydrate and sodium azide in 1:1:2 mol ratio in ethanol. There was no change of structure even after addition of excess azide, and a binuclear double end-to-end azido-bridged complex was always obtained. The diffraction-quality crystals for structural studies were obtained by slow evaporation of the solutions. The complexes are moderately soluble in acetonitrile and ethanol but insoluble in dichloromethane and acetone. The two complexes gave satisfactory microanalytical data, and the crystal structures show that the complexes have two end-to-end azide ions bridged between the metal centers.

Table1. Crystallographic data for complexes of (1) and (3)

Chemical formula	$Ni_2C_{40}H_{60}Cl_2N_{18}O_{10}$	$Cu_2C_{36}H_{48}Cl_2N_{18}O_8$
Formula weight	1141.38	1058.90
Crystal Colour	Blue	Blue
Crystal Size (mm)	0.38 x 0.19 x 0.13	0.34 x 0.14 x 0.04
Temperature (K)	293(2)	100(2) K
Crystal System	Monoclinic	Monoclinic
Space Group	*P21/c*	C2/c
a(Å)	10.921(3)	28.996(2)
b(Å)	15.380(4)	11.5951(10)
c(Å)	16.175(5)	14.3321(12)
α(º)	90	90
β(º)	106.898(5)	110.2190(10)
γ(º)	90	90
Z	2	4
V(Å^3)	2599.4(13)	4521.6(7)
Density (Mg/m^3)	1.458	1.556
Absorption Coefficient(mm^{-1})	0.898	1.130
F(000)	1192	2184
Reflections Collected	13509	11890
Independent Reflections	5090	4435
$R_{(int)}$	0.0483	0.0402
Number of parameters	331	302
S(Goodness of Fit) on F2	1.069	1.145
Final R1 , *w*R2 (I>2σ(I)	0.0756/ 0.1857	0.0775/0.1642
Weighted R1,*w*R2(all data)	0.1068/ 0.2023	0.0891/0.1701

3.2. IR and UV-Vis spectroscopy

The IR spectra of the free ligand and complexes show strong bands in the region of 1,610–1,550 cm^{-1}, consistent with coordination of the pyrazole to the metals. Two strong bands at ca. 2,108 and 2,080 cm^{-1} are attributed to bridging azide ligands in all the complexes. The complexes **1** and **3** have two strong bands; one broad band around 1,091 cm^{-1} due to ν_{asmy}(Cl–O) and other sharp band at 625 cm^{-1} due to δ(O–Cl–O), confirming the presence of perchlorate as a counterion [44] [Fig. 1 and Fig. 2]. All the PF_6^- and BF_4^- containing complexes have one strong band around 844 and 1095 cm^{-1} due to $\nu_{asmy}(PF_6^-)$ and $\nu_{asmy}(BF_4^-)$, respectively. All other bands observed for the ligand are also present in the complexes. The UV–Vis spectrum of complex (**3, 4, 5**) was recorded in acetonitrile solution at room temperature. The spectrum exhibits a band at λ_{max} 695 nm, which may be attributed to the d–d transition [Fig. 3]. A second strong absorption band is observed at ca 424 nm and may be assigned to ligand- to-metal charge transfer. This type of spectrum has been previously assigned to copper(II) complexes having square pyramidal structure [45]. Bands below 400 nm is due to intraligand transitions.

3.3. Crystal structures

The molecular structure of the dimeric cationic moiety of Ni(II) complex (**1**) and the atom-labeling scheme are shown in Fig. 3. Selected bond lengths and angles related to the metal coordination sphere for the structure are given in Table 2. The structure shows that the two azide ions bridge two nickel(II) centers by adopting an end-to-end (μ-1,3) coordination mode. The ligand L is tetradentate, utilizing all potential donor atoms. Each nickel atom is six coordinated with distorted octahedral environment and is bonded to four nitrogen atoms- pyridine nitrogen (N6), tertiary amine nitrogen (N3) and the two nitrogen atoms (N7 and N9a) from the bridging azide ligands at the basal position-plus the two pyrazole nitrogen atoms (N1 and N5) at the axial positions. In the basal plane, the bond distances of Ni–N3, Ni–N6, Ni–N7 and Ni–N9a are 2.147, 2.072, 2.126 and 2.045 Å, respectively. The axial bond lengths Ni–N1 (2.095 Å) and Ni–N5 (2.080 Å) are

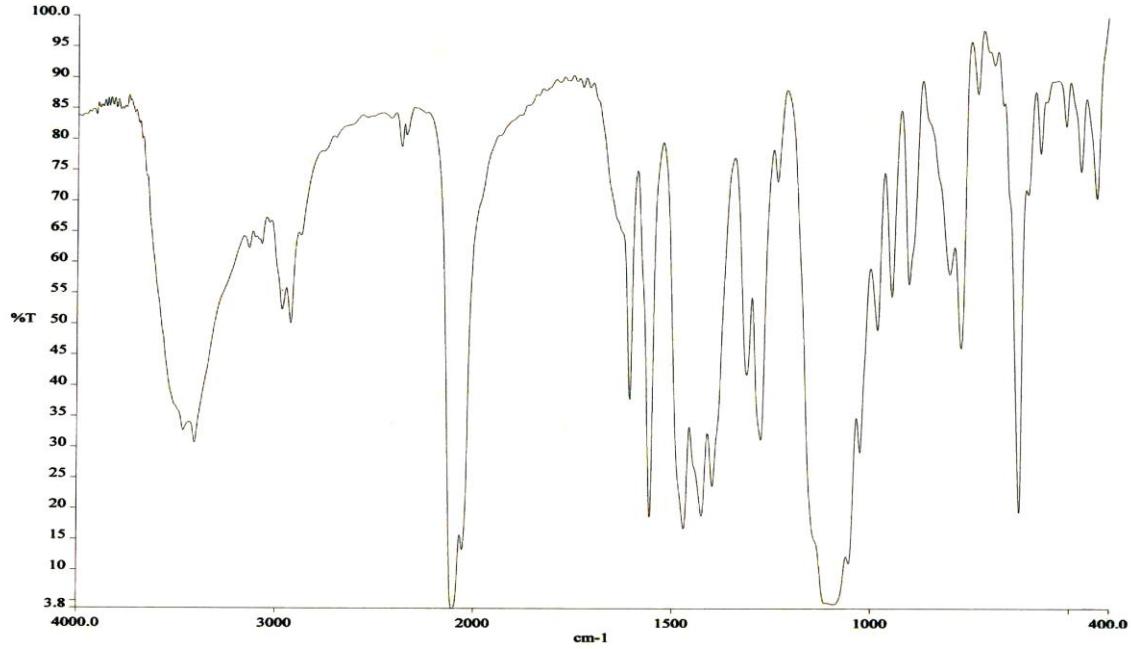

Fig. 1. IR Spectra of $[Ni_2L_2(N_3)_2](ClO_4)_2.2C_2H_5OH$

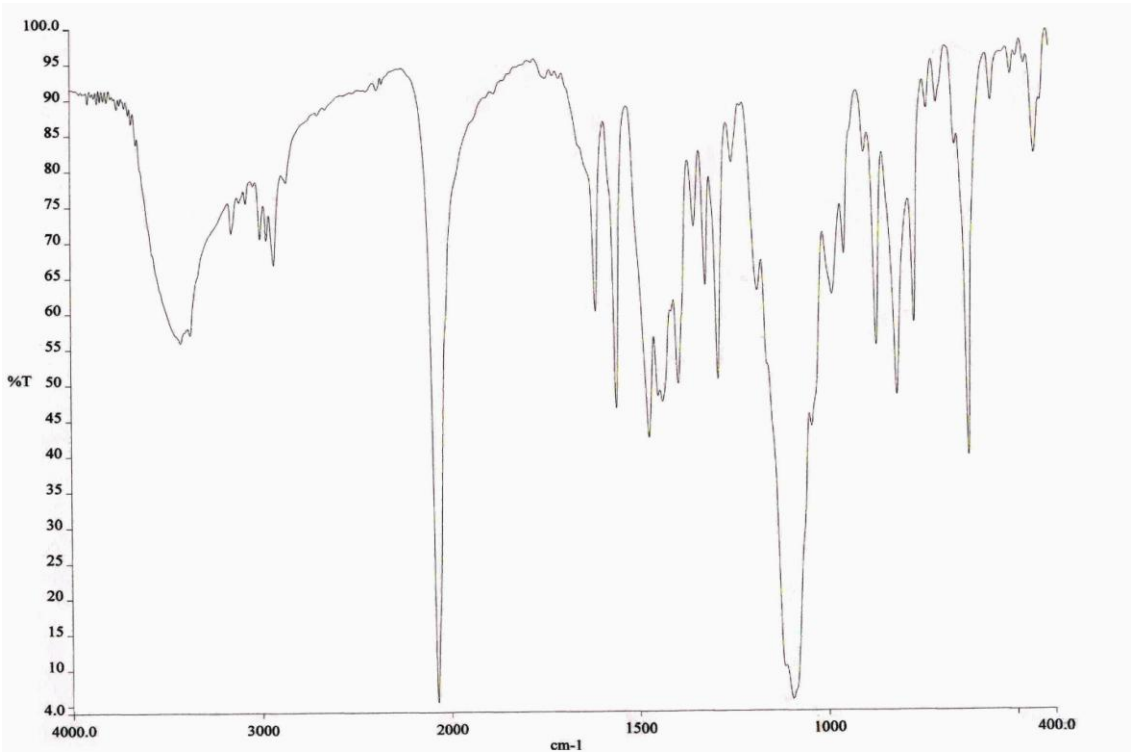

Fig. 2. IR spectra of $[Cu_2L_2(N_3)_2](ClO_4)_2$

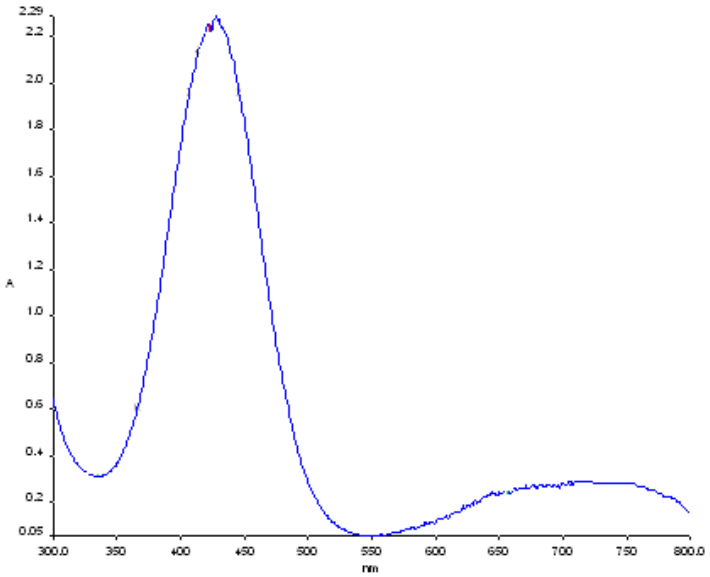

Fig. 3. UV-VIS spectra of $[Cu_2L_2(N_3)_2](ClO_4)_2$

approximately equal. The end-to-end azide bridge is linear with an N7–N8–N9 angle of 176.7(5)°. The N(8a)–N(9a)–Ni(1) angle of 137.6(4)° differs considerably from N(8)–N(7)–Ni(1) of 120.1(3)°.The Ni⋯Ni distance is 5.060 Å. This is consistent with the structural results obtained for other end-to-end azido bridging complexes [41].

The molecular structure of the dimeric cationic moiety of complex (**3**) and the atom-labeling scheme are shown in Fig.4. Selected bond lengths and angles related to the metal coordination sphere for this structure are given in Table 2. The structure shows that the two azide ions bridge two copper(II) centers by adopting end-to-end (μ-1,3) coordination. Each copper atom is six coordinated with a distorted octahedral environment and is bonded to four nitrogen atoms; pyridine nitrogen (N1), tertiary amine nitrogen (N3), pyrazole nitrogen atoms (N4) and one bridging azide ion (N7) at the basal position and one pyrazole nitrogen atom (N6) and one bridging azide nitrogen (N9a) at the axial positions. In the basal plane, the bond distances of Cu–N1, Cu–N4, Cu–N2 and Cu–N7 are 2.009, 1.987(4), 2.007(4) and 1.962(4) Å, respectively. The axial bond lengths Cu–N6 (2.443 Å) and Cu–N9a (2.637 Å) are not equal and much higher than the basal plane bond length. The end-to-end azido bridge is linear with N7–N8–N9 angle of 175.5(5)°. The N8a–N9a–Cu(1) angle of 132.4(4)° differs considerably from N8–N7–

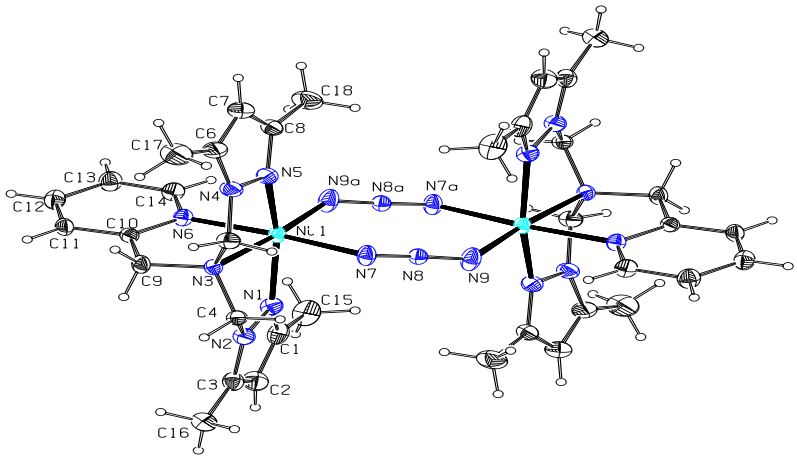

Fig. 4. ORTEP diagram depicting the dimeric cationic moiety of the complex 1 with crystallographic atom-numbering scheme (30% probability factor for the thermal ellipsoids)

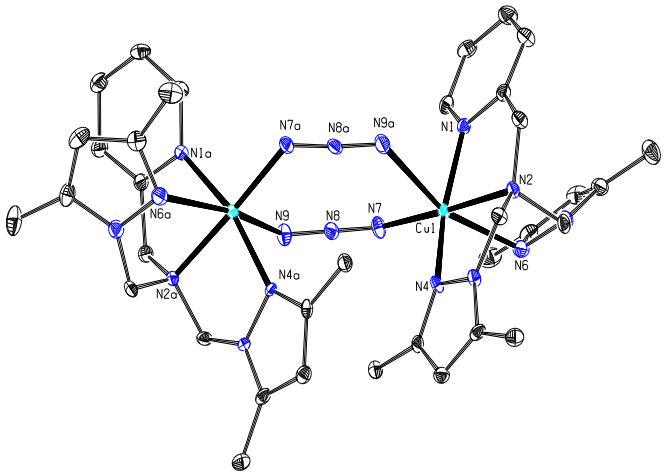

Fig. 5 ORTEP diagram depicting the dimeric cationic moiety of the complex 3 with crystallographic atom-numbering scheme (30% probability factor for the thermal ellipsoids)

Cu(1) of 121.2(4)º. The Cu···Cu distance is 5.323 Å. Cu(1) shows a distorted octahedron with four short equatorial Cu–N bonds (<2.08 Å) and two much longer axial Cu–N bonds (>2.4 Å). However, the Cu–N9a bond (2.673 Å) is very weak and does not contribute any bridging interaction. Hence, the local environment around Cu(1) might be best considered as distorted square pyramidal. A similar long axial bond distance in a copper complex with weak interactions has been reported in the literature [42, 43].

Table 2. Important bond lengths [Å] and angles [deg] for complexes **1** and **3**

$[Ni_2L_2(N_3)_2](ClO_4)_2.2C_2H_5OH$

Ni(1)-N(9)	2.045(5)	N(5)-Ni(1)-N(1)	158.62(16)
Ni(1)-N(6)	2.072(4)	N(9)-Ni(1)-N(3)	173.97(16)
Ni(1)-N(5)	2.080(4)	N(9)-Ni(1)-N(1)	101.7(2)
Ni(1)-N(1)	2.095(4)	N(6)-Ni(1)-N(5)	89.77(15)
Ni(1)-N(7)	2.126(4)	N(9)-Ni(1)-N(5)	99.5(2)
Ni(1)-N(3)	2.147(4)	N(9)-Ni(1)-N(6)	92.50(16)

$[Cu_2L_2(N_3)_2](ClO_4)_2$

Cu(1)-N(7)	1.962(4)	N(7)-Cu(1)-N(4)	100.96(18)
Cu(1)-N4)	1.987(4)	N(7)-Cu(1)-N(1)	95.40(18)
Cu(1)-N(1)	2.009(4)	N(4)-Cu(1)-N(1)	162.45(17)
Cu(1)-N(2)	2.007(4)	N(7)-Cu(1)-N(2)	177.14(18)
Cu(1)-N(6)	2.443(5)	N(8)- N(7)- Cu(1)	121.2(4)
N(7)-N(8)	1.191(6)	N(9)- N(8)-N(7)	175.5(5)

3.4. Cyclic Voltammetry and EPR data

The electrochemical behavior of complexes $[Cu_2L_2(N_3)_2](Y)_2$ (**3, 4, 5**) has been examined by cyclic voltammetry using platinum electrodes in acetonitrile solution (containing 0.1

M tetraethyl ammonium tetrafluoroborate as supporting electrolyte) in the potential range -1.6 to + 1.6 V versus Ag/AgCl reference electrode. It shows a reduction process ($E_{1/2}$ ~ -0.43 V) corresponding to a Cu(II)/Cu(I) electron transfer. The peak potential separation (ΔE_p) is 160 mV at a scan rate 100 mVs^{-1}, indicating quasi-reversible one-electron transfer [Fig. 6].

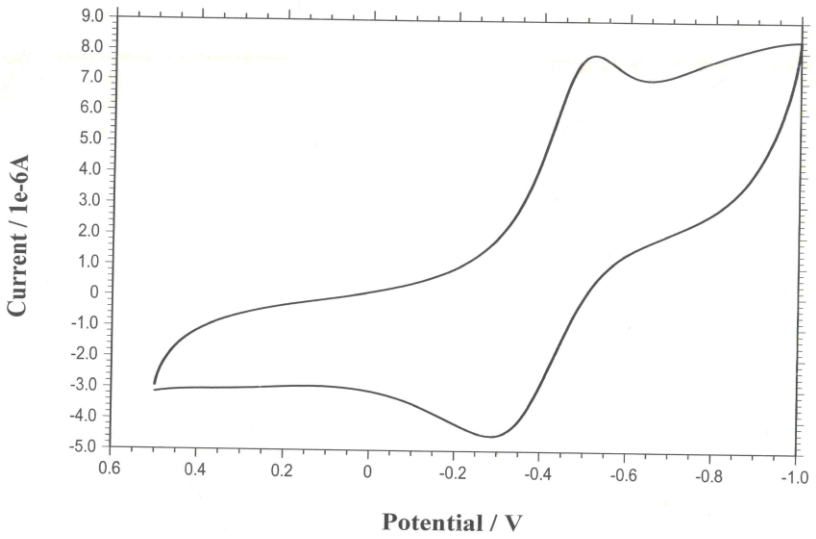

Fig.6. Cyclic voltammograms of $Cu_2L_2(N_3)_2](Y)_2$ (conc. 1 x 10^{-3}M) in MeCN solution of 0.1 M tetraethyl ammonium tetrafluoroborate , using platinum electrode., scan rate 100 mVs^{-1}

The X-band EPR spectrum of complex $[Cu_2L_2(N_3)_2](ClO_4)_2$ in frozen acetonitrile solution (78 K) exhibited a typical four-line splitting pattern with g_{II} = 2.237 and $g_{\perp}$ = 2.022 due to interaction of the unpaired electron with the nuclear spin of the copper nucleus (^{63,65}Cu: I = 3/2). The observed feature $g_{II}>g^{\perp}$ is diagnostic of a pseudotetragonal site symmetry for copper(II) (Fig.7).

3.5. Magnetic properties

The temperature dependence of the magnetic property of complex (1), shown as a plot of $\chi_M T$ versus T plot (χ_M is the molar magnetic susceptibility for two nickel(II) ions), and the reduced magnetization data as M/Nμ_B versus H at 2 K are shown in Fig. 8. The value of $\chi_M T$ at 300 K is close to 2.00 cm^3 mol^{-1}K, which is lower than that expected for two

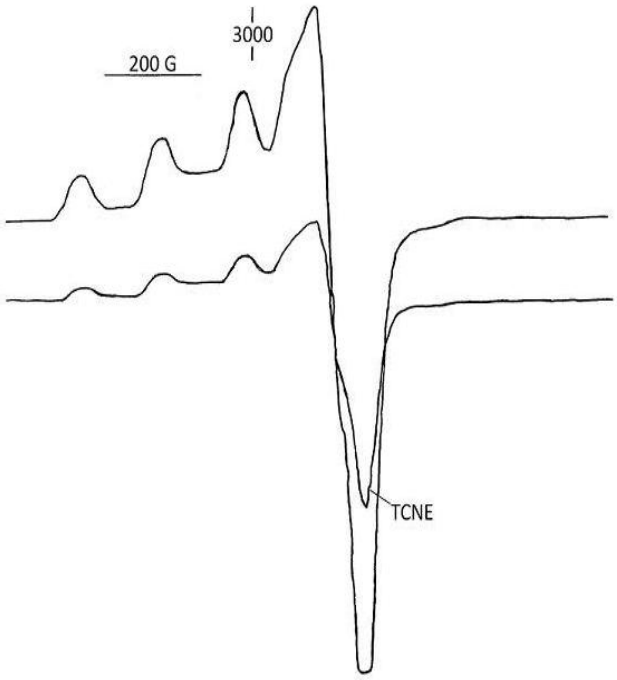

Fig. **7**.X-Band EPR spectrum of $[Cu_2L_2(N_3)_2](ClO_4)_2$in CH_3CN at 78 K

magnetically isolated spin triplets (g > 2.00). Starting from room temperature, the $\chi_M T$ values decrease with decreasing temperature, reaching a very small value (0.3 cm^3 mol^{-1} K) at 2 K. This magnetic behavior is characteristic of a significant intramolecular antiferromagnetic interaction between the two nickel(II) centers with the presence of some amount of paramagnetic impurities, which are clearly manifested at low temperature.

Complex (1) is, actually, a binuclear nickel(II) complex. From the Hamiltonian $H = -JS_1S_2$, the fit of the susceptibility data has been carried out applying the hypothesis of paramagnetic impurities (denoted by R). The best fit parameters obtained are J = -84.5 ± 1.3 cm^{-1}, g = 2.24 ± 0.01 and R = 0.03 (i.e. close to 3%). This J value agrees perfectly with data reported in the literature for $[Ni(NNN)_2Ni]$ entities in which the dihedral [Ni(NNN)Ni] angle δ is the dominant factor; the more planar the structure (i.e. dihedral angle δ close to 0°), the more antiferromagnetic is the coupling. In complex (**1**), this dihedral angle is small, 19.17°, so the J value can vary -40 to -90 cm^{-1} according to the literature [24]. The reduced molar magnetization at 2 K clearly corroborates the influence

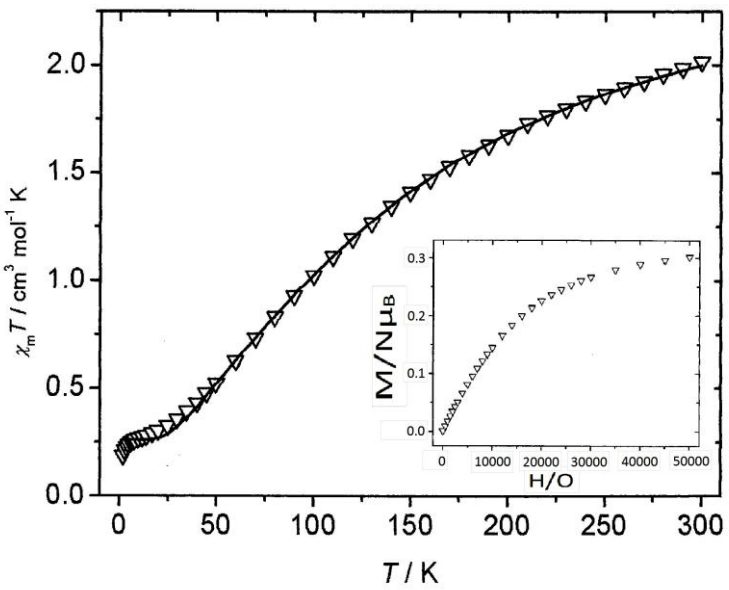

Fig. **8.** Temperature dependence of the magnetic moment (χ_m vs *T*) of the complex **1**. The *solid lines* represent the best fit of the data. [*onset*] A plot of the reduced magnetization ($M/N\mu_B$ vs. H) at 2 K of complex(**1**).

of the antiferromagnetic character: the $M/N\mu_B$ plot clearly lies below the theoretical Brillouin function for g = 2.2. In fact, this theoretical value should be close to 4 $N\mu_B$. Variable temperatures magnetic behavior of complex **2** was not measured but we expect magnetic behavior of complex **2** will be same type as that of complex **1**.

The temperature dependence of the magnetic properties of complex (3), shown as a plot of $\chi_M T$ versus *T* plot (χ_M is the molar magnetic susceptibility for two copper(II) ions) and the reduced magnetization data as $M/N\mu_B$ versus H at 2 K are shown in Fig.9. Starting from room temperature, the $\chi_M T$ values showed no change in magnetic susceptibility with decreasing temperature, remaining constant except at very low temperature. This magnetic behavior is characteristic of a mononuclear copper complex, and there is no noticeable magnetic interaction ($J = 0$) between the two copper(II) atoms. This is due to weak interaction between azido N(9) and Cu(1), as indicated by the longer Cu(1)–N(9) distance. So, the local environment around Cu(1) might be best considered as distorted square pyramidal.

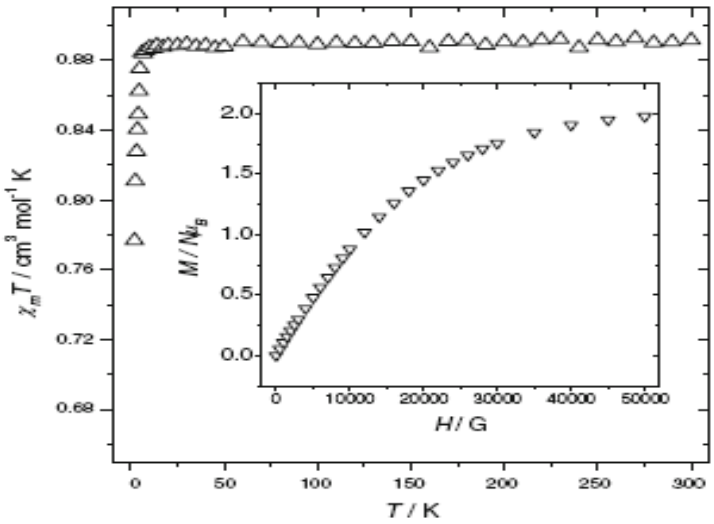

Fig.**9**. Temperature dependence of the magnetic moment (χ_m vs *T*) of the complex **3**. The *solid lines* represent the best fit of the data. [*onset*] A plot of the reduced magnetization (M/Nμ_B vs. H) at 2 K of complex 3.

4. Conclusion

We have described synthesis and characterization of five new binuclear azido bridged nickel(II) and copper(II) complexes with tetradentated ligand *N*,*N*-bis(3,5-dimethylpyrazol-1-ylmethyl)aminomethylpyridine. The variable-temperature magnetic study of $[Ni_2L_2(N_3)_2](ClO_4)_2.2C_2H_5OH$ complex shows antiferromagnetic behavior at low temperature with J = -84.5 ± 1.3 cm^{-1}, but $[Cu_2L_2(N_3)_2](ClO_4)_2$ complex shows behavior typical of mononuclear copper complexes with distorted square pyramidal geometry and therefore has no magnetic interactions.

Supplementary materials

Crystallographic data for the structural analysis have been deposited with the Cambridge Crystallographic data center, CCDC 734805 and CCDC 771329 for complex (**1**) and complex (**3**), respectively. Copies of this information may be obtained free of charge from the Director, 12 Union Road, Cambridge, CB2 1EZ, UK; (fax: +44-1223-336033; e-mail: deposit@ccdc.cam.ac.uk or www: http://www. ccdc.cam.ac.uk).

References

1 Ribas J, Monfort M, Ghosh BK, Solans X Angew Chem Int Ed Engl, 1994, 33: 2087. doi:10.1002/anie.199420871

2 Ribas J, Monfort M, Diaz C, Basto C, Solans X Inorg Chem, 1993, 32:3557. doi:10.1021/ic00068a029

3 Ribas J, Monfort M, Ghosh BK, Cortes R, Solans X, Font-Bardia M Inorg Chem, 1996, 35:864. doi:10.1021/ic9510573

4 Goher MA, Escuer A, Mautner FA, Al-Salem NA Polyhedron, 2002, 21:1876. doi:10.1016/s0277-5387(02)01061

5 Zhang Z-H, Bu X-H, Ma Z-H, Bu W-M, Tang Y, Zhao Q-H Polyhedron, 2000, 19:1559. doi:10.1016/s0277-5387(00)00411-3

6 Liu G-F, Ren ZG, Li H-X, Chen Y, Li Q-H, Zhang Y, Lang J-P Eur J Inorg Chem, 2007, 35:5511. doi:10.1002/ejic.200700657

7 Tandon SS, Bunge SD, Rakosi R, Xu Z, Thompson LK J Chem Soc Dalton Trans, 2009, 33:6536. doi:10.1039/b903617b

8 Monfort M, Resino I, Ribas J, Solans X, Font-Bardia M, Stockli- Evans H New J Chem, 2002, 11:1601. doi:10.1039/b205404c

9 Maji TK, Mukherjee PS, Mostafa G, MAllah T, Cano-Boquera J, Caudhury NR Chem Commun, 2001, 11:1012. doi:10.1039/b100529o

10 Mukherjee PS, Dalai S, Mustafa G, Lu T-H, Rentschler E, Raychaudhury NR New J Chem, 2001, 9:1203. doi:10.1039/b104596m

11 Biani FD, Ruiz E, Cano J, Novoa JJ, Alvarez S Inorg Chem, 2000, 39:3221. doi:10.1021/ic000005x

12 Wang X-T, Wang X-H, Wang Z-M, Gao S Inorg Chem,2009, 48:1301. doi:10.1021/ic801505a

13 Chaudhuri P, Wagner R, Khanra S, Weyhermuller T J Chem Soc Dalton Trans, 2006, 4962. doi: 10.1039/b610308a

14 Chaudhuri P, Weyhermuller T, Bill E, Weighardt K Inorg Chim Acta, 1996, 252:195. doi:10.1016/s0020-1693(96)05314-5

15 Li L, Liao D, Jiang Z, Monesca ReyP Inorg Chem, 2006, 45:7665. doi:10.1021/ic0606429

16 Konar S, Saha S, Mallah T, Okamoto K-I Inorg Chem, 2004, 43:840. doi:10.1021/ic034347p

17 Song Y, Massera C, Roubeau O, Gamez P, Maria A, Lanfredi AMM, Reedijk J Inorg Chem, 2004, 43:6842. doi:10.1021/ic049317g

18 Karmakar TK, Chandra SK, Ribas J, Mostafa G, Lu TH, Ghosh BK Chem Commun, 2002, 2364. doi: 10.1039/b205375f

19 Liu F-C, Zhao J-P, Hu B-W, Zeng Y-F, Ribas J, Bu X-H J Chem Soc Dalton Trans, 2010, 39:1185. doi:10.1039/b915616j

20 Bai S-Q, Gao E-Q, He Z, Fang C-J, Yau C-H New J Chem, 2005, 29:935. doi:10.1039/b418239a

21 Miao ZX, Li MX, Shao M, Liu HJ Inorg Chem Commun, 2007, 10:1117. doi:10.1016/j.inoche.2007.06.014

22 Koner S, Saha S, Okamoto K-I, Tuchagues J-P Inorg Chem, 2003, 42:4668. doi:10.1021/ic020526f

23 Song XY, Li W, Li LC, Liao DX, Jiang ZH Inorg Chem Commun, 2007, 10:567. doi:10.1016/j.inoche.2007.01.028

24 Ribas J, Escuer A, Monfort M, Vicente R, Cortes R, Lezama L, Rojo T Coord Chem Rev, 1999, 193–195:1027. doi:10.1016/ s0010-8545(99)00051-X

25 Sridhar R, Perumal PT, Etti S, Shanmugam G, Ponnuswamy MN, Prabavathy V, Mathivanna RN Bioorg Med Chem Lett, 2004, 14:6035. doi:10.1016/j.bmcl.2004.09.066

26 Jain AK, Moore SM, Yamaguchi K, Eling TE, Back SJ J Pharmacol Exp Ther, 2004, 311:885. doi:10.1134/jpet.104.070664

27 Haanstra WG, Donk WAJWV, Drissen WL, Reedijk J, Wood JS, Drew MGB J Chem Soc Dalton Trans, 1990, 3123. doi: 10.1039/DT9900003123

28 Sorrell TN, Vankai VA, Garrity ML Inorg Chem, 1991, 30:207. doi:10.1021/ic00002a014

29 Bouwman E, Driessen WL, Reedijk J Inorg Chem, 1985, 24:4730. doi:10.1021/ic00220a059

30 Blonk HL, Driesen WL, Reedijk J J Chem Soc Dalton Trans, 1985, 1699. doi: 10.1039/DT9850001699

31 Veldhuis JBJ, Drissen WL, Reedijk J J Chem Soc Dalton Trans, 1986, 537. doi: 10.1039/DT9860000537

32 Hulsbergen FB, Driessen WL, Reedijk J, Verschoor GC Inorg Chem, 1984, 23:3588. doi:10.1021/ic00190a031

33 Sheu S-C, Tien M-J, Cheng M-C, Ho T-I, Peng S-M, Lin Y-C J Chem Soc Dalton Trans, 1995, 3503. doi: 10.1016/DT99 50003503

34 Barszcz B, Glowiak T, Jezierska J, Tomkiewicz A Polyhedron, 2004, 23:1309. doi:10.1016/j.poly.2004.01.024

35 Kovacs A, Nemesok D, Pokol G, Szecsenyi KM, Leovac VM, Jacimovic ZK, Evans IR, Howard JAK, Tomic ZD, Giester G New J Chem, 2005, 29:833.

36 Driessen WL Recl Trav Chim Pays-Bas, 1982, 101:441

37 Sheldrick GM (1995) SAINT 5.1 ed. Siemens Industrial Automation Inc, Madison WI

38 SADABS (1997) empirical absorption correction program. University of Go¨ttingen, Go¨ttingen, Germany

39 Sheldrick GM (1997) SHELXTL reference manual: version 5.1. Bruker AXS, Madison, WI

40 Sheldrick GM, SHELXL-97: program for crystal structure refinement. University of Go¨ttingen: Go¨ttingen

41 Pierpont CG, Hendrickson DN, Duggan DM, Wagner R, Barefield FEK Inorg Chem, 1975, 14:604. doi:10.1021/ic50145a034

42 Liu J-C, Fu D-G, Zhuang J-Z, Duan C-Y, You X-Z J Chem Soc Dalton Trans, 1999, 2337. doi: 10.1039/a900619b

43 Matsumoto OS, Nakatsuka K, Mori W, Suzuki S, Nakahara A, Nakao Y J Chem Soc Dalton Trans, 1985, 2095. doi: 10.1039/ DT9850002095

44 Nakamoto K (1978) Infrared and Raman Spectra of Inorganic and Coordination Compounds, 3rd edn. Wiley Interscience, New York

45 Bhattacharyya S, Kumar SB, Dutta SK, Tiekink ERT, Chaudhury M Inorg Chem, 1996, 35:1967. doi:10.1021/ic950594k

CHAPTER IV B

Syntheses, Characterization, Structure and Magnetic Properties of Cyanate bridged Nickel(II) and Copper(II) complexes with Pyridylpyrazole ligand

Chapter IV B

Abstract

Binuclear cyanate bridged nickel(II) complexes $[Ni(L)(NCO)]_2(X)_2$ (X = PF_6^-(**1**) and BF_4^- (**2**)) and copper(II) complexes $[Cu(L)(NCO)]_2(Y)_2$ (Y = PF_6^- (**3**) and BF_4^- (**4**)), where L is *N*,*N*-bis(3,5-dimethylpyrazol-1-ylmethyl)aminomethylpyridine, a tetradentate N_4-coordinated ligand have been synthesized and characterized by microanalysis and physico-chemical method. The structures of complexes **1** and **3** have been studied by single crystal X-ray diffraction analysis. The structure analysis reveals that both nickel(II) and copper(II) center are coordinated in distorted octahedral fashion and coordination mode of cyanate ligand is end-to-end (μ-1,3) for complex **1** but it is double end-on (μ -1,1) mode for complex **3**. The variable temperature magnetic susceptibility data, measured from 2 to 300 K, show weak antiferromagnetic interaction with *J* value -6.2(1) cm^{-1} for complex **1**, whereas complex **3** has very weak ferromagnetic interaction with *J* value +0.5(1) cm^{-1}.

1. Introduction

The important aspect of the pseudohalides bridged transition metal complexes is that pseudohalide can coordinate with metal ions in different ways namely end-to-end and end-on bridging mode. Among the pseudohalides, azide bridged complexes have been studied widely because azide is a versatile ligand [1]. Among the thiocyanate and cyanate bridged complexes, number of cyanate bridged complexes is less as compared to thiocyanate bridged complexes. The cyanate ion, like azide ion, can coordinate with end-to-end (μ-1,3) and end-on (μ-1,1) coordination mode (Scheme1) and also forms single or double bridged binuclear complexes. The number of cyanate bridged polynuclear copper(II) complexes reported in the literature is less. There are only few reported end-to-end cyanate bridge binuclear copper(II) complexes [2–4] and most of the studied cyanate-bridged binuclear copper(II) complexes have end-on coordination mode [5–16]. Among these, there are only two oxygen coordinated end-on cyanate bridged complexes reported in the literature [5, 13]. All the reported end-on cyanate bridged copper(II) complexes show weak ferromagnetic behavior. In comparison to cyanate bridged polynuclear copper(II) complexes, the number of cyanate bridged polynuclear nickel(II) complexes is scare and only few binuclear complexes have been structurally characterized. It has been found that cyanate ion coordinated with nickel(II) in end-to-end coordination mode and the complexes are weakly antiferromagnetic (AF) [17–19]. In an effort to synthesis polynuclear pseudohalide bridged complexes, we report here synthesis, characterization and structure of double cyanate bridged binuclear complexes $[Ni(L)(NCO)]_2(X)_2$ (X = PF_6^- (**1**) and BF_4^- (**2**)) and $[Cu(L)(NCO)]_2(Y_2)$ (Y = PF_6^-(**3**) and BF_4^-(**4**)), where L is *N*,*N*-bis(3,5-dimethylpyrazol-1-ylmethyl)aminomethylpyridine, a tetradentate N_4-coordinated ligand. Here, cyanate ion bridged as double end-to-end (μ-1,3) coordination mode in complexes **1** and **2**, whereas double end-on (μ-1,1) mode in complex **3** and **4**. Magnetic properties of the two complexes **1** and **3** have been discussed in detail.

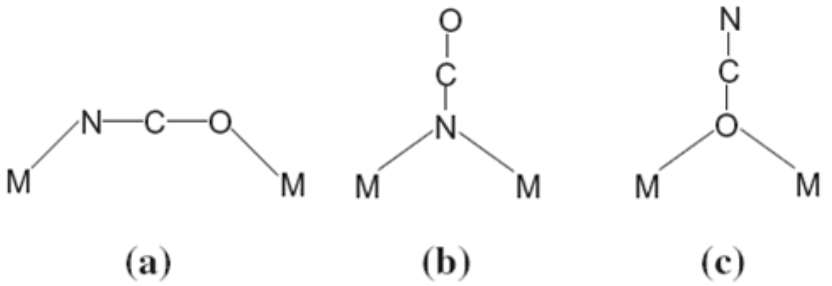

Scheme 1. Bridging mode of cyanate ion

2. Experimental

2.1. Materials and methods

All the chemicals and solvents were of analytical grade reagents. 2-(aminomethyl)pyridine (Aldrich), hydrazine hydrate (GR, Loba, India), acetylacetone (GR, Loba, India), paraformaldehyde (GR, Loba, India), copper acetate and nickel acetate (Loba, India), sodium cyanate (Qualigens, India), NH_4BF_4, NH_4PF_6 (Aldrich) were of reagent grade and used as received. *N*,*N*-bis(3,5-dimethylpyrazol-1-ylmethyl) aminomethylpyridine (L) was synthesized and characterized by published procedure [20]. Solvents used in this study were purified following the standard procedures.

2.2. Synthesis of $[Ni(L)(NCO)]_2(X)_2$ X = PF_6^- (**1**) and BF_4^-(**2**)

A methanol solution (10 mL) of ligand L (0.162 g, 0.5 mmol) was added to a stirring solution of $Ni(CH_3COO)_2.4H_2O$ (0.125 g, 0.5 mmol) in methanol (10 mL) drop wise. After 10 min, NaNCO (0.035 g, 0.5 mmol) in minimum quantity of water was added. Finally, NH_4PF_6/NH_4BF_4 (0.5 mmol) in minimum quantity of water was added and stirring was continued for another 2 h. The solution was filtered and the filtrate was kept for slow evaporation. Blue crystals were obtained after 7 days.

Analytical data of $[Ni(L)(NCO)]_2(PF_6)_2$ **(1)**. Yield 0.130 g (48%). Anal. Calc. for $C_{38}H_{48}F_{12}N_{14}Ni_2O_2P_2$: C, 39.99; H, 4.20; N, 17.18%. Found: C, 39.94; H, 4.10; N, 17.57%. IR (KBr pellet) cm^{-1}; ν(NCO^-), 2243 vs; ν(C=C) + ν(C=N)/pyrazole ring, 1607 s, 1556 vs; ν(PF_6^-), 844 vs.

Analytical data of $[Ni(L)(NCO)]_2(BF_4)_2$ **(2).** Yield 0.120 g (48%).Anal. Calc. For $C_{38}H_{48}F_8N_{14}Ni_2O_2B_2$: C, 44.57; H, 4.69; N, 19.75. Found: C, 44.12; H, 4.72; N, 19.85 %. IR (KBr pellet) cm^{-1}; ν(NCO^-), 2243 vs; ν(C=C) + ν(C=N)/pyrazole ring, 1607 s, 1556 vs; ν(PF_6^-), 1043 vs.

2.3. Synthesis of $[Cu(L)(NCO)]_2(Y)_2$ Y = PF_6^- (**3**) and BF_4^- (**4**)

To a methanol solution of $Cu(CH_3COO)_2.H_2O$ (0.108 g, 0.5 mmol), ligand L (0.162 g, 0.5 mmol) in methanol (10 mL) was added with stirring. After 15 min, NaNCO (0.035 g, 0.5 mmol) in minimum quantity of water was added drop wise with stirring. Finally, NH_4PF_6 (0.085 g, 0.5 mmol) in minimum quantity of water was added in the mixture and the light blue solution was stirred for another 4 h and filtered. The filtrate was kept for slow evaporation. Blue crystals were obtained after 7 days.

Analytical data for $[Cu(L)(NCO)]_2(PF_6)_2$ **(3)** Yield 0.122 g (40%). Anal. Calc. for $C_{38}H_{48}F_{12}N_{14}Cu_2O_2P_2$: C, 39.65; H, 4.17; N, 17.06%. Found: C, 39.65; H, 4.20; N, 17.28%. IR (KBr pellet) cm^{-1}; ν(NCO^-), 2213 vs; ν(C=C) + ν(C=N)/pyrazole ring, 1604 s, 1557 vs; ν(PF_6^-), 844 vs; UV–Vis spectra: λ_{max}/nm (ε_{max}/mol^{-1} cm^{-1}): 623 (120), 313 (22 559).

Analytical data for $[Cu(L)(NCO)]_2(BF_4)_2$ **(4)** Yield 0.116 g (46%).Anal. Calc. for $C_{38}H_{48}F_8N_{14}Cu_2O_2B_2$: C, 39.65; H, 4.17; N, 17.04. Found: C, 39.72; H, 4.10; N, 17.12%. IR (KBr pellet) cm^{-1}; ν(NCO^-), 2213 vs; ν(C=C) + ν(C=N)/pyrazole ring, 1604 s, 1557 vs; ν(BF_4^-), 1045 vs; UV–Vis spectra: λ_{max}/nm (ε_{max}/mol^{-1} cm^{-1}): 627 (110), 313 (22 469).

2.4. Physical measurements

The IR spectrums were recorded on a Perkin-Elmer FT-IR spectrometer RX1 spectrum using KBr pellets. The microanalysis (C, H and N) was carried out using Perkin-Elmer IA 2400 series elemental analyzer. UV–Vis spectra (900–190 nm) were recorded on a Perkin-Elmer spectrophotometer model Lambda 35 in CH_3CN solution. The magnetic susceptibility of a powder sample was carried out in the magneto chemistry Service of Universidad de Barcelona, on polycrystalline samples with a DSM5 Quantum Design SQUID magnetometer working in the 2–300 K range. The magnetic field was 0.1 T between 300 and 30 K and 0.03 T between 30 and 2 K to avoid saturation effects. The

contribution of the sample holder was determined separately in the same temperature range and magnetic field. The diamagnetic corrections were evaluated from Pascal's constants.

2.5. X-ray crystallography

The crystallographic data, details of data collection and some important features of the refinement for the compound **1** and **3** are given in Table 1. Blue crystals of suitable size of complex **1** and **3** were obtained by slow evaporation of methanol solution. Crystals suitable for **1** and **3** were selected and mounted on the glass fire using epoxy resin. Data for both complexes were collected with Mo-Kα radiation (λ = 0.71073Å) at 293 K on a Bruker SMART APEX diffractometer equipped with CCD area detector. Data for both the compounds were processed with SAINT software [21] and empirical absorption correction was applied with SADABS [22] software programs. The structure was solved by direct method using SHELXTL [23] and refined by the full-matrix least-squares technique using SHELXL-97 [24] program package. All non-hydrogen atoms were refined anisotropically till convergence is reached. The H atoms positions were calculated from the difference Fourier map.

3. Results and discussion

3.1. Synthesis

The binuclear complexes of the type $[M(L)(NCO)]_2(X)_2$ (M = Ni^{2+} and Cu^{2+}, X=$PF_6^-$and BF_4^-) are readily obtained through one-pot reaction of metal salt like acetate, L, sodium cyanate and PF_6^-/BF_4^- ion in 1:1:1:1 mole ratio in methanol and water. There was no change of structure even after addition of excess cyanate salt and binuclear complexes were always obtained. All complexes gave satisfactory microanalytical results confirming their composition. The diffraction quality crystal for structural studies was obtained by slow evaporation of the solution. The complexes are moderately soluble in acetonitrile and ethanol and insoluble in dichloromethane, acetone etc. One important observation was that the ligand L formed double end-to-end azido bridged binuclear complexes with nickel(II) and copper(II) [20] but only mononuclear complexes with thiocyanate [25]. However, the Cu–O1 bond distance in complex **3** is 2.777 Å which is close to Cu–N9a

Table 1. Crystal data and structure refinements for complex **1** and **3.**

	Complex **1**	Complex **3**
Empirical formula	$C_{38}H_{48}F_{12}N_{14}Ni_2O_2P_2$	$C_{38}H_{48}F_{12}N_{14}Cu_2O_2P_2$
Formula weight	1140.26	574.96
Temperature (K)	293(2)	293
Wavelength (Å)	0.71073 Å	0.71073
Crystal system	Triclinic	Triclinic
Space group	*P1*	*P1*
a (Å)	11.641(2)	9.885(2)
b (Å)	12.605(2)	11.783(3)
c (Å)	17.357(3)	12.017(3)
α (°)	93.549	111.553(4)
β (°)	106.675(3)	108.199(4)
γ (°)	96.818(3)	95.817(4)
Volume $Å^3$	2410.2(8)	1199.1(5)
Z	2	1
Density(calculated) (mg/m^3)	1.571	1.592
Absorption coefficient(mm^{-1})	0.945	1.051
F(000) (mm)	1168	586
Crystal size	0.24 x 0.18 x 0.10	0.24 x 0.18 x 0.10
Theta range for data collection(º)	1.64 to 24.00	2.24 to 21.35
Index ranges	$-13\leq h\leq 13$	$-11\leq h\leq 11$
	$-14\leq k\leq 14$, $-19\leq l\leq 19$	$-13\leq k\leq 13$, $-13\leq l\leq 13$
Reflections collected	15743	7894
Independent reflections	7527 [R(int) = 0.0467]	2969[R(int) = 0.0555]
Absorption correction	MULTI SCAN	OMEGA-PHI SCAN
Max. and min. transmission	0.9115 and 0.8050	0.9022 and 0.7865
Refinement method	Full-matrix least-squares on F^2	Full-matrix least-squares on F^2
Data / restraints / parameters	7527 / 0 / 639	3748/0/320
Goodness-of-fit on F^2	1.099	1.165

(2.637 Å) bond distance in azido bridged copper complex with the same ligand [20].

3.2. IR and UV–Vis spectroscopy

The IR spectrum for all the complexes (**1–4**) have common two absorption bands in the region of 1607–1556 cm^{-1} resulting from the vibration ν(C=N) + ν(C=C) of the pyrazole ring of L. This indicates coordination of the pyrazole group in all the copper and nickel complexes. The strongest intensity band in the infrared spectrum is shown at 2243 cm^{-1} and at 2213 cm^{-1} for complexes (**1–4**), corresponding to the asymmetric stretching vibration of ν(CN) of cyanate ligand. The complexes **1** and **3** have one strong band at ca. 844 cm^{-1} due to ν(PF_6^-) ion and complexes **2** and **4** have one strong band at ca. 1093 cm^{-1} due to ν(BF_4^-). All other bands of the ligand appeared in the IR spectra of the complexes [Fig.1 and 2]. Nature of the coordination mode of cyanate ion is confirmed by the crystal structure. Electronic spectrum of complex **3** and **4** in CH_3CN solution at room temperature exhibits a band at 623 nm, which may be attributed to d–d transition [Fig.3]. This type of absorption band has been previously assigned to copper(II) complex with square–pyramidal geometry [26]. Bands below 400 nm are due to intraligand transitions.

3.3. Crystal structure

The molecular structure of the binuclear cation moiety of complex **1** and the atom labeling scheme are shown in Fig. 4. Selected bond lengths and angles related to metal coordination sphere for the structure are given in Table 2. The structure shows each nickel atom is six coordinated with distorted octahedral environment and the two NCO^- ions bridges two nickel(II) centers by adopting end- to-end coordination mode. Each nickel atom is in six-coordinate surrounded by four nitrogen atoms (N5, N3, N1 and N6) from ligand L and N7 and O1 from two cyanate bridging ligands. In the basal plane, there are three nitrogen atoms – N3, N6, N7 and one oxygen atom O1 and two nitrogen atoms – N1 and N5 in the axial position. The bond distances Ni–N3, Ni–N6, Ni–N7 and Ni–O1 are 2.151, 2.068, 1.991 and 2.175 Å, respectively, and are very close to each other. Two axial bond distances Ni–N1 and Ni–N5 are 2.089 and 2.131 Å, respectively, and are

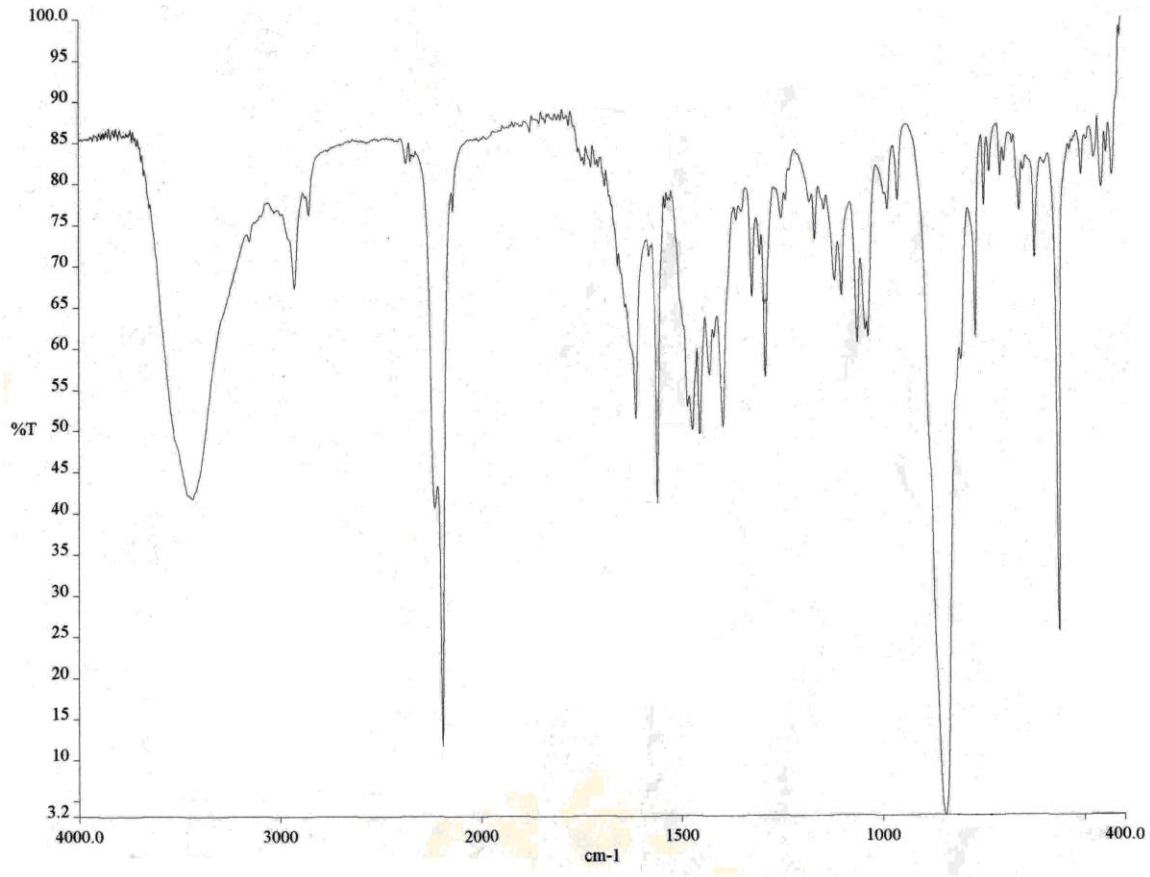

Fig. 1. IR spectra of $[NiL(NCO)]_2(PF_6)_2$

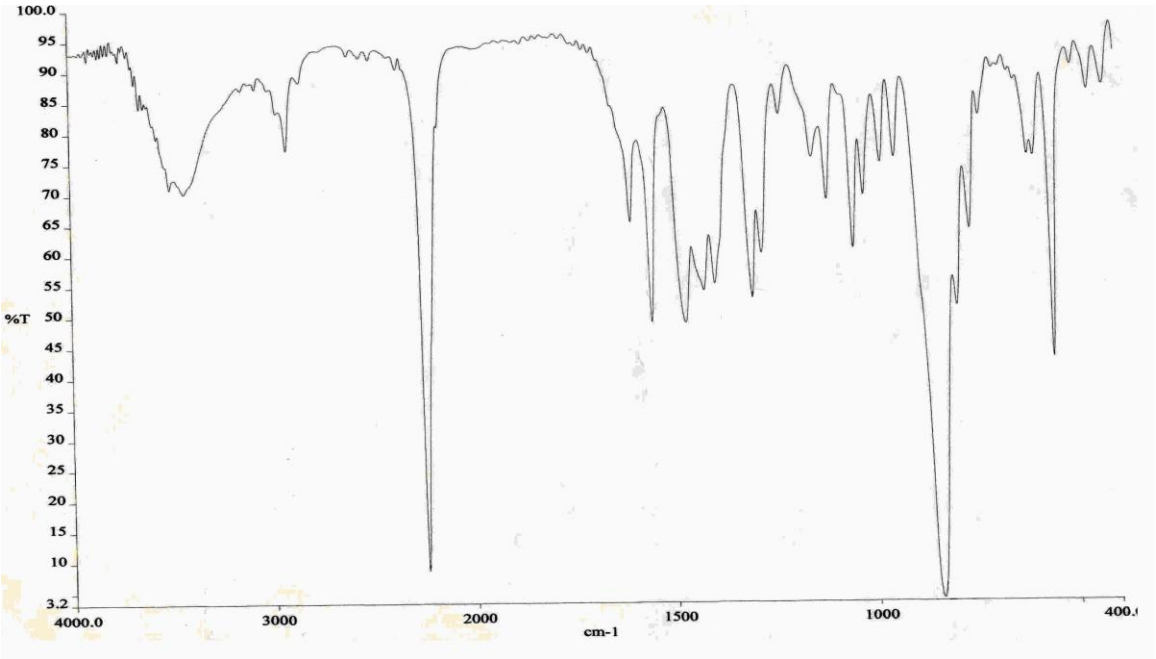

Fig.2. IR spectra of $[Cu(L)(NCO)]_2(PF_6)_2$

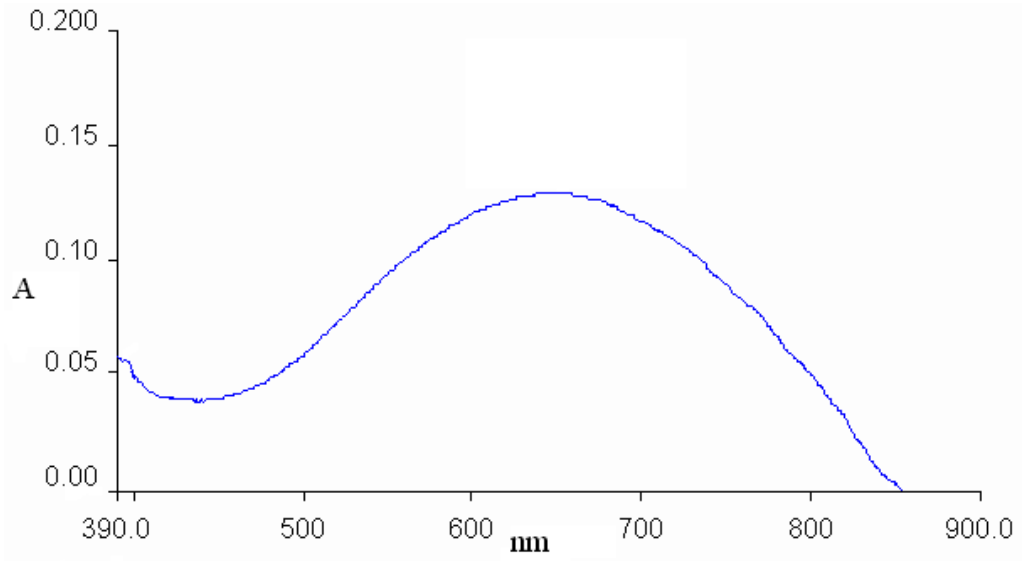

Fig. 3. Electronic spectra of $[Cu(L)(NCO)]_2(PF_6)_2$ in CH_3CN (conc. = 1.0 $x10^{-3}$ M)

Table 2. Main bond lengths (Å) and angles (°) for complex 1 and 2.

$[Ni_2L_2(NCO)_2](PF_6)_2$		$[Cu_2L_2(NCO)_2](PF_6)_2$	
Ni1-N7	1.991(7)	Cu1-O1	1.937(7)
Ni1-N6	2.068(7)	Cu1-N4	2.032(7)
Ni1-N1	2.089(6)	Cu1-N1	2.038(6)
Ni1-N5	2.131(7)	Cu1-N2	2.082(6)
Ni1-N3	2.151(6)	Cu1-N6	2.473(7)
Ni1-O1	2.175(6)	Cu1-O1a	2.777
N7-Ni1-N6	96.7(3)	O1-Cu1-N4	101.0(3)
N7-Ni1-N1	100.3(3)	O1-Cu1-N1	96.8(3)
N6-Ni1-N1	98.8(3)	N1-Cu1-N4	161.4(3)
N7-Ni1-N5	99.9(3)	O1-Cu1-N2	178.0(3)
N6-Ni1-N5	85.0(3)	O1-Cu1-N6	
N1-Ni1-N5	158.8(3)	O1a-Cu1-N6	
N7-Ni1-N3	178.0(3)	N1-Cu- N2	81.6(2)
N6-Ni1-N3	81.5(3)	O1-Cu1-N6	102.5(3)
N1-Ni1-N3	79.3(3)	N4-Cu1-N6	99.4(2)
N5-Ni1-N3	80.7(3)	N1-Cu1-N6	82.3(2)
N7-Ni1-O1	93.5(3)	N2-Cu1-N6	78.5(2)
N6-Ni1-O1	166.8(2)	O1-Cu1-O1a	
N1-Ni1-O1	87.5(3)		
N5-Ni1-O1.	85.0(3)		
N3-Ni1-O1.	88.4(2)		
N8-Ni2-N14.	97.3(3)		

almost similar. Bond angles involving the cyanate ligand Ni(1)–N(7)–C(19), N(7)–C(19)–O(2) and O(1)–Ni(1)–N(7) are 147.9°, 177.9° and 93.5°, respectively. The two (OCN) bridges are in the same plane. The Ni1----Ni2 intradimer distance is 5.091 Å. This is consistent with other structural data obtained for end-to-end azido bridging complex with the same ligand [20] and is lower than other end-to-end cyanate bridging complex [17].

The structure of **3** consists of the binuclear units $[Cu(L)(NCO)]_2^{2+}$ isolated by hexafluorophosphate anions. An ORTEP drawing with the atom-labeling scheme is shown in Fig. 5. Selected bond lengths and angles related to metal coordination sphere for the mononuclear unit are given in Table 2. The copper(II) atoms are bridged by cyanate ions in double end-on fashion. The copper atom is octahedrally surrounded by four nitrogen atoms – N1, N2, N4 and N6 from ligand L and O1 and O1a from two bridging ligands. The atoms N5, N2, O1 and O1a are in the basal plane and N1 and N7 are in the axial plane. The bond distances of Cu–N1, Cu–N2, Cu–N4, Cu–O1, Cu–N6 and Cu–O1a are 2.038, 2.082, 2.032, 1.937, 2.473 and 2.777 Å, respectively. So the coordination polyhedron around the copper atom consists of a distorted octahedron with four short bonds (<2.09 Å) and two much longer bond (>2.4 Å). The intradimer Cu----Cu distance is 3.509 Å and this is consistent with structural data obtained with other binuclear end-on cyanate bridging complex [7]. However, the Cu–O1 bond (2.777 Å) is very high and probably does not contribute any bridging interaction.

3.4. Magnetic studies

The temperature dependence of the magnetic response of the complex **1** as plot of $\chi_M T$ versus T (χ_M is the molar magnetic susceptibility for two nickel(II) ions) can be seen in Fig. 6. The value of $\chi_M T$ at 300 K is 2.25 cm^3 mol^{-1} K, slightly higher than the expected value for two isolated S = 1 spin carriers (2.00 cm^3 mol^{-1} K for g = 2.0). Starting from room temperature, the $\chi_M T$ values decreases very slowly with decreasing temperature until 50 K (2.0 cm^3 mol^{-1} K) and below this temperature it decreases fast reaching a final value of 0.15 cm^3 mol^{-1} K at 2 K. This shape of the magnetic plot is typical for an antiferromagnetically coupled system. Magnetic data were fitted from the conventional

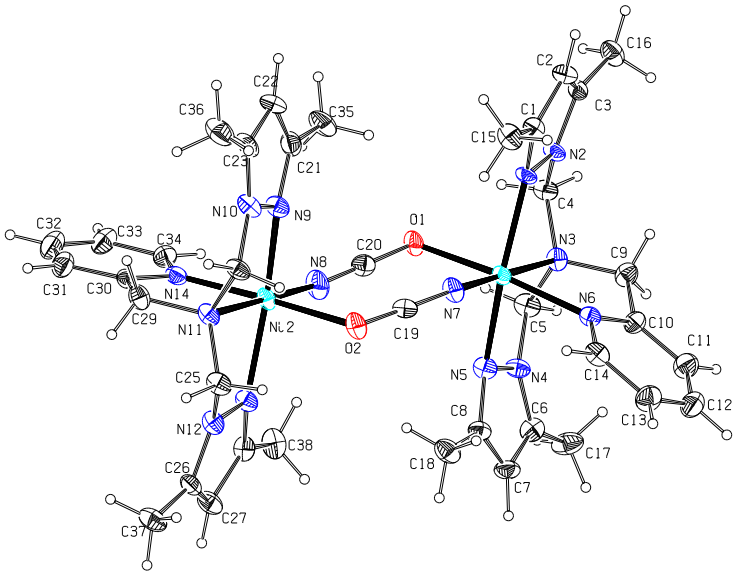

Fig.4. ORTEP diagram of the cationic part of complex **1** with atom numbering scheme (30% probability factor for the thermal ellipsoids).

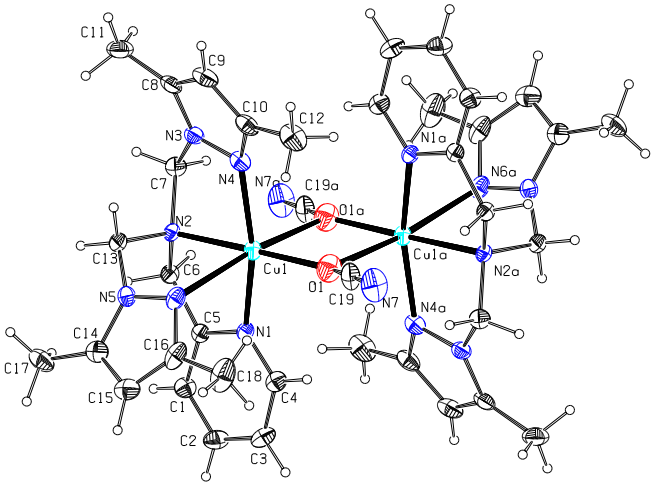

Fig.5. ORTEP diagram of the cationic part of the complex **3** with atom numbering scheme (30% probability factor for the thermal ellipsoids).

analytical expression derived from the isotropic Hamiltonian H = -*J* (S_1. S_2), including a correction term to take into account the paramagnetic impurities (denoted by ρ). The best fit parameters obtained are *J* = -6.2(1) cm^{-1}, g = 2.163(3) with ρ = 3.1%. Fit of the $1/\chi_M$ versus *T* plot gives the Weiss value of -41 K for the complex 1. MO calculations [17] show that super exchange mediated by cyanato ligand follows a similar pattern of interactions than azido ligand: the maximum antiferromagnetic character should be expected for Ni–O–C and Ni–N–C bond angles of 120°and 105°, respectively. Larger bond or Ni–NCO–Ni torsion angles reduce the antiferromagnetic components of the superexchange and for large (close to linear) bond angles, the system can be even ferromagnetic as has been experimentally found for $[Ni(323\text{-tet})(NCO)]_n(ClO_4)_n$ (323-tet = *N,N′*-bis(3-aminopropyl)ethane ligand) [17]. The main difference in comparison

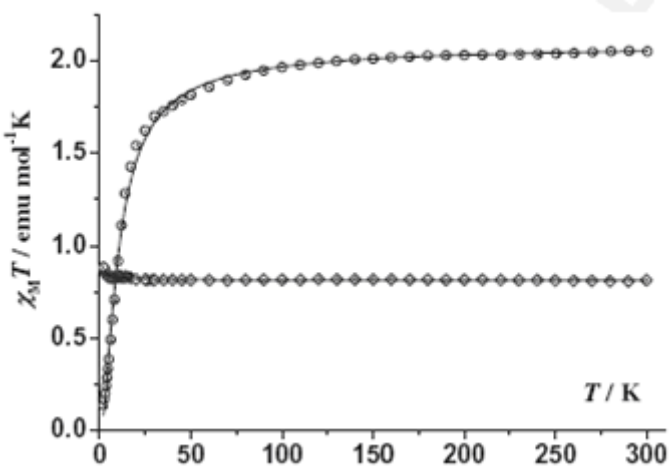

Fig. 6. Plot of $\chi_M T$ product vs. *T* for complex 1(circles) and complex 3 (diamonds). Solid lines show the best fit obtained for the experimental data.

with azido ligand lies in the comparatively lower *J* values found for cyanato bridges as consequence of the lower spin density on the N and O atoms and the experimentally found large Ni–N–C bond angles. Comparison of the structural data for **1** with the previously reported similar systems show a similar Ni–N–C bond angles, slightly lower Ni–O–C bond angles and a clearly larger chair distortion of the Ni–$(OCN)_2$–Ni fragment (Table 3). The calculated *J* coupling constant of -6.2 cm^{-1} for compound **1** perfectly lies in the expected range of *J* values reported until now and its lower value should be attributed to the loss of overlap derived of the lower planarity of the bridging region.

Copper system **3** shows a quasi constant $\chi_M T$ value of 0.81 $cm^3\ mol^{-1}$ K between 300 and 10 K. Below this temperature $\chi_M T$ increases slightly reaching 0.89 $cm^3\ mol^{-1}$ K at 2 K, indicating a very weak ferromagnetic interaction. Experimental data were fitted from the conventional analytical expression derived from the isotropic Hamiltonian $H = -J(S_1.S_2)$

Table 3. Magneto-structural parameters for end-to-end cyanato bridged nickel(II) complexes.

Compound	Ni-O-C (º)	Ni-N-C (º)	Dihedral (º)	J(cm^{-1})	Ref.
$[Ni(tren)(NCO)]_2(BF_4)_2$	117.1	155.0	9.1	-8.8	15
$[Ni(L1)(NCO)]_2(BF_4)_2$	122.0	150.1	4.8	-10.7	16,17
$[Ni(L)(NCO)]_2(PF_6)_2$	110.9/111.4	147.9/152.0	18.6/20.8	-6.2	This work

Abbreviation used: Tren, 2,2',2''-triaminotriethylamine; L1, DL-5,5,7,12,12,14-hexamethyl-1,4,8,11-tetraazacyclotetradecane; L, *N*,*N*-bis(3,5-dimethylpyrazol-1-ylmethyl)aminomethylpyridine. Dihedral angle defined as the angle between mean cyanato plane and O–Ni–N planes.

resulting a *J* value of +0.5(1) cm^{-1} and g = 2.083(1). The magnetization data measured at 2 K shows a Brillouin shape with a comparable g value of 2.094(4). The practically negligible value of *J* coupling constant is derived of the poorly favorable superexchange pathway between the copper atoms which involves large axial distances of 2.777 Å which practically induces a quasi-monomeric magnetic response. Fit of the $1/\chi_M$ versus *T* plot gives the Weiss value of 3.4 K for the complex **3**.

4. Conclusion

We have presented the synthesis, structural and magnetic characterization of new binuclear double end-to-end cyanate bridge nickel(II) complex $[Ni(L)(NCO)]_2(X)_2$ (X = PF_6^-(**1**) and BF_4^-(**2**)) and double end-on cyanate bridge copper(II) complex $[Cu(L)(NCO)]_2(Y)_2$ (Y = PF_6^- (**3**) and BF_4^- (**4**)). Variable temperature magnetic study of complex **1** shows weak antiferromagnetic interaction with *J* = -6.2(1) cm^{-1} whereas complex **3** has very weak ferromagnetic interaction with *J* = +0.5(1) cm^{-1}.

Supplementary material

Crystallographic data for the structural analysis have been deposited with the Cambridge Crystallographic Data Center, CCDC 782334 for compound **1** and CCDC 78233 for compound **3**. Copies of this information can be obtained free of charge from the Director, CCDC, 12 Union Road, Cambridge CB12 1EW, UK (fax: +44-1223-336 033; e. mail: deposit@ccdc.cam.ac.uk or http://www.ccdc.cam.ac.uk).

References

1 J. Ribas, A. Escuer, M. Monfort, R. Vicente, R. Cortes, L. Lezama, T. Rojo, Coord. Chem. Rev. 1999, 193–195, 1027.

2 J. Luo, X.-G. Zhou, L.-H. Weng, X.-F. Hou, Acta Crystallogr., Sect. C Cryst. Struct. Commun. 2003, 59, m519.

3 C.J. Harding, F.E. Mabbs, E.J.L. MacInnes, V. McKee, J. Nelson, J. Chem. Soc., Dalton Trans. 1996, 3227.

4 A. Escuer, M. Font-Bardia, E. Penalba, X. Solans, R. Vicente, Inorg. Chim. Acta 1999, 286, 189.

5 T. Mallah, O. Kahn, J. Gouteron, S. Jeannin, Y. Jeannin, J. O'Connor, Inorg. Chem. 1987, 26, 1375.

6 C. Diaz, J. Ribas, M.S. El Fallah, X. Solans, M. Font-Bardia, Inorg. Chim. Acta 2001, 312, 1.

7 S. Youngme, J. Phatchimkun, U. Suksangpanya, C. Pakawatchai, G.A. Van Albada, J. Reedijk, Inorg. Chem. Commun. 2005, 8, 882.

8 T. Rojo, R. Cortes, L. Lezama, J.L. Mesa, J. Via, M.I. Arriortua, Inorg. Chim. Acta 1989, 165, 91.

9 O.J. Parker, M.P. Wolther, G.L. Breneman, Acta Crystallogr., Sect. C 1996, 52, 1089.

10 A.E. Mauro, S.I. Klein, J.S. Saldana, C.A. De Simone, J. Zukerman-Schpector, E.E. Castellano, Polyhedron 1990, 9, 2937.

11 J. Carranza, J. Sletten, F. Lloret, M. Julve, J. Mol. Struct. 2008, 890, 31.

12 F. Valach, M. Dunaj-Jurco, J. Garaj, M. Hvastijova, Collect. Czech. Chem. Commun. 1974, 39, 380.

13] M.-L. Boillot, O. Kahn, C.J. O'Connor, J. Gouteron, S. Jeannin, Y. Jeannin, J. Chem. Soc., Chem. Commun. 1985, 178.

14 T. Mallah, M.-L. Boillot, O. Kahn, J. Gouteron, S. Jeannin, Y. Jeannin, Inorg. Chem. 1986, 25, 3058.

15 O. Kahn, T. Mallah, J. Gouteron, S. Jeannin, Y. Jeannin, J. Chem. Soc., Dalton Trans. 1989, 1117.

16 M. Mikuriya, S. Kida, I. Murase, Bull. Chem. Soc. Jpn. 1987, 60, 1355.

17 A. Escuer, R. Vicente, M.S.E. Fallah, X. Solans, M. Font-Bardia, J. Chem. Soc., Dalton Trans. 1996, 1013.

18 D.M. Duggan, D.N. Hendrickson, Inorg. Chem. 1974, 13, 2056.

19 D.M. Duggan, D.N. Hendrickson, Inorg. Chem. 1974, 13, 2929.

20 M. Zala, S.B. Kumar, E. Suresh, J. Ribas, Trans. Met. Chem. 2010, 35, 757.

21 G.M. Sheldrick, SAINT 5.1 ed, Siemens Industrial Automation Inc., Madison, WI, 1995. 329

22 SADABSEmpirical Absorption Correction Program, University of Göttingen, Göttingen, Germany, 1997.

23 G.M. Sheldrick, SHELXTL Reference Manual: Version 5.1, Bruker AXS, Madison, WI, 1997.

24 G.M. Sheldrick, SHELXL-97: Program for Crystal Structure Refinement, University of Göttingen, Göttingen, 1997.

25 M. Zala, E. Suresh, S.B. Kumar, J. Coord. Chem. 2011, 64, 483.

26 S. Bhattacharyya, S.B. Kumar, S.K. Dutta, E.R.T. Tiekink, M. Chaudhury, Inorg. Chem. 1996, 35, 1967.

CHAPTER V

Syntheses, Characterization and Structure of Pseudohalides containing Cadmium(II) and Zinc(II) complexes with Pyridylpyrazole ligand

Chapter V

Abstract

The synthetic details and characterization of pseudohalides (NCS^-, N_3^- and NCO^-) containing cadmium(II) and zinc(II) complexes of the type $[M(L)(NCS)_2]$, $[M(L)(N_3)]PF_6$ and $[M_2(L)_2(NCO)_2](PF_6)_2$, where M = Cd(II) and Zn(II) and L = *N*,*N*-bis(3,5-dimethylpyrazol-1-ylmethyl)aminomethylpyridine are described. All complexes were characterized by microanalysis and physico-chemical method. Crystal structure of the complexes $[Cd_2(L)_2(NCO)_2](PF_6)_2$ and $[Zn(L)(N_3)]PF_6$ have been solved by single crystal X-ray diffraction studies and it shows $[Cd_2(L)_2(NCO)_2]^{+2}$ has binuclear double end-on (μ-1,1) NCO^- bridged distorted octahedral geometry whereas $[Zn(L)(N_3)]^+$ has square pyramidal geometry.

1. Introduction

Pyrazole containing tripodal ligands and their metal complexes has been the subject of active area of research owing to their rich coordination chemistry and to model for the biologically active sites in metalloproteins and metalloenzymes [1-8]. Pyrazole containing ligands are used in drug design and in herbicides and fungicides and also in the building of polynuclear complexes [9-10]. Cadmium and zinc are involved in many biochemical reactions [11] and their complexes with nitrogen containing tripodal ligands have potential applications in the areas of catalysis, luminescent materials etc [12-14]. A large number of zinc and cadmium complexes with pseudohalides are known in the literature [15-20].

We have recently synthesized and characterized a number of mono- and binuclear Ni(II) and Cu(II) complexes containing pyridylpyrazole ligand and studied their magnetic properties and also check the coordination behaviour of the ligand [21-23]. As our interest was in new polynuclear complexes with pyridylpyrazole ligand, we were interested in metal complexes with pseudohalide containing cadmium(II) and zinc(II) complexes with the ligand. Herein, we report on the synthesis and characterization of cadmium(II) and zinc(II) complexes using different pseudohalide like N_3^-, NCS^- and NCO^- with ligand *N,N*-bis(3,5-dimethylpyrazol-1-ylmethyl)aminomethylpyridine (L). The complexes are characterized by various physo-chemical methods and structural confirmation of the complexes $[Cd_2(L)_2(NCO)_2](PF_6)_2$ and $[Zn(N_3)(L)]PF_6$ by single crystal X-ray diffraction studies.

1. Experimental

2.1. Materials and methods

All chemicals and solvents were of analytical grade reagents. Zinc acetate, cadmium acetate, KSCN, NaN_3, NaNCO (Loba, India) and NH_4PF_6 (Aldrich) were of reagent grade and used as received. $Zn(ClO_4)_2.6H_2O$ and $Cd(ClO_4)_2.6H_2O$ were synthesized by treating $ZnCO_3$ and $CdCO_3$ with dilute $HClO_4$ acid solution, followed by slow evaporation of the solution over steam bath. Solvents used for synthesis and for spectroscopic studies were purified following the standard procedures.

2.3. Synthesis of Complexes

2.3.1. Synthesis of $[Cd(L)(NCS)_2]$ (**1**)

Ligand L (0.162 g, 0.5 mmol) in methanol (10 ml) was added to methanol solution (10 ml) of $Cd(ClO_4)_2.6H_2O$ (0.210 g, 0.5 mmol) slowly with stirring. After 5 min, 0.096 g (0.5 mmol) of KSCN in little amount of water was added with stirring and finally light yellow solution was stirred for 6 h. Filtered the solution and white powder material was obtained after slow evaporation. Compound was collected by filtration and washed with ether. Yield 0.152 g (60%). Found. C = 43.20, H = 4.32, N = 20.03%; Anal calc for $C_{20}H_{24}N_8S_2Cd$: C = 43.45, H = 4.34 , N = 20.27%; MS (EI): *m/z* 506 $(C_{19}H_{24}N_7SCd)^+$.IR (KBr pellet) cm^{-1}; ν(C=C) + ν (C=N)/pyrazole ring, 1,604 s, 1,555 vs; ν(NCS^{-1}), 2100 vs; ^1H NMR (400 MHz, $CDCl_3$, 20 $^{\circ}C$). *δ*/ppm: 2.19 (s, 6H, CH_3/pz ring), 2.51 (s, 6H, CH_3/pz ring), 4.23 (s, 2H, pyridine-CH_2N), 5.35 (s, 4H, CH_2), 5.82 (s, 2H, CH/pz ring), 7.02 (m, 1H, C^5H/py ring), 7.54 (d, J_{HH} = 8 Hz, 1H,C^3H/py ring), 8.76 (ddd, J_{HH} = 7.6, 1.6, 1.6 Hz, C^4H/py ring), 7.84 (d, J_{HH} = 5.2 Hz, 1H, C^6H/py ring). $\Lambda_M(CH_3CN)$ $(\Omega^{-1}cm^2mol^{-1})$; 8.

2.3.2. Synthesis of **[**$Cd(L)(N_3)]PF_6$ (**2**)

650 mg (2 mmol) of ligand L in methanol (10 ml) was added to a stirred solution of $Cd(CH_3COO)_2$, $2H_2O$ (0.533 g, 2 mmol) in methanol (15 ml). After 10 min, a solution of sodium azide (0.26 g, 4 mmol) in methanol (15 ml) was added slowly to the mixture and stirring was continued for another 3 h. Filtered the solution and the filtrate was left to evaporate slowly. Yield 0.260 g (60%). Found. C = 35.34, H = 3.85 , N = 16.88%; Anal calc for $C_{18}H_{24}N_9CdPF_6$: C = 34.65, H = 3.84, N = 20.21%; MS (EI): *m/z* 480 $(C_{18}H_{24}N_9Cd)^+$. IR (KBr pellet) cm^{-1}; ν(PF_6^-) 844 vs; ν(C=C) + ν(C=N)/pyrazole ring, 1,602 s, 1,553 vs; ν(N_3^-), 2,055 vs; ^1H NMR (400 MHz, $CDCl_3$, 20 ^0C). *δ*/ppm: 2.39 (s, 6H, CH_3/pz ring), 2.45 (s, 6H, CH_3/pz ring), 4.30 (s, 2H, pyridine-CH_2N), 5.1 (s, 4H, CH_2), 6.02 (s, 2H, CH/pz ring), 7.02 (m, 1H, C^5H/py ring), 7.54 (d, J_{HH} = 8 Hz, 1H,C^3H/py ring), 8.87 (ddd, J_{HH} = 7.6, 1.6, 1.6 Hz, C^4H/py ring), 8.01 (d, J_{HH} = 5.2 Hz, 1H, C^6H/py ring). $\Lambda_M(CH_3CN)(\Omega^{-1}cm^2mol^{-1})$; 120.

2.3.3**.** Synthesis of $[Cd_2L_2(NCO)_2](PF_6)_2$ (**3**)

To a methanol solution (10 ml) of $Cd(CH_3COO)_2.H_2O$ (0.125 gm, 0.5 mmol), ligand L (0.162 gm, 0.5 mmol) in methanol (10 ml) was added slowly. After 5 min, 0.065 g (0.5 mmol) of NaNCO in little amount of water was added. Finally, NH_4PF_6 (0.082 g, 0.5 mmol) in little amount of water added with stirring and light yellow solution was stirred for 24 h. Filtered the solution and filtrate was left to evaporate slowly. It was possible to obtain diffraction quality crystal after 5 days. Yield. 0.240 g (44%). Found. C = 40.40, H = 4.50, N = 23.00%; Anal calc for $C_{36}H_{48}N_{18}Cd_2P_2F_{12}$: C = 39.55, H = 4.16, N = 22.73%; MS (EI): *m/z* 480 $(C_{18}H_{24}N_9Cd)^+$.IR (KBr pellet) cm^{-1}; ν(PF_6^-) 844 vs; ν(C=C) + ν(C=N)/pyrazole ring, 1,604 s,1,554 vs ; ν(NCO^-), 2,213 vs; ^{1}H NMR (400 MHz, $CDCl_3$, 20 °C). *δ*/ppm: 2.19 (s, 6H, CH_3/pz ring), 2.44 (s, 6H, CH_3/pz ring), 4.34 (s, 2H, pyridine-CH_2N), 5.87 (s, 4H, CH_2), 6.04 (s, 2H, CH/pz ring), 7.21 (m, 1H, C^5H/py ring), 7.54 (d, J_{HH} = 8 Hz, 1H,C^3H/py ring), 8.80 (ddd, J_{HH} = 7.6, 1.6, 1.6 Hz, C^4H/py ring), 8.01 (d, J_{HH} = 5.2 Hz, 1H, C^6H/py ring).

2.3.4. Synthesis of $[Zn(L)(SCN)_2]$ **(4)**

Ligand L (0.162 g, 0.5 mmol) in methanol (5 ml) was added slowly to a methanol solution (10 ml) of $Zn(ClO_4)_2.6H_2O$ (0.185 g, 0.5 mmol). After 5 min, 0.096 g (0.5 mmol) of KSCN in little amount of water was added with stirring and light yellow solution was stirred for 6 h. Filtered the solution and white powder material obtained by slow evaporation was collected by filtration and washed with ether. Yield 0.152 g (60%). Found. C = 47.20, H = 4.74, N = 24.03%; Anal calc for $C_{20}H_{24}N_8S_2Zn$: C = 47.48, H = 4.74, N = 22.16%; MS (EI): *m/z* 506 $(C_{20}H_{24}N_8S_2Zn)^+$. IR (KBr pellet) cm^{-1}; ν(NCS^-), 2100; ν(C=C) + ν(C=N)/pyrazole ring, 1,604 s, 1,555 vs; ^{1}H NMR (400 MHz, $CDCl_3$, 20 °C). *δ*/ppm: 2.28 (s, 6H, CH_3/pz ring), 2.51 (s, 6H, CH_3/pz ring), 3.99 (s, 2H, pyridine-CH_2N), 4.52 (s, 4H, CH_2), 5.94 (s, 2H, CH/pz ring), 6.05 (m, 1H, C^5H/py ring), 7.67 (d, J_{HH} = 8 Hz, 1H,C^3H/py ring), 9.01 (ddd, J_{HH} = 7.6, 1.6, 1.6 Hz, C^4H/py ring), 8.08 (d, J_{HH} = 5.2 Hz, 1H, C^6H/py ring). $\Lambda_M(CH_3CN)(\Omega^{-1}cm^2mol^{-1})$; 10.

2.3.5. Synthesis of $[Zn(L)(N_3)]PF_6$ (**5**)

A solution of ligand L (0.65 g, 2 mmol) in methanol (10 ml) was added to a stirred solution of $Zn(CH_3COO)_2$. $2H_2O$ (0.5 g, 2 mmol) in methanol (15 ml). After 10 min, a solution of sodium azide (0.26 g, 4 mmol) in methanol (15 ml) was added slowly to the mixture. The mixture was stirred for 2 h, the solution was filtered off, and the filtrate was left to evaporate slowly. It was possible to obtain diffraction quality crystal after 5 days. Yield 0.260 g (60%). Found. C = 36.66, H = 4.22, N = 21.56%; Anal calc for $C_{18}H_{24}N_9ZnPF_6$: C = 36.89, H = 4.27, N = 21.52%; MS (EI): *m/z* 430 $(C_{18}H_{24}N_9Zn)^+$. IR (KBr pellet) cm^{-1}; ν (N_3^-), 2,080 vs; ν(PF_6^-) 844 vs; ν(C=C) + ν(C=N)/pyrazole ring, 1,604 s, 1,555 vs; $\nu_{asym}(N_3^-)$, 2,080 vs; ^{1}H NMR (400 MHz, $CDCl_3$, 20°C). *δ*/ppm: 2.37 (s, 6H, CH_3/pz ring), 2.55 (s, 6H, CH_3/pz ring), 4.35 (s, 2H, pyridine-CH_2N), 5.07 (s, 4H, CH_2), 6.08 (s, 2H, CH/pz ring), 6.05 (m, 1H, C^5H/py ring), 7.67 (d, J_{HH} = 8 Hz, 1H,C^3H/py ring), 9.01 (ddd, J_{HH} = 7.6, 1.6, 1.6 Hz, C^4H/py ring), 8.08 (d, J_{HH} = 5.2 Hz, 1H, C^6H/py ring). $\Lambda_M(CH_3CN)(\Omega^{-1}cm^2mol^{-1})$; 116.

2.3.6. Synthesis of $[Zn_2L_2(NCO)_2](PF_6)_2$ (**6**)

To a methanol solution (10 ml) of $Zn(CH_3COO)_2.2H_2O$ (0.110 g, 0.5 mmol), ligand L (0.162 g,0.5 mmol) was added slowly. After 5 min, (0.065 g, 0.5 mmol) of NaNCO in little amount of water added slowly. Finally, 0.082 g (0.5 mmol) of NH_4PF_6 in little amount of water was added with stirring and light yellow solution was stirred for 24 h. and white crystalline material was obtained by slow evaporation of solution. Yield 0.260 g (60%). Found. C = 39.49, H = 4.48 , N =16.72%; Anal calc for $C_{36}H_{48}N_{18}Zn_2P_2F_{12}$: C = 39.55 , H = 4.16 , N = 17.00% ; MS (EI): m/z 430 $(C_{18}H_{24}N_9Zn)^+$. IR (KBr pellet) cm^{-1}; ν(PF_6^-), 844vs; ν(C=C) + ν C=N)/pyrazole ring, 1,604 s,1,555 vs ; $\nu_{asym}(NCO^-)$, 2,230 vs; ^{1}H NMR (400 MHz, $CDCl_3$, 20 °C). *δ*/ppm: 2.36 (s, 6H, CH_3/pz ring), 2.53 (s, 6H, CH_3/pz ring), 4.35 (s, 2H, pyridine-CH_2N), 5.05 (s, 4H, CH_2), 6.06 (s, 2H, CH/pz ring), 7.58 (m, 1H, C^5H/py ring), 7.65 (d, J_{HH} = 8 Hz, 1H,C^3H/py ring), 9.06 (ddd, J_{HH} = 7.6, 1.6, 1.6 Hz, C^4H/py ring), 8.08 (d, J_{HH} = 5.2 Hz, 1H, C^6H/py ring). $\Lambda_M(CH_3CN)$ $(\Omega^{-1}cm^2mol^{-1})$; 180.

2.4. Physical measurements

The infrared spectrum (4000-400 cm^{-1}) was recorded on a Perkin-Elmer FT-IR spectrometer RX1 spectrum using KBr pellets. Elemental analysis (C, H and N) were carried out using a Perkin-Elmer IA 2400 series elemental analyzer. UV-Vis spectra (900 - 190 nm) were recorded on a Perkin-Elmer spectrophotometer model Lambda 35 in acetonitrile solution. Solution conductivity were measured in CH_3CN solution using Equip-Tronics conductivity meter (model no. EQ-660A)..

2.5. X-ray Crystallography

The crystallographic data and details of data collection and refinement of the compound **3** and **5** are given in Table 1. Crystal of suitable size was selected from the mother liquor and immersed in partone oil, then mounted on the tip of a glass fiber and cemented using epoxy resin. Intensity data for both the crystals was collected using Mo-K_α X-ray (λ = 0.71073Å) radiation on a Bruker SMART APEX diffractometer equipped with CCD area detector at 293 K and 100 K for compound **3** and **5**, respectively. The data integration and reduction were processed with SAINT [24] software. An empirical absorption correction was applied to the collected reflections with SADABS [25] software programs. The structure was solved by direct methods using SHELXTL [26] and was refined on F^2 by the full-matrix least-squares technique using the SHELXL-97 [27] program package. All non-hydrogen atoms were refined anisotropically till convergence is reached. Hydrogen atoms attached to the ligand moiety are either located from the difference Fourier map or stereochemically fixed.

3. Results and Discussion

3.1. General synthesis

The complexes $[M(L)(NCS)_2]$, $[M(L)(N_3)]PF_6$ and $[M_2(L)_2(NCO)_2](PF_6)_2$, where M = Cd(II) and Zn(II) and L = *N*,*N*-bis(3,5-dimethylpyrazol-1-ylmethyl)aminomethylpyridine were obtained in good yield through one-pot synthesis of a 1:1:1:1 mole ratio of the metal salt (perchlorate/ acetate), ligand L, the pseudohalides and counter anion PF_6^- (except for**1** and **4**) in methanol solution.

Table 1. Crystal data and structure refinement for complexes **3** and **5**

	Complex 3	Complex 5
Empirical formula	$C_{19}H_{24}Cd_1F_6N_7O_1P_1$	C_{18} H_{24} F_6 N_9 P Zn
Formula weight	623.00	576.80
Temperature (K)	293(2)	100(2) K
Wavelength (Å)	0.71073	0.71073 A
Crystal system	Triclinic	Orthorhombic
Space group	*P-1*	*Pbcn*
a (Å)	10.1019(10)	17.4952(11) A
b (Å)	11.9950(12)	14.0882(9) A
c (Å)	12.2293(11)	18.7841(12
α(°)	115.369(9)	90
β(°)	91.390(8)	90
γ(°)	110.603(9)	90
Volume ($Å^3$)	1226.2(2)	4629.8(5)
Z	2	8
Density (Mg/m^3)	1.687	1.655
Absorption coefficient (mm^{-1})	0.298	1.206
F(000)	540	2352
Crystal size (mm)	0.35 x 0.28 x 0.26	0.34 x 0.30 x 0.26
Theta range for data collection (°)	3.1743 to 29.048	2.15 to 27.99
Index ranges	-12≤h≤13,-14≤k≤ 15, -5≤l≤ 15	-21≤h≤20, -11≤k≤18, -23≤l≤24
Reflections collected	8247	22194
Independent reflections	5137 [*R*(int) = 0.0760]	5373 [R(int) = 0.0282]
Absorption correction	Semi-empirical from equivalents	Semi-empirical from
Max. and min. transmission	0.8726 and 0.6570	0.7446 and 0.6846
Refinement method	Full-matrix least-squares on F^2	Full-matrix least-squares on F^2
Data / restraints / parameters	5137/ 0 / 316	5373 / 0 / 310
Goodness-of-fit on F^2	0.993	1.055
Final *R* indices [I>2sigma(I)]	R1 = 0.0760, wR2 = 0.1452	R1 = 0.0709, wR2 = 0.1982
R indices (all data)	R1 = 0.1607, wR2 = 0.2062	R1 = 0.0802, wR2 = 0.2064
Largest diff. peak and hole (eA^{-3})	0.931 and -0.345	1.611 and -0.839

Among these, complexes **1**, **2**, **4** and **5** are mononuclear. IR data and conductance measurement show complex **1** and **4** are non ionic and two NCS^- ion are bonded with cadmium(II) or zinc(II). Crystal structures of $[Cd_2(L)_2(NCO)_2](PF_6)_2$ (**3**) and $[Zn(L)(N_3)]PF_6$ (**5**) have been solved by single crystal X-ray diffraction study. Crystal structure of $[Cd_2(L)_2(NCO)_2](PF_6)_2$ (**3**) shows that two NCO^- ions bridges two cadmium (II) centers by adopting end-on (μ-1,1) coordination mode and both the cadmium has octahedral geometry with CdN_6 coordination environment. Similar mononuclear complexes with NCS^- ion and binuclear double NCO^- bridged nickel(II) and copper(II) complexes were reported with this ligand [21-23]. $[Zn(L)(N_3)]PF_6$ (**5**) complex is mononuclear with ZnN_5 coordination environment and it has distorted square pyramidal geometry. On the basis of the above results and other physico-chemical data, we expect that NCS^- containing cadmium complex **1** and zinc complex **4** and N_3^- containing cadmium complexes **2** will be mononuclear and zinc complexes **6** will also be binuclear. There was no change on complex structure even after addition of excess N_3^- or NCO^- in the mixture. All complexes were characterized by microanalysis and physico-chemical method. The complexes are soluble in ethanol, methanol, dichloromethane and acetonitrile. Conductivity measurement in CH_3CN solution shows that complex **1** and **4** are non-electrolytes whereas complexes **2** and **4** have 1:1 conductance indicating the presence of 1:1 PF_6^- as counter anion. Complexes **3** and **6** have also 1:2 conductance. The ESI-MS spectral measurement showed an intense peak at 506 $(C_{19}H_{24}N_7SCd)^+$ for complex **1**, 480 $(C_{18}H_{24}N_9Cd)^+$ for complex **2** and 480 $(C_{19}H_{24}N_7OCd)^+$ for complex **3** indicating the integrity of the complex in solution. For zinc(II) complexes, the ESI-MS spectral measurement showed an intense peak at *m/z* 506 $(C_{20}H_{24}N_8S_2Zn)^+$ for complex **4** [Fig.1], 430 $(C_{18}H_{24}N_9Zn)^+$ for complex **5** and 430 $(C_{18}H_{24}N_9Zn)^+$for complex **6** indicating the integrity of the complex in solution. Due to unavailability of diffraction quality crystal, crystal structure of 1, **2**, **4** and **6** could not be solved. The coordination of L with zinc and cadmium ions were verified by the ^1H NMR studies.

3.2 Spectral studies

The IR bands were assigned by comparing with the free ligand L band. The IR spectra of all the complexes show two strong characteristic bands at ~ 1610 and ~1590 cm^{-1} due to

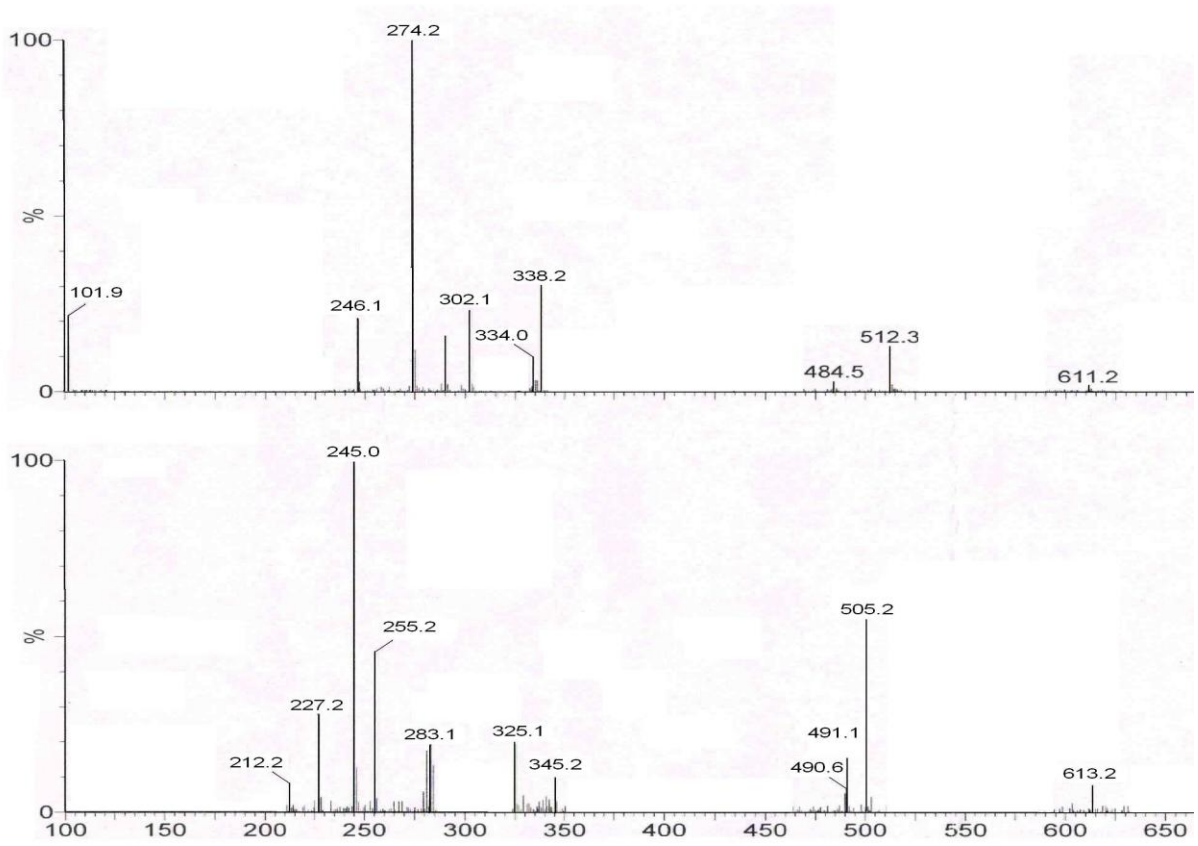

Fig.1. Mass spectra (ESI) of $[ZnL(SCN)_2]$

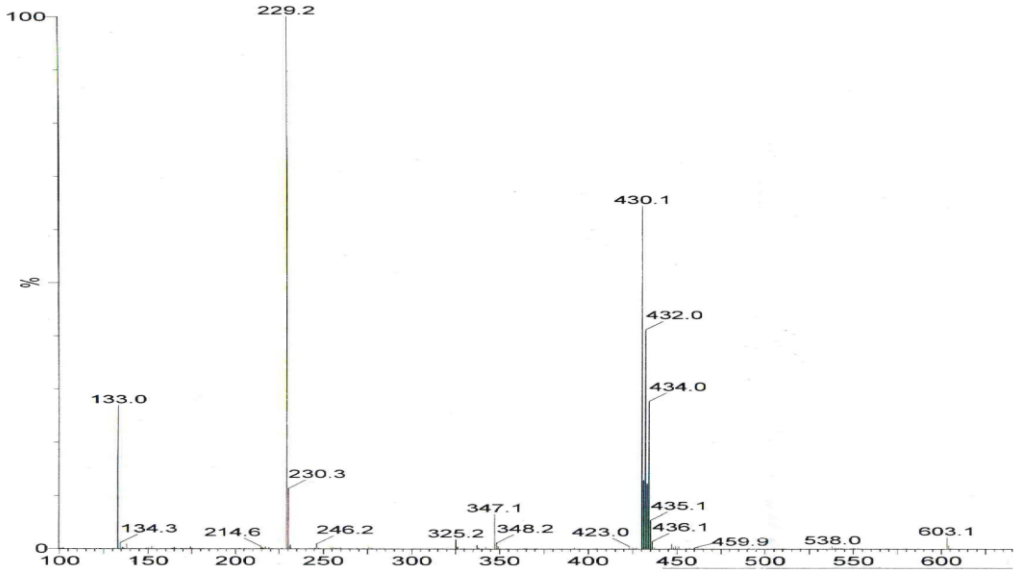

Fig. 2. Fig.1. Mass spectrum (ESI) $[Zn_2L_2(NCO)_2](PF_6)_2$

pyrazole ν(C=N) + ν(C=C) indicating coordination of pyrazole to the cadmium and zinc. Complexes **2**, **3, 5**, and **6** show strong band at ca. 844 due to ν(PF_6^-). One strong band appears at 2100 cm^{-1} for ν(NCS^-) for complexes **1** and **4** indicates coordination of NCS^- with metal atoms. The azide complexes **2** and **5** show a sharp peak at ~2070-2080 cm^{-1} which supports coordination of N_3^- with zinc(II) and cadmium(II) [29]. Similarly, the cyanate complexes **3** and **6** show a sharp peak at ~2070-2080 cm^{-1}, indicating bridging NCO^- in the complexes and this was supported by the single crystal X-ray structure data of complex **3** [Fig. 3 and 4]. All other bands of the ligand are also present in the complexes.

The electronic spectra of the complexes were recorded in the range of 250-550 nm in CH_3CN solution and no characteristic bands were obtained in the visible region All the complexes as well as the ligand exhibit two intense bands in the region of 262 and 229 nm and the transitions are presumably due to intra-ligand π-π*/and n- π* transitions. The photoluminescence properties of the ligand L and its complexes were studied at room temperature (298 K) in CH_3CN solution. Ligand L does not exhibits photoluminescence upon excitation at 262 nm as well as 229 nm. The emission energy of all the complexes in CH_3CN solution is very low in the range of 340 to 370 nm at both the excitation energy states. No emission originating from metal-centered excited states are expected for the Zn(II) and Cd(II) complexes, since they are difficult to oxidize or reduce due to their d^{10} configuration. Thus, the emission observed in the complexes is assigned to the (π-π*) intraligand fluorescence.

The ^1H NMR Spectra were recorded in $CDCl_3$ solution. The assignment has been made on the basis of spin-spin interaction and on comparison with free ligand values. All compounds NMR data are given in the experimental section. All protons of the ligand suffer down field shifting in the complexes compared to the ligand values. In all zinc and cadmium complexes with ligand L, C15, C16, C23 and C24 methyl protons are shifted by +0.16 to +0.412 ppm to higher δ value and C13 and C21 protons are shifted by +0.244 to +0.303 ppm to higher δ value in pyrazole ring. Similarly, the C7 protons (2H) is shifted to +0.34 to +0.64 ppm to higher δ value and C9 and C17 protons are shifted to 0.03 to 0.34 ppm to higher δ value. In pyridine ring, C4 proton is shifted to +0.425 to +0.515 ppm to higher δ value. The C6 proton is shifted to +0.3 to +0.507 ppm to higher δ

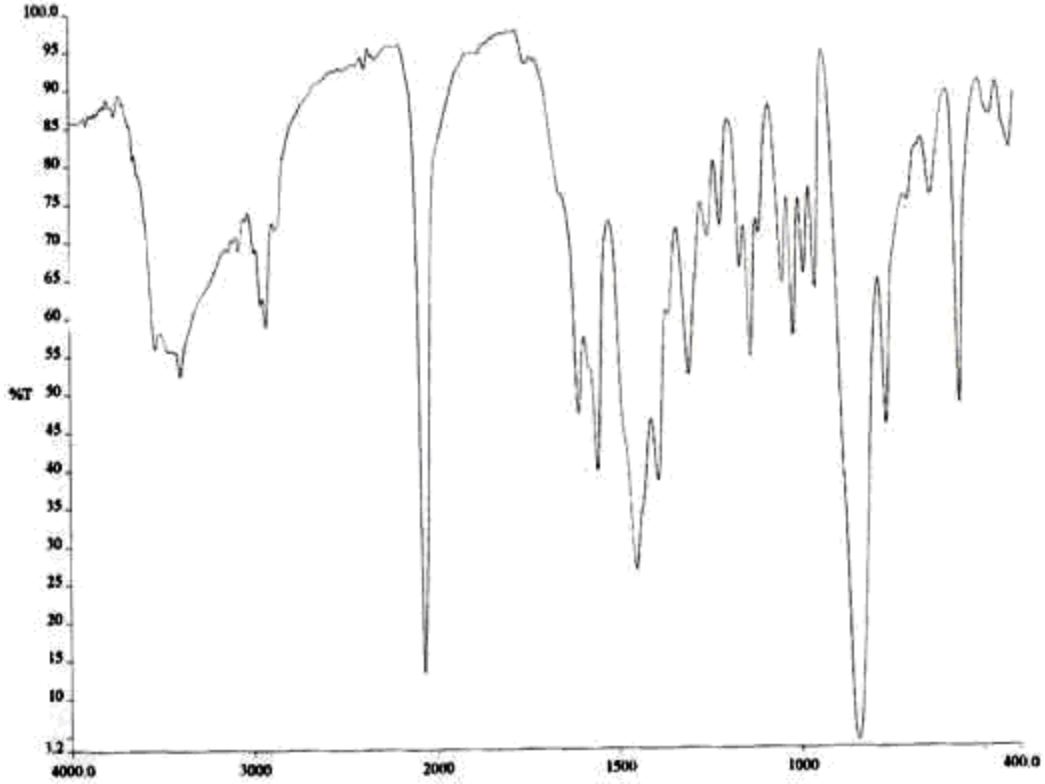

Fig.3. IR Spectra of $[Cd(L)(N_3)]PF_6$

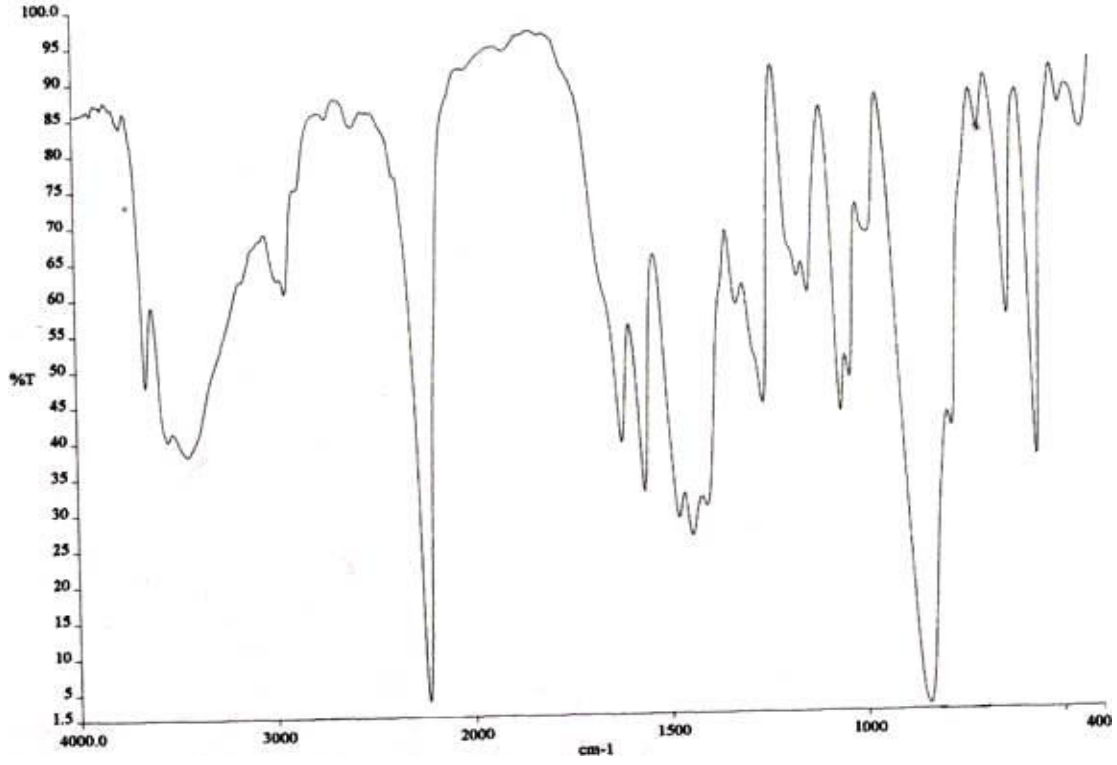

Fig.4. IR Spectra of $[Zn_2(L)_2(NCO)_2](PF_6)_2$

value. ^{1}H NMR spectra of the complexes of $[Cd(L)(N_3)]PF_6$ and $[Zn_2(L)_2(NCO)_2](PF_6)_2$ are shown in Fig. 5 and 6, respectively.

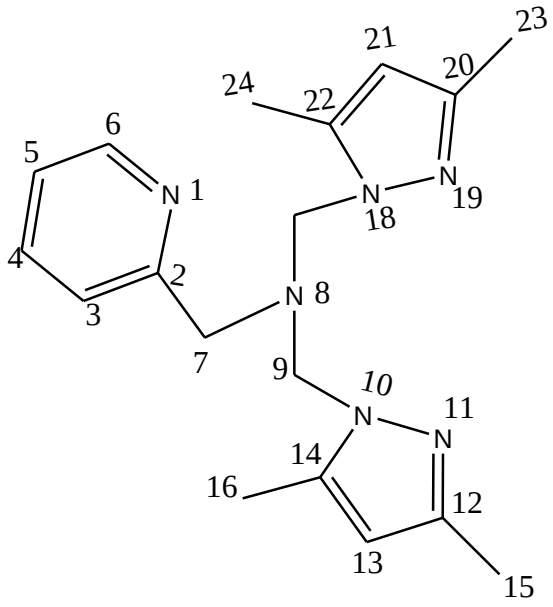

3.2. Crystal structure of $[Cd_2L_2(NCO)_2](PF_6)_2$ (3)

The molecular structure of the cation in $[Cd_2L_2(NCO)_2](PF_6)_2$ and the atom-labeling scheme are shown in Fig.7. Selected bond lengths and angles related to metal coordination sphere for the structure are given in Table 2. The structure shows that the two NCO^- ions bridges two cadmium(II) centers by adopting end-on (μ-1,1) coordination mode. The ligand L is tetradentate, utilizing all potential donor atoms-pyridine nitrogen (N1), tertiary amine nitrogen (N2), and two pyrazole nitrogen atoms (N4 and N6). Each cadmium atom has six coordination with distorted octahedral environment being bond to four nitrogen atoms- pyridine nitrogen (N1), tertiary amine nitrogen (N2) and two nitrogen atoms (N7 and N7a) from the bridging cyanate ions at the equatorial plane and the two pyrazole nitrogen atoms N6 and N4 at the axial position. In the equatorial plane, the bond distances of Cd – N1, Cd – N2, Cd - N7 and Cd –N7a are 2.322, 2.458, 2.237 and 2.513 Å, respectively. The distance between two Cd-NCO are not same and the distance Cd – N7a (2.513 Å) is longer than Cd - N7 (2.237 Å). The axial bond lengths

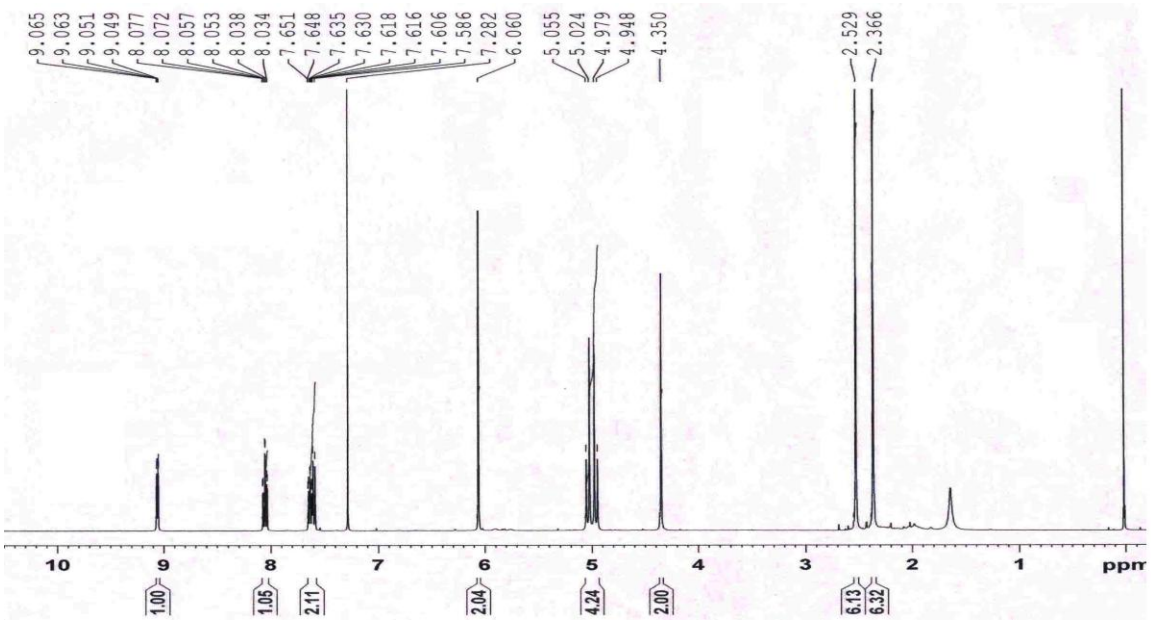

Fig. 5. ^{1}H NMR spectra of $[Cd(L)(N_3)]PF_6$

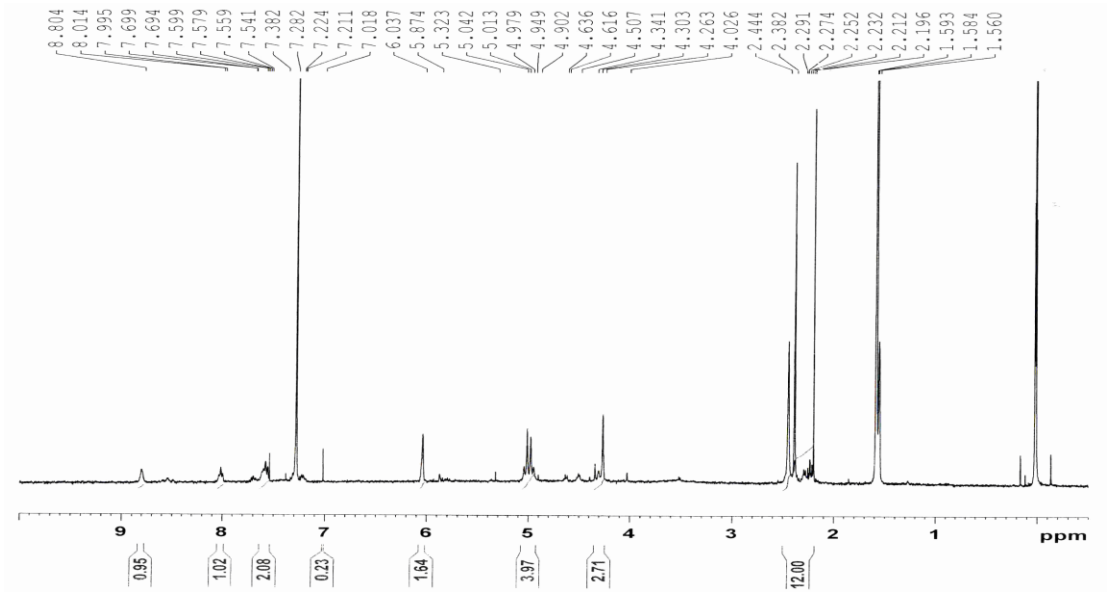

Fig.6. ^{1}H NMR spectra of $[Zn_2(L)_2(NCO)_2](PF_6)_2$

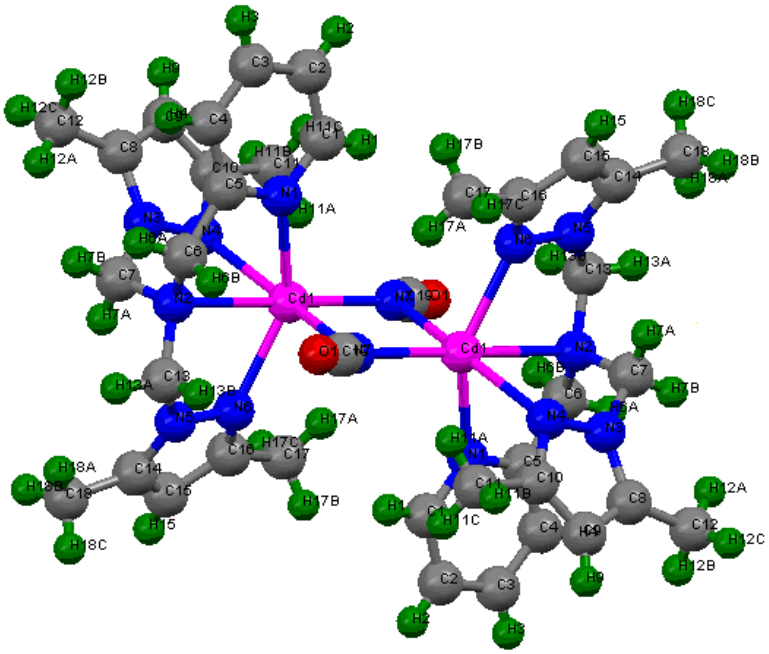

Fig. 7. ORTEP diagram depicting the cationic part of the complex **3** with atom numbering scheme (30% probability factor for the thermal ellipsoids).

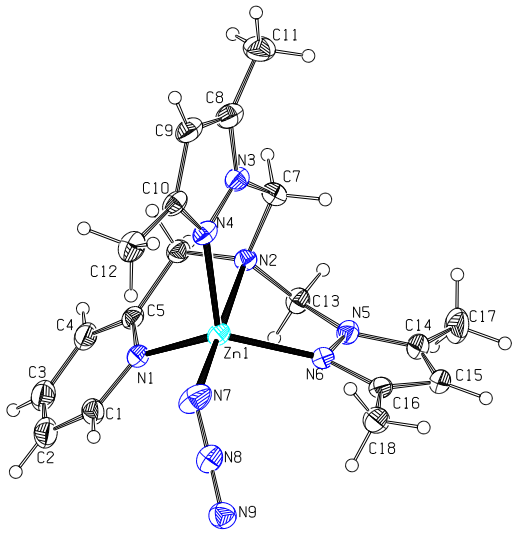

Fig. 8. ORTEP diagram depicting the cationic part of the complex $[Zn(L)(N_3)]PF_6$ with atom numbering scheme(30% probability factor for the thermal ellipsoids)

Cd-N4 (2.425 Å) and Cd – N6 (2.286 Å) are not equal and little different from each other. The cyanate ion is nearly linear with N7-C19-O1 angle of 175.3(16)°. The Cd····Cd distance is 3.4744(12) Å.

Table 2. Bond lengths (Å) and bond angles (°) of $Cd_2(L)_2(NCO)_2](PF_6)_2$ and $[Zn(L)(N_3)]PF_6$ complexes

$Cd_2(L)_2(NCO)_2](PF_6)_2$

Cd1 -N1	2.322(6)	N7-Cd1-N6	108.7(3)
Cd1 -N4	2.425(6)	N7-Cd1-N1	106.5(3)
Cd1- N2	2.458(7)	N6-Cd1-N1	144.5(3)
Cd1 -N7a	2.513(6)	N6-Cd1-N4	93.8(2)
Cd1- N7	2.237(8)	N7-C19-O1	175.3(16)
Cd1 -N6	2.286(7)	N7-Cd1-N2	177.78(19)
Cd1-Cd1	3.4744(12)	N1-Cd1-N7	86.2(2)

$[Zn(L)(N_3)]PF_6$

Zn-N1	2.062(4)	N(7)-Zn(1)-N(4	107.05(17)
Zn-N2	2.377(3)	N(7)-Zn(1)-N(6)	105.09(16)
Zn-N6	2.057(3)	N(4)-Zn(1)-N(6)	113.42(14)
Zn-N4	2.026(4)	N(7)-Zn(1)-N(1)	102.14(19)
Zn-N7	1.978(4)	N(4)-Zn(1)-N(1)	107.83(14)
		N(6)-Zn(1)-N(1)	119.95(13)
		N(7)-Zn(1)-N(2)	177.98(17)
		N(9)-N(8)-N(7)	176.9(5)

3.3.Crystal structure of $[Zn(L)(N_3)]PF_6$ (**5**)

The molecular structure of the cation in $[Zn(L)(N_3)]PF_6$ and the atom-labeling scheme are shown in Fig.8. Selected bond lengths and angles related to metal coordination sphere for the structure are given in Table 2. The structure shows it is a mononuclear and five

coordinate with ZnN_5 coordination environment and zinc has distorted square pyramidal structure. The ligand L is tetradentate, utilizing all potential donor atoms-pyridine nitrogen (N1), tertiary amine nitrogen (N2), and two pyrazole nitrogen atoms (N4 and N6). Each zinc atom has distorted square pyramidal geometry being bond to four nitrogen atoms- pyridine nitrogen (N1), tertiary amine nitrogen (N2), pyrazole nitrogen N6 and azide nitrogen N7 are in the equatorial plane and pyrazole nitrogen N4 is in the axial plane. The coordination geometry around Zn(II) ion is distorted square pyramidal as is evidenced from the values of trigonality index, τ (τ for the complex is 0.18) defined as $\tau = [\theta-\varphi/60]$, where θ and φ are the two largest coordination angles[28].

2. Conclusion

Here, we report synthesis and characterization of mononuclear complexes of the type $[M(L)(NCS)_2]$, $[M(L)(N_3)]PF_6$ and binuclear NCO^- bridged complexes $[M_2(L)_2(X)_2](PF_6)_2$ where M = Cd(II) and Zn(II) and L = *N*,*N*-bis(3,5-dimethylpyrazol-1-ylmethyl)aminomethylpyridine. The single crystal structure of $[Cd_2(L)_2(NCO)_2](PF_6)_2$ shows two NCO^- ions bridged with cadmium centers by end-on coordination mode and structure of $[Zn(L)(N_3)]^+$ shows it has distorted square pyramidal structure.

Supplementary material

Crystallographic data for the structural analysis have been deposited with the Cambridge Crystallographic Data Center, CCDC 834084 for compound **3** and CCDC 834083 for compound **5**. Copies of this information can be obtained free of charge from the Director, CCDC, 12 Union Road, Cambridge CB12 1EW, UK (fax: +44-1223-336 033; e. mail: deposit@ccdc.cam.ac.uk or http://www.ccdc.cam.ac.uk).

Reference:

1. S. Trofimenko, Chem. Rev. 1993, 93, 943
2 R. Mukherjee, Coord. Chem. Rev. 2000, 203, 151
3 N. Kitajima, W. B. Tolman, Prog. Inorg. Chem. 1995, 43, 419
4 K. D. Karlin, Z. Tyeklar, Bioinorganic Chemistry of Copper, Chapman and Hall, London, 1973
5 W. G. Haansta, W. A. J. W. V. Donk, W. L Drissen, J. Reedijk, J.S. Wood, M.G.B. Drew, J Chem Soc Dalton Trans 1990, 3123
6 E . Bouwman, W.L. Driessen, J. Reedijk, Inorg. Chem. 1985, 24, 4730.
7 B. Barszcz, A. J.-Wawrzycka, K. Stadnicka, J. Jezierska, Polyhedron, 2009, 27, 3500.
8 B. Barszcz, Coord. Chem. Rev. 2005, 249, 2259.
9 R. Evans, J. A. K. Howard, L. E. M. Howard, J. S. O. Evans, Z. K. Jacimovic, V. S. Jetovic, V. M. Leovac, Inorg. Chim. Acta, 2004, 357, 4528.
10. T. Rachid, R. Abdelkrim, E. K. Sghir, Int. J. Phy. Sci., 2009, 4(13), 906.
11. C. Peifer, D. R. Alessi, Chem. Med. Chem. 2008, 3, 1810.
12. H. Berta, Z. D. Tomic´, P. Pogány, A. Kovács, V. M. Leovac, K. M. Szécsényi, Polyhedron, 2009, 28, 3881.
13. H.A. Habib, A. Hoffmann, H.A. Höppe, G. Steinfeld, C. Janiak, Inorg. Chem. 2009, 48, 2166.
14. H.-Z. Dong, J. Zhao, S.-H. Gou, H.-B. Zhu, Polyhedron, 2009, 28, 1040.
13 Tuoping Hu, Longjie Liu, Xiaoli Lv, Xiaohui Chen, Haiyan He, Fangna Dai, Guoqing Zhang, Daofeng Sun, Polyhedron, doi:10.1016/j.poly.2009.05.015.
15 N. Mondal, M.K. Saha, S. Mitra and V. Gramlich, J. Chem. Soc. Dalton Trans, 2000, 3218.
16 J.M Clemente-Juan, B. Chansou, B. Donnadieu & J-P. Tuchagues, *Inorg. Chem*, 39 2000, 39, 5515.
17 X. Zhu Shi, G. Fang, G. Wu Q, G. Tian, R. Wang, D. Zhang, M. Xue & S. Qiu, Eur. J. Inorg. Chem, 2004, 185.
18 R. Wang, M. Hong, D. Yuan, Y.Xu L, J.Luo, R. Cao, A. S. C. Chan, Eur. J. Inorg.

Chem, 2004, 37.

19 M.K. Patra, J. Dinda, T.-H. Lu, A. R. Paital, C. Sinha, Polyhedron, 2007, 26, 4140

20 H. Chaudhury, R. Ghosh, S. H. Rahaman, G. M. Rosair, B. K. Ghosh, Ind. J. Chem. 2005, 44A, 687.

21 M. Zala, S.B. Kumar, E. Suresh, J. Ribas, Trans. Met. Chem. 2010, 35, 757.

22 M. Zala, E. Suresh, S.B. Kumar, J. Coord. Chem. 2011, 64, 483.

23 M. Zala., A. Solanki, S. B. Kumar, A. Escuer, E. Suresh, Inorg.Chim.Acta. 2011 (in press)

24 G.M. Sheldrick. SAINT, 5.1 ed. Siemens Industrial Automation Inc., Madison, WI (1995).

25 G.M. Sheldrick. SADABS, Empirical Absorption Correction Program, University of Gottingen, Gottingen, Germany (1997).

26 G.M. Sheldrick. SHELXTL Reference Manual (Version 5.1), Bruker AXS, Madison, WI (1997).

27 G.M. Sheldrick. SHELXL-97: Program for Crystal Structure Refinement, University of Gottingen, Gottingen (1997).

28 A.W. Addition, T. N. Rao, J. Reedijk, J. V. Rinj, G. C. Verschoor, J. Chem. Soc., Dalton Trans., 1984, 1349.

29. K. Nakamoto. Infrared and Raman Spectra of Inorganic and Coordination Compounds. Part B, Application in Coordination, Organometallic, and Bioinorganic Chemistry, John Wiley & Sons Inc., New York (1997

CHAPTER VI

Study of Cytotoxic Activity of Copper(II), Nickel(II), Cobalt(II), Cadmium(II) and Zinc(II) Complexes with Pyridylpryazole Ligand.

Chapter VI

Abstract

Cytotoxic activity of copper(II), nickel(II), cobalt(II), zinc(II) and cadmium(II) complexes with ligand *N*,*N*-bis(3,5-dimethyl-1-ylmethyl) aminomethylpyridine (L) have been evaluated. The cytotoxic activity was carried out with HL 60 cell line. After 96 hours, MTT assay was carried out to understand the effect of the metal complexes on cells. All the statistical analyses were carried out using Graphpad Prism 5, and the test for significance was compared using one-way analysis of variance. The pharmacological properties of thiocyanate and selenocyante containg Cu(II) and Ni(II) complexes showed completely different activity than salt or ligand. The results showed that activity of $[CuL(NCS)]PF_6$ and $[NiL(SeCN)(H_2O)](ClO_4)_2$ complexes were mainly attributed to its ligand structure. This activity was quite comparable and dose dependent.

1. Introduction

Metals have played an important role in medicine for years, ever since humans have walked the planet. Many are essential in our diets in varying quantities, although people have recently realized their significance. Many metallic elements play a crucial role in living systems. Copper, Cobalt and Zinc belongs to the essential metals, which are indispensable for plants and animals [1]. These metals, in general called essential bioelements, in optimal concentration provide important functions in cell metabolism: they are components of the enzymes, structural proteins, assimilation pigments, they maintain osmotic potential in the cells. As these metals are having biological role, a new approach has been made in recent years to explore these metals for developing pharmacological drugs. However, as these metals are toxic in high concentrations, new therapeutic inventions tries to form various metal complexes using organic ligands to reduce the toxicity of these elements and enhance their bioefficacy [2].

An Important characteristic of metals is that they easily lose electrons from the familiar elemental or metallic state to form positively charged ions which tend to be soluble in biological fluids. It is in this cationic form that metals play their role in biology whereas metal ions are electron deficient, most biological molecules such as proteins and DNA are electron rich. The attraction of these opposing charges leads to a general tendency for metal ions to bind to and interact with biological molecules. This same principle applies to the affinity of metal ions for many small molecules and ions crucial to life, such as oxygen. Given this wide scope for the interaction of metals in biology, it is not surprising that natural evolution has incorporated many metals into essential biological functions [1]. Metals perform a wide variety of tasks such as carrying oxygen throughout the body and shuttling electrons. Haemoglobin, an iron-containing protein that binds to oxygen through its iron atom, carries this vital molecule to body tissues. Metal ions such as zinc provide the structural framework for the zinc fingers that regulate the function of genes in the nuclei of cells [3]. Similarly, calcium-containing minerals are the basis of bones, the structural framework of the human body. Zinc is a natural component of insulin, a substance crucial to the regulation of sugar metabolism. Metals such as copper, zinc, iron

and manganese are incorporated into catalytic proteins the metalloenzymes-which facilitate a multitude of chemical reactions needed for life [4].

Medicinal inorganic chemistry as a discipline has only existed for about the last 30 years, since the discovery of antitumor activity of cisplatin. Pt-based combination chemotherapy is still the mainstay for the treatment of solid malignancies (especially testicular, ovarian and small cell lung cancers) [5]. Medicinal inorganic chemistry has been practiced, however, for almost 5000 years. As far back as 3000BC the Egyptians used copper to sterilize water. Gold was used in a variety of medicine in Arabia and China 3500 years ago, more as a result of the precious nature of gold than of its known medicinal activities. Various iron remedies were used in Egypt about 1500BC, around the same time that zinc was discovered to promote the healing of wounds. In Renaissance era Europe, mercurous chloride was used as a diuretic and nutritional essentiality of iron was discovered. It is in the last 100years, however, that the medicinal activity of inorganic compounds has slowly been developed in a rational manner, starting in the early 1900s with $K[Au(CN)_2]$ for tuberculosis, various antimony compounds for leishmaniasis, and the antibacterial activity of various gold salts in a number of different conditions [1]. When one thinks of drugs, one often thinks of organic compounds such as the antibacterial penicillins, the nutrient vitamin C and the psychoactive drugs, such as LSD, THC, etc. The Biochemical literature of the last 30years chronicles the burgeoning understanding that many of the biological activities of proteins and enzymes can be ascribed to the metal centers, with the organic backbone acting as a scaffold to hold the metal ion in place for the requisite transformation. Because of this rapid growth of biological inorganic chemistry, it seems logical to explore in parallel the medicinal properties of the various metal ions that are found naturally and even of those that are not found naturally and even of those that are not known to have essential benefit. In the last 50 years, knowledge of the central importance of inorganic elements in organisms has opened up the possibility for inorganic chemists to contribute to health and well-being of man and all other organisms [6].

The area of optimum physiological response of any inorganic drug vary greatly according to the element, its speciation and oxidation state and the biochemistry of the

specific compound in which it is found. Therefore, the areas of deficiency, toxicity and optimum physiological response can be dramatically varied by considering a combination of these variables, as well as design features of the potential ligand which may be altered to tune the delivery of that metal ion into the biological system. This refinement of the biological properties of metal complexes by ligand modification along with the design of ligands to alter the homeostasis of endogenous metal ions, will provide many therapeutic and diagnostic agents over the coming years and will direct medicinal inorganic chemistry into discipline of central importance in medicine and science. Metals can be toxic, but so can some organic molecules that are used as drugs [7]. One of these complexes could destroy a target, and then move on to another, eventually destroying many targets. So a smaller dose of a metal complex could do the work of a larger dose of a traditional drug. Completely destroying the target molecule also lowers the chance that a virus will develop a drug-resistant strain. These metal complexes represent a good first step towards the development of multi-functional drugs called dual activity agents. A number of drugs and potential pharmaceutical agents also contain metal-binding or metal-recognition sites, which can bind or interact with metal ions and potentially influence their bioactivities and might also cause damages on their target biomolecules [8].

There are also a number of metallodrugs and metallopharmaceuticals which have been utilized for the treatment of diseases and disorders or as diagnostic agents, such as gold antiarthritic drug, bismuth antiulcer drugs, gadolinium MRI contrast agents, technetium radiopharmaceuticals, metal based X-ray contrast agents and photo-and radio-sensitizers, vanadium as insulin mimics, and lithium psychiatric drugs [9]. The metal ion Li^{+} can be considered the smallest effective metallo drug whose carbonate and citrate salts exhibit significant therapeutic benefit in the treatment of manic depression [10]. The metal ion Sb^{3+} may be regarding as the simplest "metalloantibiotics" whose salts (including N-methylglucamine antimonite and Na-stibogluconate) have been utilized for the treatment of leishmaniasis against the protozoan parasite Leishmania. The antiprotozoal mechanism of Sb^{3+} is thought to be attributed to its binding to trypanothione that is essential for the growth of the parasite.

The medicinal uses and applications of metals and metal complexes are of increasing clinical and commercial importance. The field of inorganic chemistry in medicine may usefully be divided into two main categories: firstly, ligands as drugs which target metal ions in some form, whether free or protein-bound; and secondly metal-based drugs and imaging agents where central metal ion is usually the key feature of the mechanism. The application of inorganic compounds to medicine requires detailed examination of the fundamental aqueous chemistry of the proposed drug, including its pharmaceutics, the metabolic fate in blood and intracellularly and the effects of the drug on the target of choice [1]. The usefulness of any drug is a balance between its toxicity and activity. Developing metal complexes as drugs, hence, is not an easy task. Accumulation of metal ions in the body can lead to deleterious effects. Thus biodistribution and clearance of the metal complex as well as its pharmacological specificity are to be considered. Favorable physiological responses of the candidate drugs need to be demonstrated by *in vitro* study with targeted biomolecules and tissues as well as in vivo investigation with xenografts and animal models before they enter clinical trials. A mechanistic understanding of how metal complexes achieve their activities is crucial to their clinical success, as well as to the rational design of new compounds with improved potency. The first step in the development of any inorganic metal complex as drug is to screen it for its *in vitro* activity [2].

Hence, we undertook this study to understand the toxicity of inorganic metal complexes we had synthesized during the entire tenure of this study and compare it with their respective salts and ligands to understand the alteration in their toxicity after forming the complex. This study is the first and pioneering study in the development novel pharmacological agents from the metal complexes synthesized in this study.

3. METHODS AND MATERIALS

2.2. Cytotoxicity testing

Dimethyl sulphoxide (DMSO) was purchased from Sigma Aldrich and cell culture reagents and equipments were purchased from High Media Chemicals, Bombay.

2.3. HL 60 cell line culture

HL 60 cell line was obtained from NCCS, Pune and cultured as described previously (Kawaii and Lansky, 2004). Briefly, the cell line was procured from the national center for cell sciences (NCCS), Pune, India. The cells were cultured in a humidified atmosphere (95% air, 5% CO_2) at 37º C in Dulbecco's Modified Eagle's Medium (DMEM, High Media, Bombay) containing 1% anti microbial anti fungal solution (High Media, Bombay), supplemented with 10% FBS (High Media, Bombay). Upon reaching confluence, the cells were removed, counted and loaded in 96 well plates (Merck Scientific, Bombay) for culturing for 96 hours.

Stock solution of the test compounds were prepared by dissolving the compounds in DMSO and stored at 4° C. Working solutions were prepared by dissolving stock solutions in culture media prior to treatment. After 96 hours, MTT assay was carried out to understand the effect of the metal complexes on cells.

2.4. Assessment of cytotoxicity, using MTT assay

Test compounds were dissolved in DMSO, diluted in culture media and used to treat cells for their cytotoxicity in 4 increasing concentration (10 µg/mL, 20 µg/mL, 100 µg/mL, 200 µg/mL) of all compounds for a period of 96 h. A miniaturized viability assay using 3-(4,5-dimethylthiazol- 2-yl)-2,5-diphenyl tetrazolium bromide (MTT) was carried out according to the method described by Mosman. Each assay was carried out using five replicates and repeated on at least three separate occasions. Viability was calculated as a percentage of solvent treated control cells, and expressed as percentage of control.

HL 60 cells were incubated in a DMEM containing 10% FBS under partial pressure of 5% CO_2 at 37 º C. after 96 hours of culture, MTT assay was carried out adding 0.5 mg/mL MTT into each well and further incubating them for 4 h; dissolving produced formazan crystals in DMSO; and measuring their absorbencies at 550 nm using ELISA reader as described previously [11].

2.5. Statistical Analysis

All the statistical analyses were carried out using Graphpad Prism 5, and the test for significance was compared using one-way analysis of variance (ANOVA), followed by Bonferroni post hoc test [12].

3. RESULTS

3.1. Growth of HL 60

HL 60 has been an established cell line for the purpose of cancer and cytotoxicity research. During the experimental period, there was no evidence of bacterial or fungal contamination on the well chamber. The cells were found to be growing well in the culture medium after passaging. After 96 hours of culture, the cells of the control group were found to be prominently growing in the wells.

3.2. MTT assay:

MTT assay was carried out to check for the cytotoxic potential of the metal complexes. These metal complexes were then compared with their respective metal salts and ligands to study alteration in their cytotoxic behaviour. Cisplatin was used as standard inorganic metal complex. Cisplatin showed complete dose dependent toxicity to HL 60 cells, killing 83% cells in higher doses. It was observed that copper complexes had quite contrasting effect compared to their salt and ligand. Ligand showed dose dependent toxicity to the cells and killed 68% of cells in higher doses. Copper chloride was found to be more toxic; however its toxicity was not seen in a dose dependent manner. The cytotoxic activity of the copper complexes is listed in Table 1. This study showed that metal complexes had completely altered property compared to their constituting ligand or salt, $[CuL(CH_3COO)]PF_6.H_2O$, $[Cu(Cl)L'\text{-}(\mu\text{-}Cl)\text{-}CuL'(pz)](PF_6)_2$, $[Cu_2L_2(N_3)_2](BF_4)_2$, $[Cu_2L_2(N_3)_2](ClO_4)_2$ and $[Cu_2L_2(NCO)_2](PF_6)_2$ were found to be comparatively less toxic, killing not more then 60% of cells in higher doses. Compared to these complexes, $[CuL'(SCN)_2]$ and $[CuL(NCS)]PF_6$ were most toxic, killing 90% of cells in higher doses.

Cobalt salt was not found to have any significant toxic effect in higher doses, but surprisingly it showed potent toxicity in low doses of 20 µg/ml (78% cells were killed). Cytotoxicity of the cobalt complexes is listed in table 2. Among the cobalt complexes, $[CoL(Cl)](BF_4).H_2O\ {}^1/_2CH_3OH$ was found to be least toxic and yielding 39% cell

survival. Compared to this complexes, thiocyante and selenocyanate derivatives, $[CoL(SeCN)(H_2O)](ClO_4)$ and $[CoL(SCN)_2]$ were found to be potently toxic, killing 75% of cells.

Nickel salt showed significant toxicity to HL 60 cells starting from lower doses; however, it did not showed any dose dependent effect on the MTT parameter (Table 3). Nickle salts were found to be more toxic compared to other complexes. $[Ni_2L_2(N_3)_2](ClO_4)_2.2C_2H_5OH$ and $[NiLCl_2]$ killed almost 90% of cells in higher doses. $[NiL(SeCN)(H_2O)](ClO_4)$ was found to be most toxic and killed almost of the cells in higher doses, with significant dose dependent effect.

Cadmium salt showed most potent dose dependent toxicity in all salts, killing 95% of cells in higher doses. Compared to the salt, metal complexes had lesser toxicity (Table 4), where $[Cd(L)(N_3)]PF_6$ killed 70% of cells in higher doses. $[Cd(NCS)_2L]$ showed more toxicity and killed 78% of cells in higher doses.

Zinc salts showed least cytotoxic potential compared to all salts and promoted cell growth in low doses, where the cell survival had increased by 25%. In higher doses, cell survival was reduced to 80%. Zinc complexes were also safer compared to other metal complexes and showed not more than 60% cytotoxic potential (Table 5). Thiocyanate complexes synthesized with Zinc were also safer compared to other thiocyante metal complexes and killed 60% salts compared to other complexes.

4. Discussion:

The numerous biological experiments performed so far suggest that DNA is the primary intracellular target of anticancer drugs because the interaction between small molecules and DNA can cause DNA damage in cancer cells, blocking the division of cancer cells and resulting in cell death [13]. Amongst newly synthesized drugs, metal complexes are showing promising effects as they play a crucial role in biological systems. However, as the metal complexes can be toxic in higher doses, it is essential to explore their cytotoxic potential before conducting any pharmacological studies of these drugs. Current study is this first step towards the development of new anticancer drugs from metal complexes.

Copper belongs to the essential metals, which are indispensable for plants. This metal, in general called essential bioelement, in optimal concentration provide important functions

in plant metabolism: they are components of the enzymes, structural proteins, assimilation pigments; they maintain osmotic potential in the cells. However, after application of the higher concentration, they become toxic [14]. Our study showed similar results and exhibited toxic potential of copper in higher doses. It is known to damage cell membranes by binding to the —SH groups of membrane proteins and by inducing lipid peroxidation. All the copper complexes showed potent cytotoxic activity and had IC_{50} less then 100 µg/ml dosage. Amongst copper metal complexes, maximum toxicity was seen with the complexes of thiocyanate derivative. Thiocyanate is a known inhibitor of the mitochondrial enzyme cytochrome C oxidase. As thiocyanate complexes can damage the oxidative phosphorylation, they can directly inhibit the cell metabolism and deprive the cell of ATP. This trend was pertinent in our study and we could observe maximum toxicity with cyanide complexes. In general copper complexes had potent cytotoxic property and they need further exploration for their anticancer property.

Cobalt is essential to all animals, including humans. It is a key constituent of cobalamin, also known as vitamin B12, which is the primary biological reservoir of cobalt as an "ultratrace" element. Our study showed similar profile and showed varied cytotoxicity of cobalt chloride with increase in dose. Cobalt complexes were found to be significantly toxic due to the presence of thiocyanate, which may be attributed to the presence of thiocyanate in it.

Nickel is a carcinogenic metal and can be highly toxic to living organisms. Our study showed similar profile and showed that Nickel chloride had significant cytotoxic activity. Nickel complexes were also found to be toxic, and maximum toxicity profile was observed selenocyanate complexes. Toxicity profile of the complexes was similar with the metal and hence it was easy to conclude that biological activities of the nickel metal complexes were mainly attributed to its metal content.

Cadmium is a toxic metal, contributing to many occupation diseases. Our study showed that cadmium acetate salt was highly toxic to the HL 60 cells. Compared to the salt, metal complexes had altered toxicity and metal complex formation was slightly ameliorating the toxicity of the cadmium.

Zinc is an essential mineral of having variety of biological activities including many gene regulatory mechanisms [15]. In our study Zinc was found to be boosting the cell growth

in lower doses, suggesting that in low doses zinc might be acting as a supplement which enhanced cell viability. However, a further detailed exploration is needed to understand the cell boosting potential of Zinc in increasing the cell viability. Also, one needs to explore the carcinogenic potential of Zinc, as it was found to be boosting sarcoma growth in few studies. Zinc complexes were found to be safer compared to all other metal complexes synthesized in this study.

5. Conclusion

In conclusion, it was learnt from this study that metal complexes had altered property compared to their constituting salt or ligand. Toxicity of Cadmium and Nickel complexes were mainly due to their metal content and hence they do not stand as potent candidates for further exploration as anti cancer compounds. However, complexes of copper, cobalt and zinc showed varied activity compared to their salts and hence they can be worth exploring for future avenues for developing new anticancer drugs.

Table 1: Cytotoxicity of Copper complexes.

Compound	10	20	100	200
Cisplatin	44.043010	18.637990	14.222220	17.204300
$Cu(CH_3COO)_2.H_2O$ salt	25.290320	16.516130	23.913980	49.720430
Ligand	78.090000	45.987000	34.987000	32.170000
$[Cu(Cl)L'\text{-}(\mu\text{-}Cl)\text{-}CuL'(pz)](PF_6)_2$	83.440860	57.634410	64.000000	53.677420
$[Cu_2L_2(N_3)_2](ClO_4)_2$	45.764230	34.753280	38.022160	47.828780
$[Cu_2L_2(NCO)_2](PF_6)_2$	57.291310	35.957610	40.946940	38.366250
$[CuL'(NCS)_2]$	67.234000	47.234000	12.234000	4.230000
$[Cu(L)(N_3)]_2(BF_4)_2$	57.291310	35.957610	40.946940	38.366250
$[CuL(CH_3COO)]PF_6.H_2O$	80.860210	45.763440	53.333330	51.956990
$[CuL(NCS)]PF_6$	73.807200	37.169300	23.298000	14.491000

Table 2: Cytotoxicity of Cobalt complexes.

Compound	10	20	100	200
Cisplatin	44.043010	18.637990	14.222220	17.204300
$Co(CH_3COO)_2.6H_2O$ salt	42.838710	22.709680	39.913980	71.569890
Ligand	78.090000	45.987000	34.987000	32.170000
$[CoL(Cl)](BF_4).H_2O\ {}^1/_2CH_3OH$	50.581520	38.538300	50.409470	41.635120
$[CoL(SeCN)(H_2O)](ClO_4)$	62.280640	33.376920	29.879000	25.118710
$[CoL(NCS)_2]$	62.280640	33.376920	40.430800	25.118710

Table 3: Cytotoxicity of Nickel complexes.

Compound	10	20	100	200
Cisplatin	44.043010	18.637990	14.222220	17.204300
Ni $(CH_3COO)_2.6H_2O$ salt	36.301070	18.236560	13.075270	27.354840
Ligand	78.090000	45.987000	34.987000	32.170000
$[Ni_2L_2(N_3)_2](ClO_4)_2.2C_2H_5OH$	57.291310	38.022160	32.516690	17.204600
$[NiL(NCO)]_2(PF_6)_2$	62.280640	33.721010	44.731950	36.645790
$[NiL(SeCN)(H_2O)](ClO_4)$	34.489000	19.290000	12.000000	3.989000
$[NiLCl_2]$	65.204300	30.967740	33.204300	12.215050

Table 4: Cytotoxicity of Cadmium complexes.

Compound	10	20	100	200
Cisplatin	44.043010	18.637990	14.222220	17.204300
$Cd(CH_3COO)_2.6H_2O$ salt	78.623660	39.053760	12.908000	5.987000
Ligand	78.090000	45.987000	34.987000	32.170000
$[CdL(N_3)]PF_6$	89.118280	70.365590	70.537640	32.333330
$[Cd(NCS)_2L]$	76.239000	44.298000	29.870000	22.387470

Table 5: Cytotoxicity of Zinc complexes.

Compound	10	20	100	200
Cisplatin	44.043010	18.637990	14.222220	17.204300
$Zn(CH_3COO)_2.H_2O$ salt	124.215100	74.322580	41.118280	81.720430
Ligand	78.090000	45.987000	34.987000	32.170000
$[ZnL(N_3)]PF_6$	99.612900	38.365590	62.279570	59.010750
$[ZnL(NCS)_2]$	73.634410	48.688170	68.645160	43.182800
$[Zn_2L_2(NCO)_2](PF_6)_2$	73.634410	48.688170	68.645160	43.182800

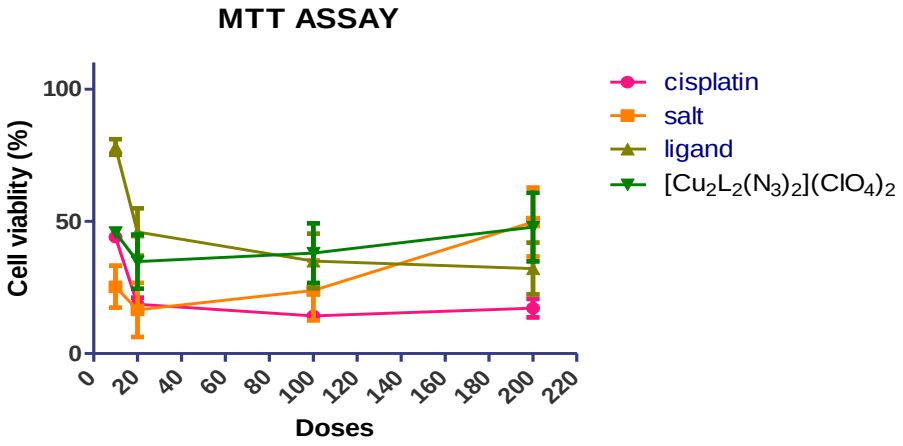
MTT ASSAY
Cell viablity (%)
100
50
0
0 20 40 60 80 100 120 140 160 180 200 220
Doses
cisplatin
salt
ligand
[Cu2L2(N3)2](ClO4)2

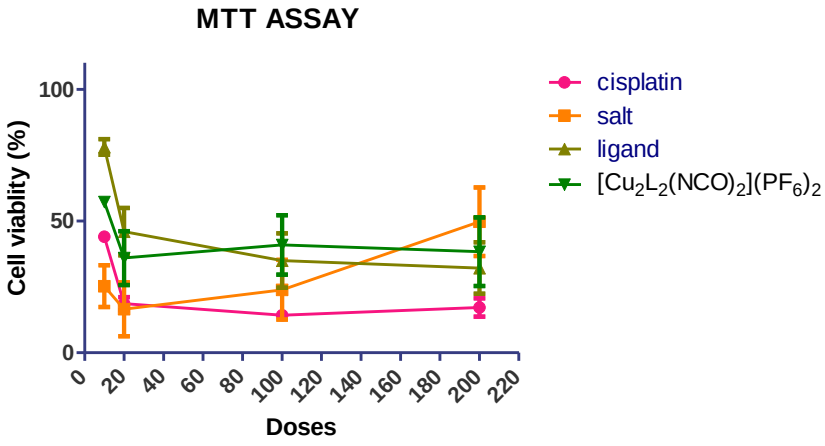
MTT ASSAY
Cell viablity (%)
100
50
0
0 20 40 60 80 100 120 140 160 180 200 220
Doses
cisplatin
salt
ligand
[Cu2L2(NCO)2](PF6)2

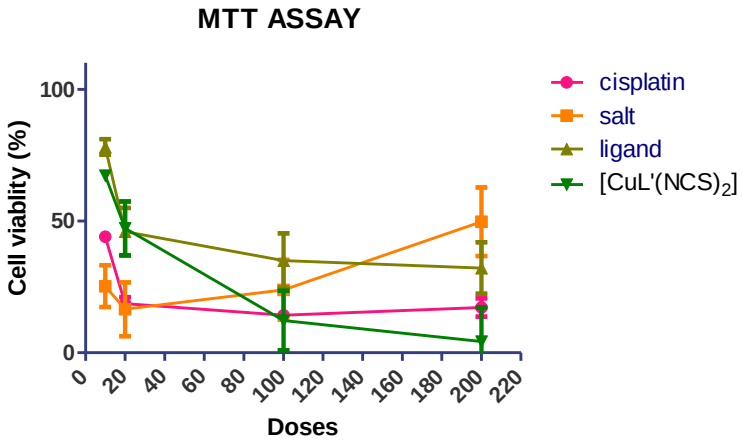
MTT ASSAY
Cell viablity (%)
100
50
0
0 20 40 60 80 100 120 140 160 180 200 220
Doses
cisplatin
salt
ligand
[CuL'(NCS)2]

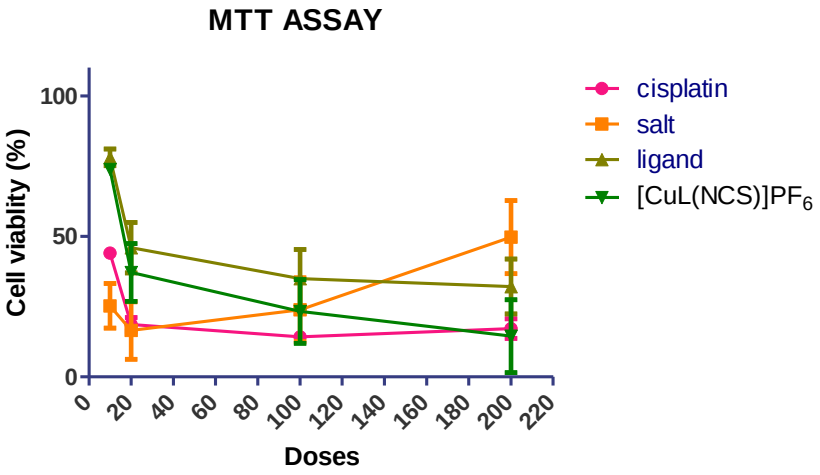
MTT ASSAY
Cell viablity (%)
100
50
0
0
20
40
60
80
100
120
140
160
180
200
220
Doses
cisplatin
salt
ligand
[CuL(NCS)]PF6

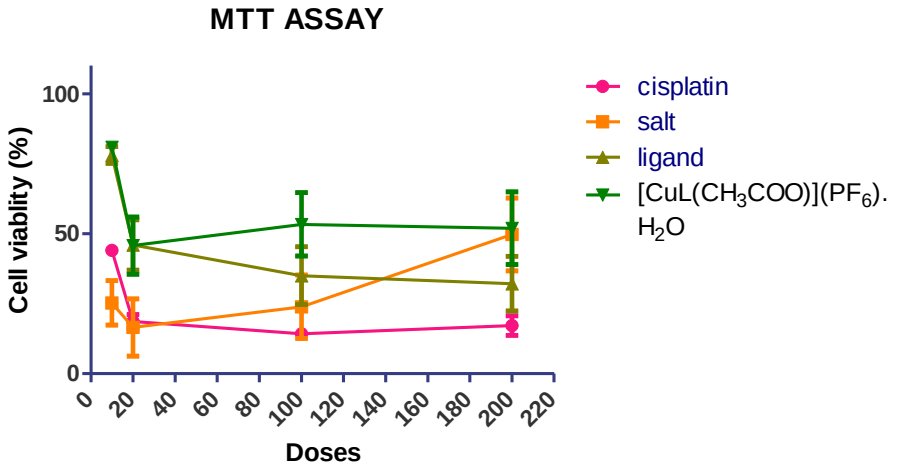
MTT ASSAY
Cell viablity (%)
100
50
0
0
20
40
60
80
100
120
140
160
180
200
220
Doses
cisplatin
salt
ligand
[CuL(CH3COO)](PF6).
H2O

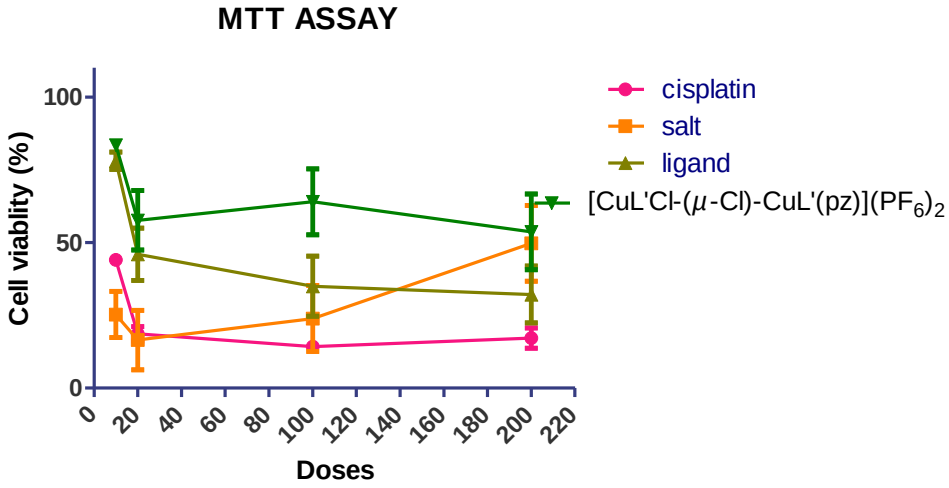
MTT ASSAY
Cell viablity (%)
100
50
0
0
20
40
60
80
100
120
140
160
180
200
220
Doses
cisplatin
salt
ligand
[CuL'Cl-(μ-Cl)-CuL'(pz)](PF6)2

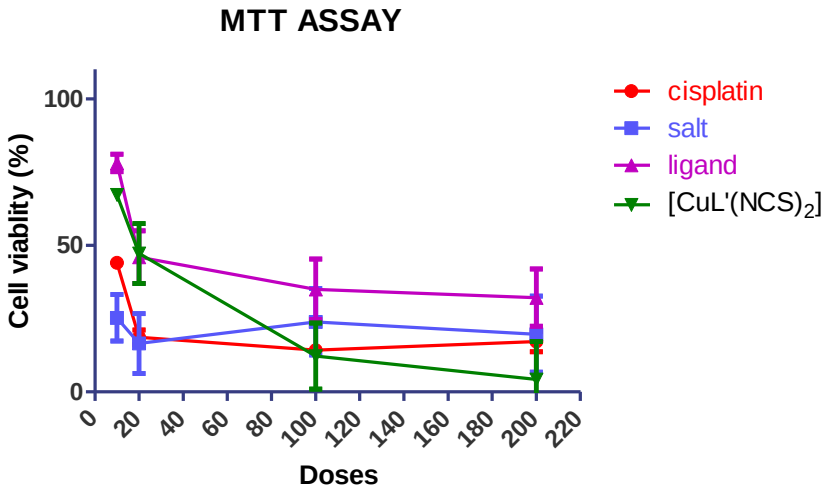
MTT ASSAY
Cell viability (%)
100
50
0
0
20
40
60
80
100
120
140
160
180
200
220
Doses
cisplatin
salt
ligand
[CuL'(NCS)2]

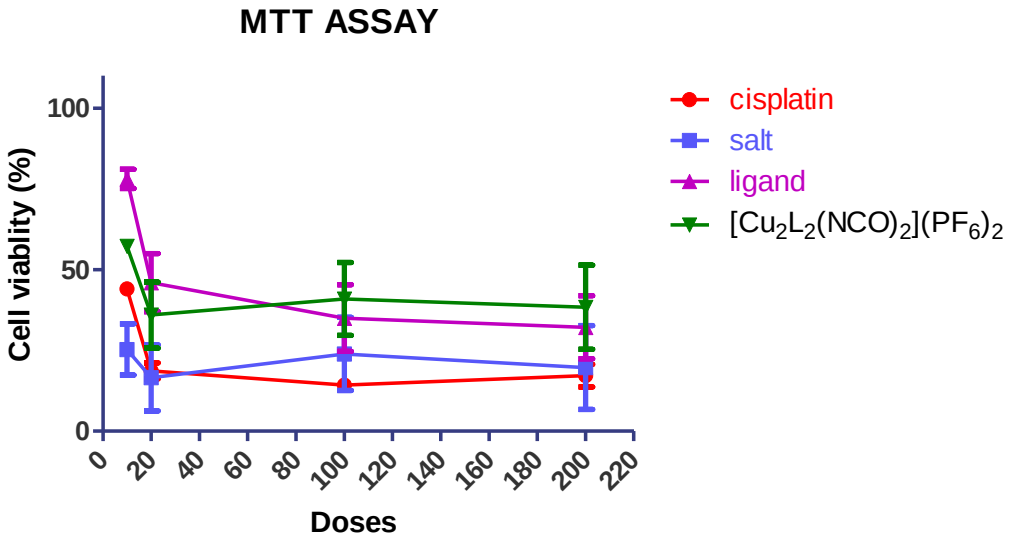
MTT ASSAY
Cell viability (%)
100
50
0
0
20
40
60
80
100
120
140
160
180
200
220
Doses
cisplatin
salt
ligand
[Cu2L2(NCO)2](PF6)2

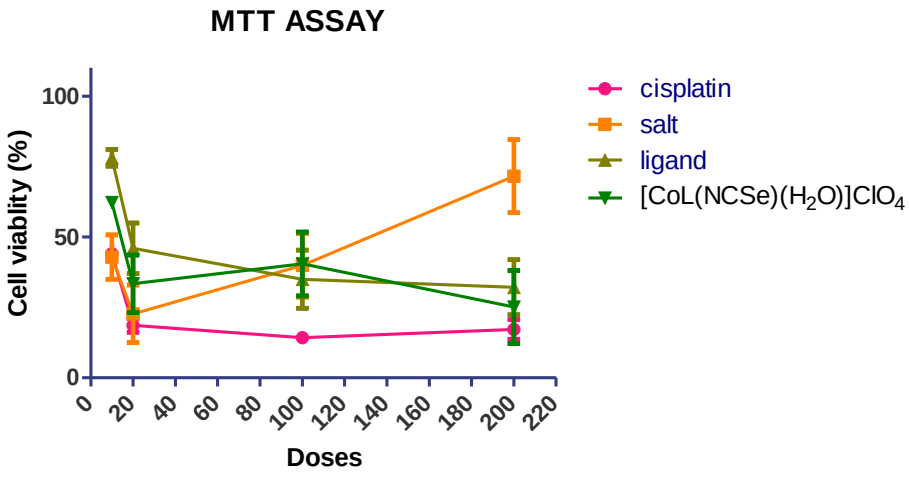
MTT ASSAY
Cell viablity (%)
100
50
0
0 20 40 60 80 100 120 140 160 180 200 220
Doses
cisplatin
salt
ligand
[CoL(NCSe)(H2O)]ClO4

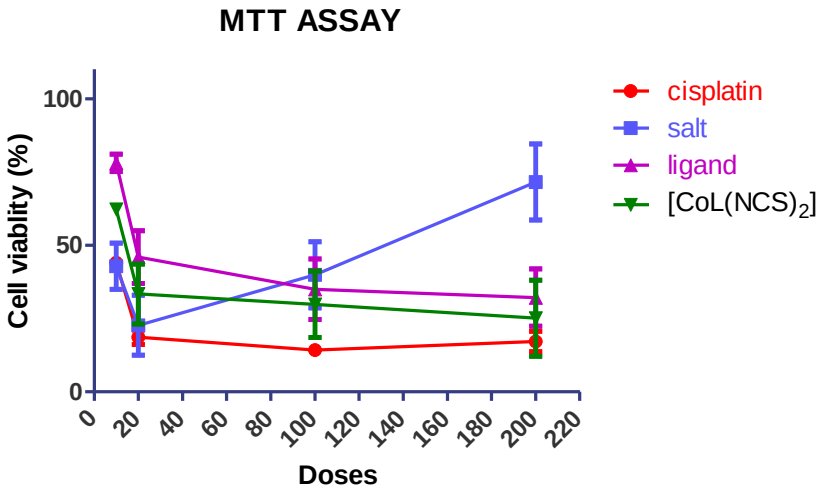
MTT ASSAY
Cell viablity (%)
100
50
0
0 20 40 60 80 100 120 140 160 180 200 220
Doses
cisplatin
salt
ligand
[CoL(NCS)2]

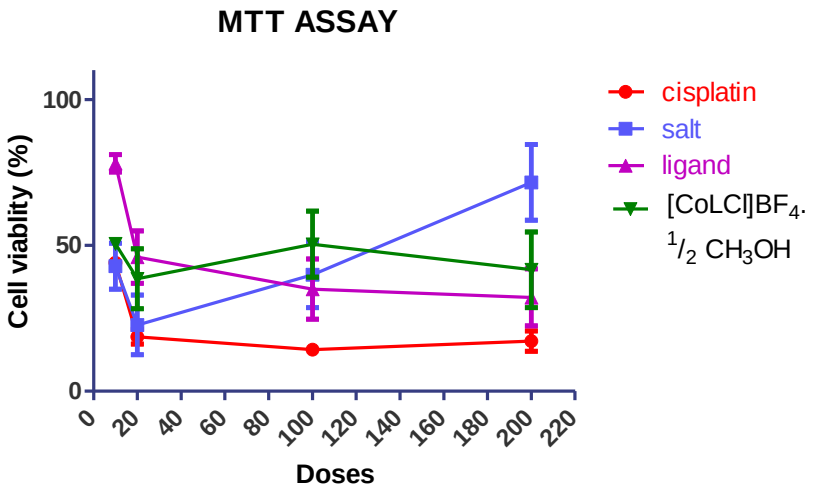
MTT ASSAY
Cell viablity (%)
100
50
0
0 20 40 60 80 100 120 140 160 180 200 220
Doses
cisplatin
salt
ligand
[CoLCl]BF4.
1/2 CH3OH

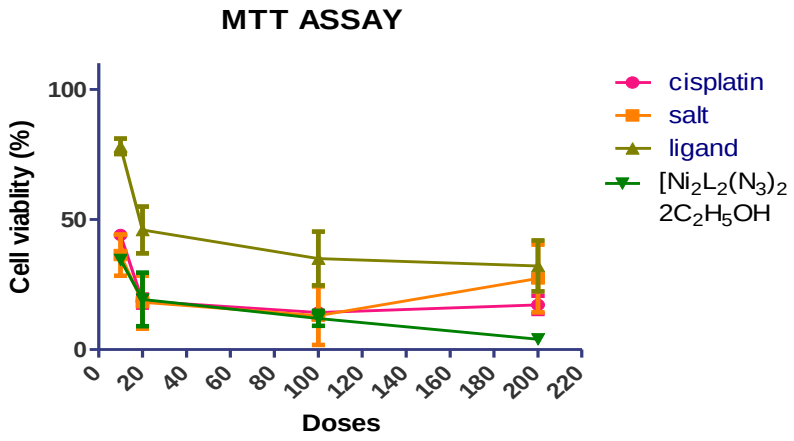
MTT ASSAY
Cell viability (%)
100
50
0
0 20 40 60 80 100 120 140 160 180 200 220
Doses
cisplatin
salt
ligand
[Ni2L2(N3)2 2C2H5OH

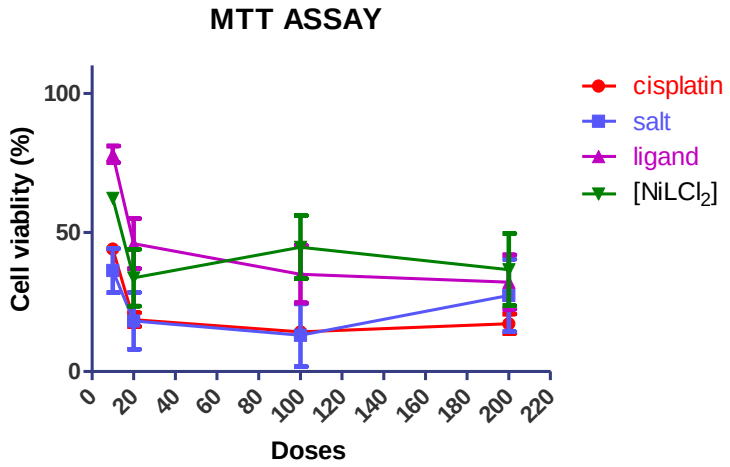
MTT ASSAY
Cell viability (%)
100
50
0
0 20 40 60 80 100 120 140 160 180 200 220
Doses
cisplatin
salt
ligand
[NiLCl2]

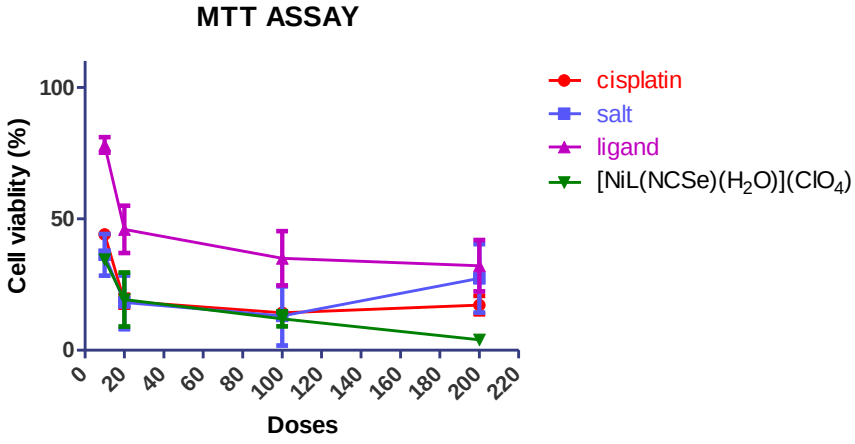
MTT ASSAY
Cell viability (%)
100
50
0
0 20 40 60 80 100 120 140 160 180 200 220
Doses
cisplatin
salt
ligand
[NiL(NCSe)(H2O)](ClO4)

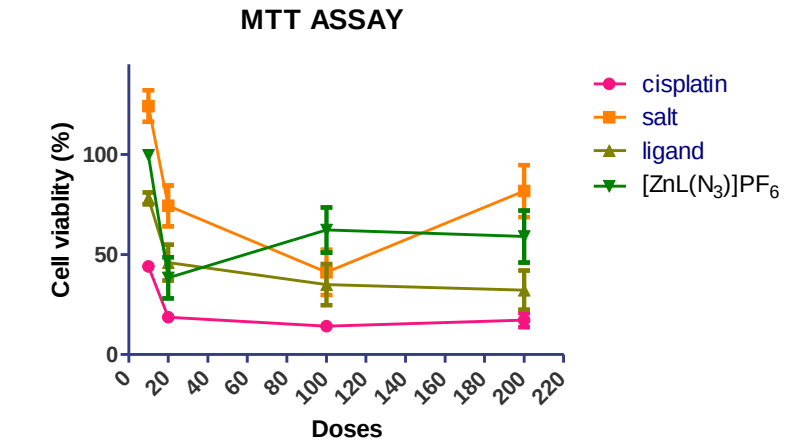
MTT ASSAY
Cell viablity (%)
Doses
cisplatin
salt
ligand
[ZnL(N3)]PF6

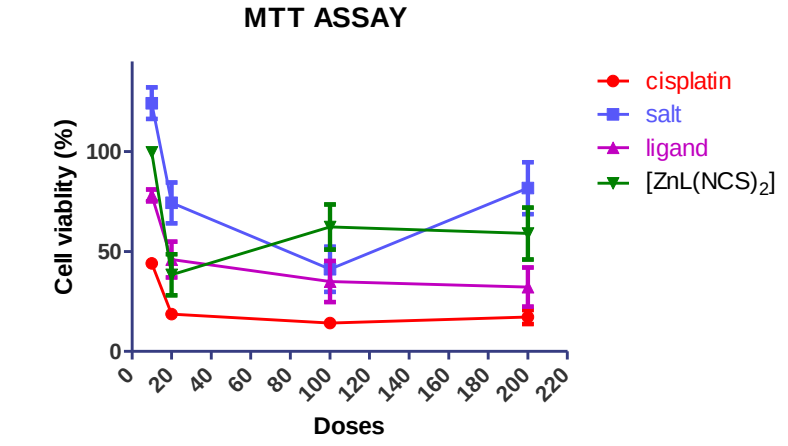
MTT ASSAY
Cell viablity (%)
Doses
cisplatin
salt
ligand
[ZnL(NCS)2]

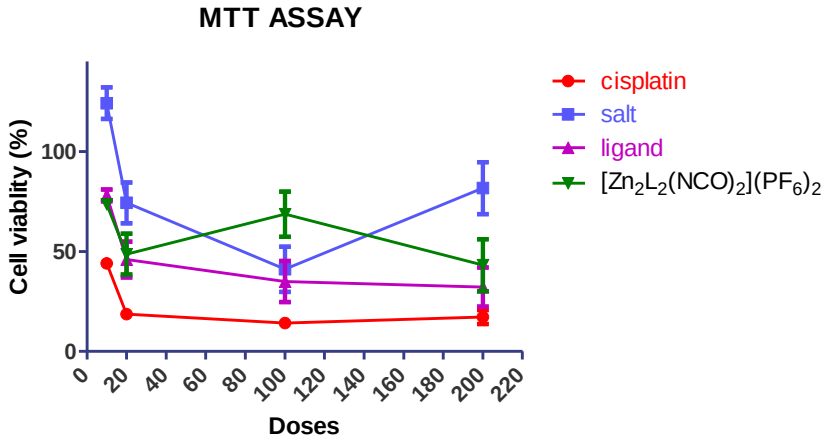
MTT ASSAY
Cell viablity (%)
Doses
cisplatin
salt
ligand
[Zn2L2(NCO)2](PF6)2

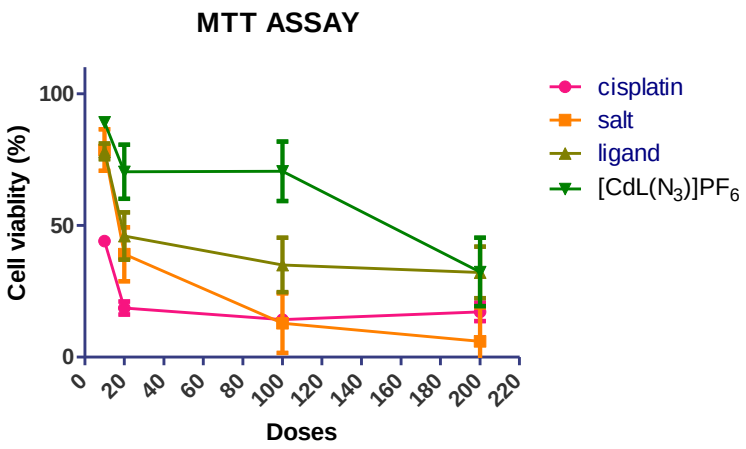
MTT ASSAY
Cell viablity (%)
100
50
0
0
20
40
60
80
100
120
140
160
180
200
220
Doses
cisplatin
salt
ligand
[CdL(N3)]PF6

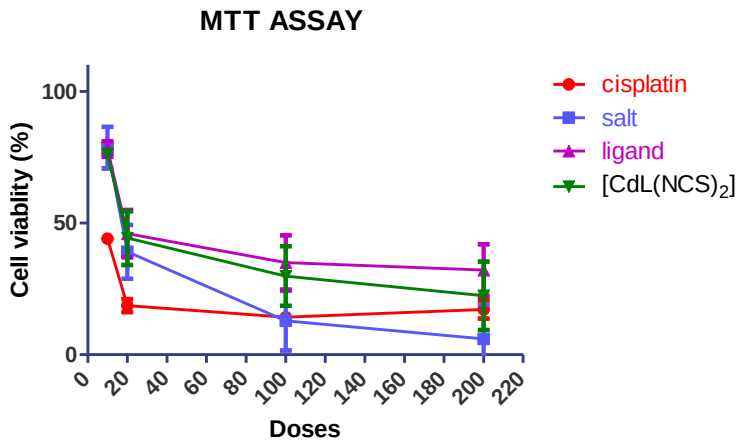
MTT ASSAY
Cell viablity (%)
100
50
0
0
20
40
60
80
100
120
140
160
180
200
220
Doses
cisplatin
salt
ligand
[CdL(NCS)2]

References:

1. Kishu Tripathi J. Research Chem.2009, 2(1): Jan.-March,
2. Ansari KI, Grant JD, Kasiri S, Woldemariam G, Shrestha B, Mandal SS. J. Inorg. Biochem. 2009,103(5): 818-26.
3. Aras MA, Hara H, Hartnett KA, Kandler K, Aizenman E. J. Neurochem. 2009,110(1): 106-107.
4. Chen D, Milacic V, Frezza M, Dou QP.Curr. Pharm. Des. 2009, 15(7): 777-791.
5. Cohen SM, Lippard SJ. Prog. Nucleic Acid Res. Mol. Biol. 2001, 67: 93-130.
6. Shazia Rafique*, Muhammad Idrees, Anwar Nasim, Haji Akbar and Amin Athar, Biotechnology and Molecular Biology Reviews April 2010,Vol. 5(2), pp. 38-45,.
7. Martins ET, Baruah H, Kramarczyk J, Saluta G, Day CS, Kucera GL Bierbach U . J. Med. Chem. 2001, 44: 4492-4496.
8. Luboldt W, Pinkert J, Matzky C, Wunderlich G, Kotzerke. J. Curr. Drug Deliv. 2009,6(3): 255-260.
9. M. Patriarca, N.A. Kratochwil and P.J. Sadler in Plasma Source Mass Spectrometry, G. Holland and S.C. Tanner, eds. Roy. Soc. Chem., Cambridge, 1999, pp199-207
10. Camins A, Crespo-Biel N, Junyent F, Verdaguer E, Canudas AM, Pallàs M . Curr. Drug Metab. 2009, 10(5): 433-47
11. Satoru Kawaii1 and Ephraim P. Lansky J. Med. Food., 7 (1) 2004, 13–18
12. Parikh, P., Suresh, B. and Rangrez, A.. Electronic Journal of Pharmacology & Therapy, 2009, 2: 81-86.
13. H. Li, P.J. Sadler and H. Sun J. Biol. Chem. 1996, 271, 9483-9489.
14. J.D. Ranford P.J. Sadler and D.A. Tocher J. Chem.Soc., Dalton Trans., 1993, 3393-3399.
15. J.H. Viles, S.U. Patel, J.B.O. Mitchell, C.M. Moody, D.E. Justice, J. Uppenbrink, P.M. Doyle, C.J. Harris, P.J. Sadler and J.M. Thornton J. Mol. Biol. 1998, 279, 973-986.

SYNOPSIS

Syntheses, Characterization and Cytotoxic Activity Of Some Metal Complexes With Pyridylpyrazole Ligand

Mr. Zala Mahendrasinh G. (M. Sc)

Department of Chemistry
Faculty of Science
The Maharaja Sayajirao University of Baroda
VADODARA – 390 002
GUJARAT, INDIA

Syntheses, Characterization and Cytotoxic Activity of Some Metal Complexes with Pyridylpyrazole Ligand

The coordination complexes of copper(II), nickel(II), cobalt(II), zinc(II) and cadmium(II) using pyridylpyrazole based ligand have been described in this work. The pyridylpyrazole ligand used in this work is *N*,*N*-bis(3,5-dimethyl-1-ylmethyl)amino-methylpyridine. The ligand has been characterized by ^{1}H NMR, ^{13}C NMR, IR and microanalysis. The compounds have been characterized by microanalysis and spectroscopic data. The general introduction of our work has been described in Chapter I and bench work is described in Chapter II to VI. In Chapter II synthesis and characterization of ligand and some mononuclear complexes of copper(II), cobalt(II) and nickel(II) and two binuclear copper(II) complexes with pyridylpyrazole ligand are described. In Chapter III mononuclear thiocyanate/selenocyanate complexes containing copper(II), nickel(II) and cobalt(II) with pyridylpyrazole ligand L are described. The complexes are characterized by IR spectra, magnetic and single crystal X-ray diffraction study. In Chapter IV synthesis, characterization, structure and magnetic study of azido and cayanato bridged nickel(II) and copper(II) complexes with pyridylpyrazole ligand has been described and it has divided into two sections. In Chapter IVA synthesis, characterization, structure and magnetic study of azido bridged nickel(II) and copper(II) complexes with pyridylpyrazole ligand has been described. Synthesis, characterization, structure and magnetic study of cyanato bridged nickel(II) and copper(II) complexes with pyridylpyrazole ligand has been described in chapter IVB. In Chapter V psuedohalides (N_3^-, NCO^- and NCS^-) containing mono- and binuclear complexes of cadmium(II) and zinc(II) with pyridylpyrazole ligand have been synthesized and characterized by microanalysis, IR spectra and X-ray diffraction study. In Chapter VI, we have checked the cytotoxic activity some of coppeer(II), cobalt(II), nickel(II), zinc(II) and cadmium(II) complexes with HL 60 (Human promyelocytic leukemia cells) and it shows that both ligand and complexes have cytotoxic activity.

Chapter II

In this chapter, synthesis of pyridylpyrazole based ligand *N*,*N*-bis(3,5-dimethylpyrazol-1-ylmethyl)aminomethylpyridine has been discussed and this ligand was characterized by ^{1}H NMR, ^{13}C NMR, IR, microanalysis [Fig.1]. Mononuclear complexes of the type $[Cu(L)(CH_3COO)]X$ (X= PF_6^- and BF_4^-), $[Co(L)(Cl)]Y$ (Y= PF_6^-, BF_4^- and ClO_4^-), and $[Ni(L)Cl_2]$ and binuclear Cu(II) complexes $[CuL'(Cl)\text{-}(\mu\text{-}Cl)\text{-}Cu(pz)L'](Z)_2$ (Z = PF_6^- and ClO_4^-) (L = *N*,*N*-bis(3,5-dimethylpyrazol-1-ylmethyl)aminomethylpyridine and L' = *N*-(3,5-dimethylpyrazol-1-ylmethyl)aminomethylpyridine) have been synthesized and characterized by elemental analysis, spectroscopic and physico-chemical method. Crystal structure of the complexes $[CuL(CH_3COO)]PF_6.H_2O$ [Fig. 2], $(CoClL)BF_4.{}^1/_2(CH_3OH)$ [Fig. 3] and $[CuL'(Cl)\text{-}(\mu\text{-}Cl)\text{-}Cu(pz)L'](PF_6)_2$ [Fig. 4] have been solved by single crystal X-ray diffraction study. Crystal structure of $[CuL(CH_3COO)]PF_6.H_2O$ shows that copper atom adopts a five coordination with distorted square bipyramidal geometry. In $(CoClL)BF_4.{}^1/_2(CH_3OH)$, cobalt(II) has penta coordination and it has trigonal bipyrmidal geometry. For binuclear chloride bridged copper(II) complex, the crystal structure of $[CuL'(Cl)\text{-}(\mu\text{-}Cl)\text{-}Cu(pz)L'](PF_6)_2$ shows that two square planer copper(II) complexes are attached by single chloride (μ-Cl) bridge and coordination environment around two copper atoms are different.

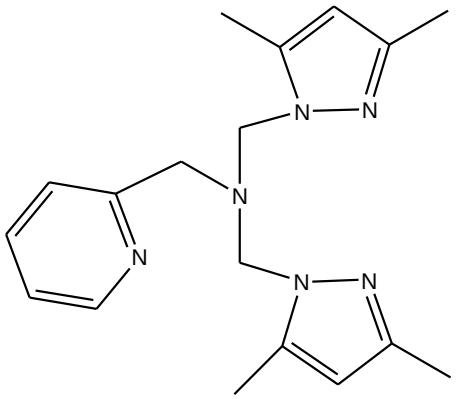

Fig.1. *N*,*N*-bis(3,5-dimethylpyrazol-1-ylmethyl)aminomethylpyridine (Ligand)

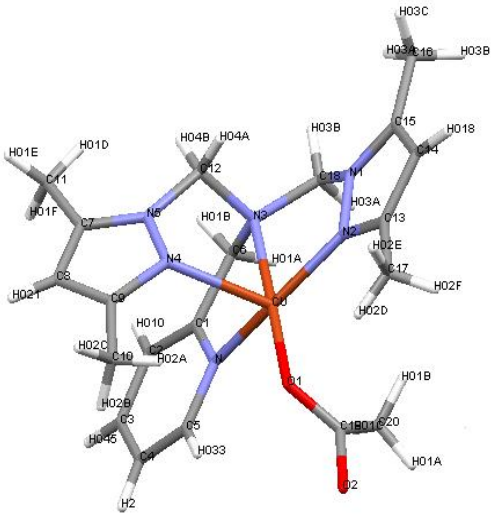

Fig. 2. ORTEP diagram depicting the cationic part of the complex $[CuL(CH_3COO)](PF_6).H_2O$

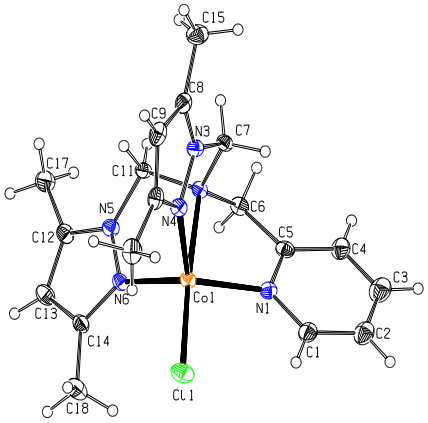

Fig. 3. ORTEP diagram depicting the part of cationic part of one molecule of the complex $[CoLCl](BF_4).^1/_2(CH_3OH)$

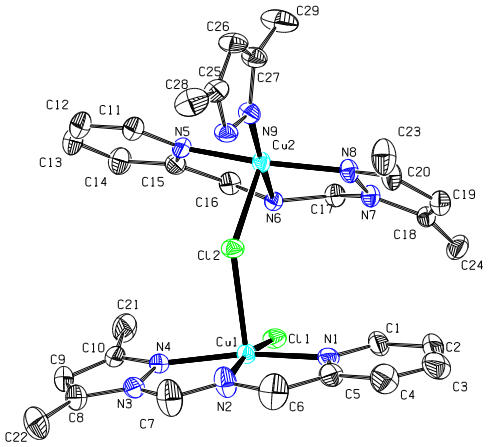

Fig. 4. ORTEP diagram depicting the cationic part of $[CuL'(Cl)\text{-}(\mu\text{-}Cl)\text{-}Cu(pz)L'](PF_6)_2$ with atom numbering scheme

Chapter III

Mononuclear NCS^- containing complexes, $[M(NCS)_2L]$ (L = *N*,*N*-bis(3,5-dimethyl pyrazol-1-ylmethyl)aminomethylpyridine), $[Cu(NCS)_2L']$ (L' = *N*-(3,5-dimethylpyrazol-1-ylmethyl)aminomethylpyridine) and $NCSe^-$ containing complexes $[ML(NCSe)(H_2O)](ClO_4)$ (M = Ni^{+2}, Co^{+2}) have been synthesized and characterized by elemental analysis, spectroscopic, and physicochemical methods. Crystal structure of $[Cu(NCS)_2L']$ [Fig. 5] and $[CuL(NCS)]PF_6$ [Fig. 6] have been solved by single crystal X-ray diffraction study. The structure of $[Cu(NCS)_2L']$ show copper has five coordination with distorted trigonal bipyramidal geometry with two NCS^- in the equatorial plane and bonded through nitrogen with copper atom whereas $[CuL(NCS)]PF_6$ has distorted square pyramidal geometry. $[M(NCS)_2L]$ and $[ML(NCSe)(H_2O)]ClO_4$ (M= Ni^{+2} and Co^{+2}) are expected to be octahedral. $[Cu(NCS)_2L']$ complex has been synthesized according to scheme 1 where tetradentate N_4- coordinated ligand L has been transformed into N_3-coordinated ligand L' during reaction but $[CuL(NCS)]PF_6$ complex has been synthesized following the scheme 2 where NCS^- is obtained from ligand 3,5-dimethyl-1-thiocarboxamide pyrazole during reaction.

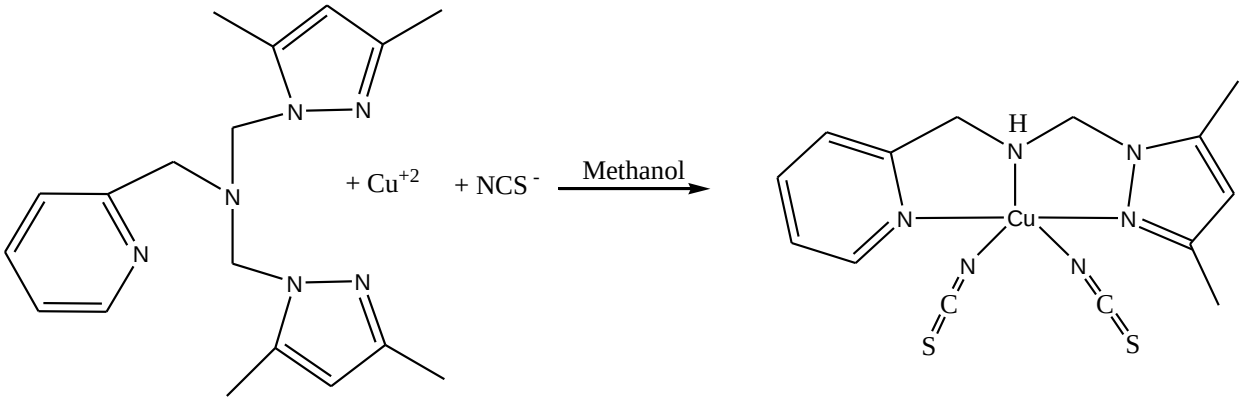

Scheme 1 Synthesis of complex $[Cu(NCS)_2L']$

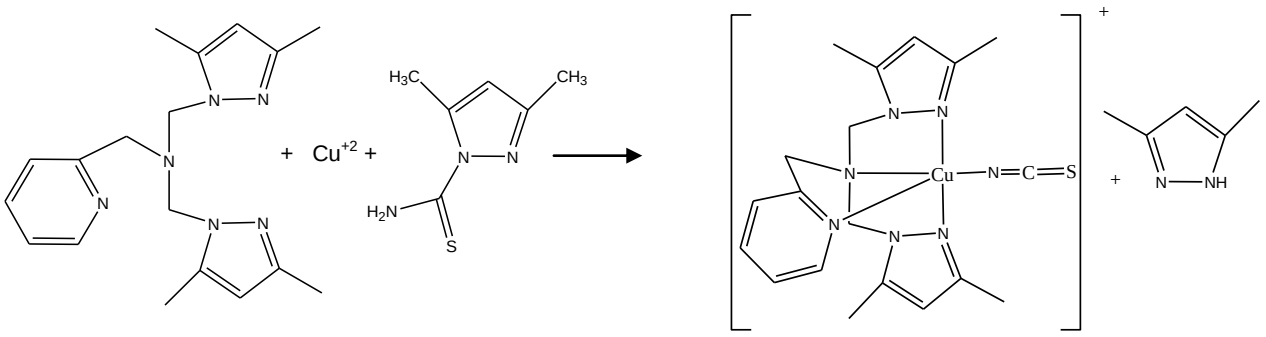

Scheme 2. Synthesis of $[CuL(NCS)]^{+}$

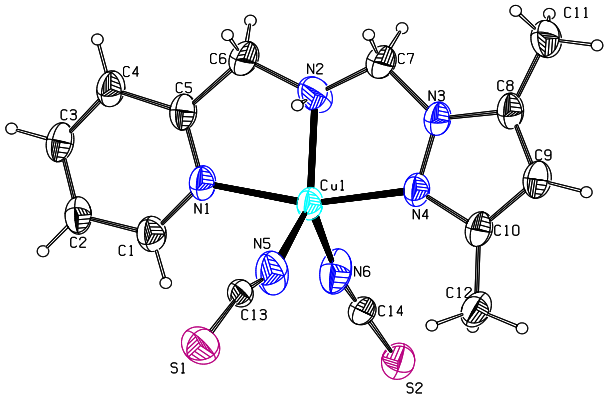

Fig. 5. ORTEP diagram of complex $[Cu(NCS)_2L']$ with atom numbering scheme

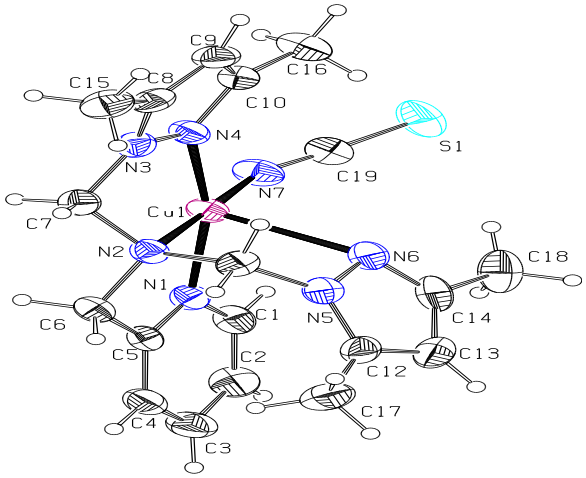

Fig. 6. ORTEP diagram of complex $[CuL(NCS)]PF_6$ with atom numbering scheme

Chapter IV-A

Two binuclear azido bridged nickel(II) complexes, $[Ni_2(L)_2(N_3)_2](X)_2.2EtOH$ ($X = ClO_4^-$ and PF_6^-) and three azido bridged copper(II) complexes, $[Cu_2(L)_2(N_3)_2](Y)_2$ ($Y = ClO_4^-$, PF_6^- and BF_4^-) have been synthesized with the ligand *N*,*N*-bis(3,5-dimethylpyrazol-1-ylmethyl)aminomethylpyridine (L) and characterized by physico-chemical and spectroscopic methods. The Crystal structures of $[Ni_2(L)_2(N_3)_2](ClO_4)_2.2EtOH$ [Fig. 7] and $[Cu_2(L)_2(N_3)_2](ClO_4)_2$ [Fig. 8] are solved by single crystal X-ray diffraction study. Each metal atom in the complexes has a MN_6 coordination environment with distorted octahedral geometry. Variable-temperature magnetic susceptibility measurements for complex $[Ni_2(L)_2(N_3)_2](ClO_4)_2.2EtOH$ show typical antiferromagnetic behavior with *J* value -84.5 ± 1.3 cm^{-1} [Fig. 9], whereas complex $[Cu_2(L)_2(N_3)_2](ClO_4)_2$ has no magnetic interactions.[Fig.10]

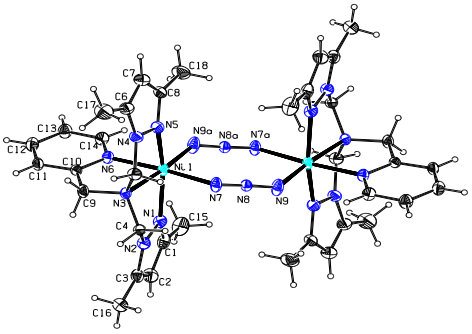

Fig.7 ORTEP diagram of complex $[Ni_2L_2(N_3)_2](ClO_4)_2.2C_2H_5OH$ with atom numbering scheme

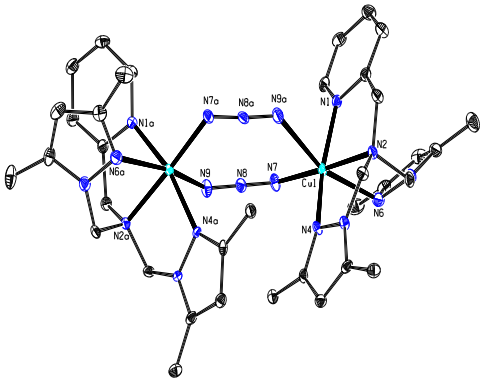

Fig.8. ORTEP diagram of complex $[Cu_2L_2(N_3)_2](ClO_4)_2$ with atom numbering scheme

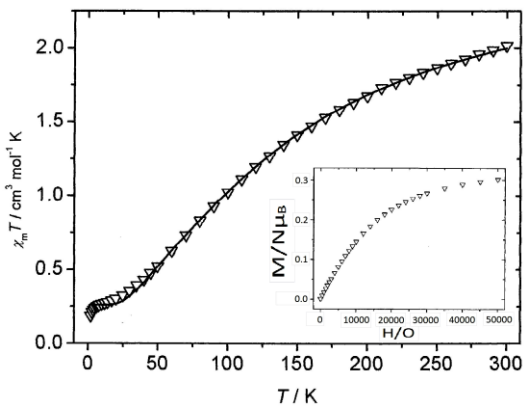

Fig.9. Variable temperature magnetic of behaviour of $[Ni_2L_2(N_3)_2](ClO_4)_2.2C_2H_5OH$ complex

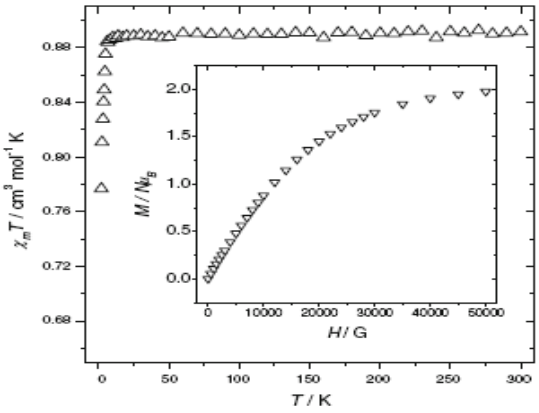

Fig.10. Variable temperature magnetic behaviuor of $[Cu_2L_2(N_3)_2](ClO_4)_2$ complex

Chapter IVB

Two binuclear cyanate bridged nickel(II) complexes $[Ni_2(NCO)_2L_2](X)_2$ (X= PF_6^- and BF_4^-) and two binuclear cayanate bridged copper(II) complexes $[Cu_2(NCO)_2L_2](Y)_2$ (Y= PF_6^- and BF_4^-), where L is *N*,*N*-bis(3,5-dimethylpyrazol-1-ylmethyl)aminomethyl-pyridine, a tetradentate N_4-coordinated ligand have been synthesized and characterized by physicochemical method. Crystal structure of the complexes $[Ni_2(NCO)_2L_2](PF_6)_2$ [Fig. 11] and $[Cu_2(NCO)_2L_2](PF_6)_2$ [Fig. 12] have been solved. Coordination mode of cyanate ligand is end-to-end (μ-1,3) for complex $[Ni_2(NCO)_2L_2](PF_6)_2$, but it is end-on (μ-1,1) mode for complex $[Cu_2(NCO)_2L_2](PF_6)_2$. Magnetic susceptibility data, measured from 2-300 K, show weak antiferromagnetic interaction with *J* value -6.2(1) cm^{-1} for complex $[Ni_2(NCO)_2L_2](PF_6)_2$, whereas complex $[Cu_2(NCO)_2L_2](PF_6)_2$ has very weak ferromagnetic interaction with *J* value +0.5(1) cm^{-1} [Fig. 13].

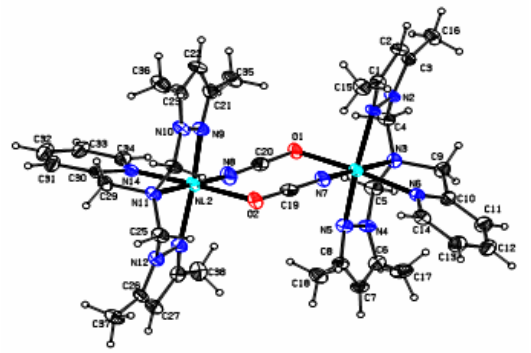

Fig.11. ORTEP diagram of complex $[Ni_2L_2(NCO)_2](PF_6)_2$ with atom numbering scheme

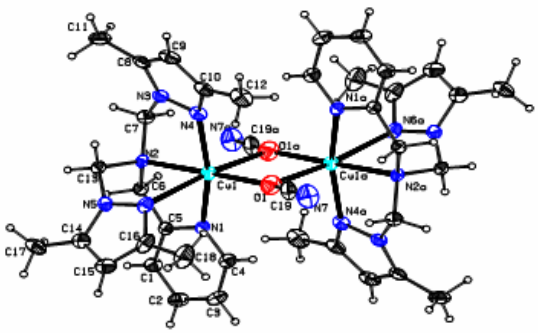

Fig. 12. ORTEP diagram of complex $[Cu_2L_2(NCO)_2](PF_6)_2$ with atom numbering scheme

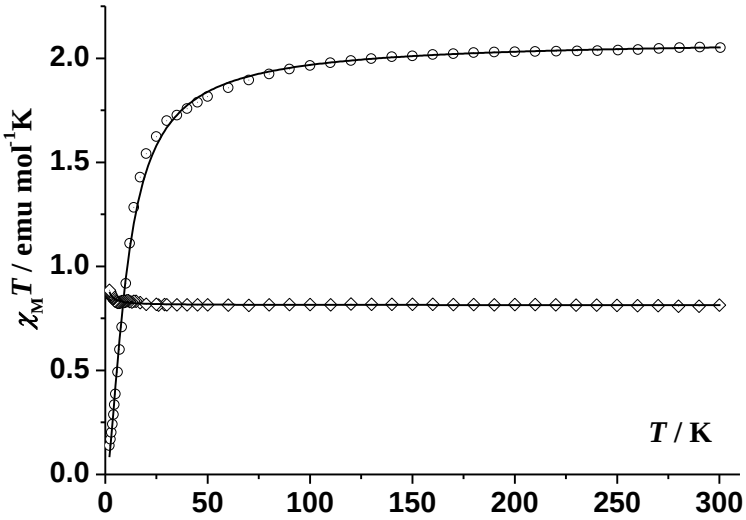

Fig. 13 Variable temperature (2-300K) magnetic study of the $[Ni_2L_2(NCO)_2](PF_6)_2$ (ooo) and $[Cu_2L_2(NCO)_2](PF_6)_2$ (◊◊◊) Complexes.

Chapter V

In this chapter we discussed synthesis of psuedohalides (NCS^-, N_3^-, NCO^-) containing zinc(II) and cadmium(II) complexes with ligand L and these complexes were characterized by IR, ^1H NMR, mass, physico-chemical method. Crystal structure of the complexes $[Cd_2L_2(NCO)_2](PF_6)_2$ [Fig.14] and $[ZnL(N_3)]PF_6$ [Fig.15] have been solved by single crystal X-ray diffraction study. The crystal structure of $[Cd_2L_2(NCO)_2](PF_6)_2$ shows it is a binuclear NCO^- bridged complex and two NCO^- attached with cadmium using end-on coordination mode whereas $[ZnL(N_3)]PF_6$ complex has square pyramidal geometry. All the zinc(II) and cadmium(II) complexes have very weak fluorescence at room temperature.

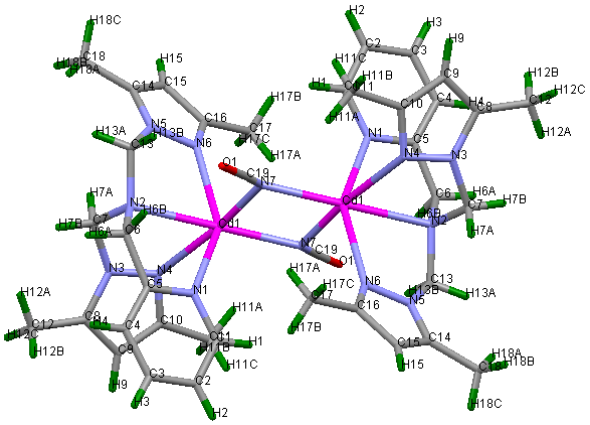

Fig.14. ORTEP diagram of complex $[Cd_2L_2(NCO)_2](PF_6)_2$ with atom numbering scheme

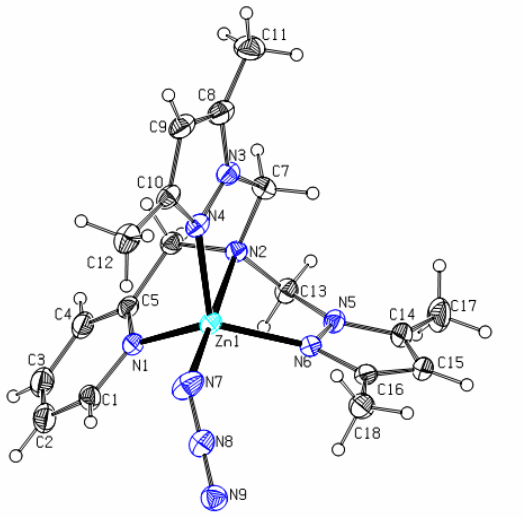

Fig.15. ORTEP diagram of complex $[ZnL(N_3)]PF_6$ with atom numbering scheme

Chapter VI

In this chapter, we evaluate the cytotoxic activity of copper(II), nickel(II), cobalt(II), zinc(II) and cadmium(II) complexes with ligand *N*,*N*-bis(3,5-dimethyl-1-ylmethyl) aminomethylpyridine (L) .

MTT test

HL 60 cell line was obtained from NCCS, Pune and cultured. Upon reaching confluence, the cells were removed, counted and loaded in 96 well plate (Merck Scientific, Bombay) for culturing for 96 hours in 4 increasing concentration (10 µg/mL, 20 µg/mL, 100 µg/mL, 200 µg/mL) of all compounds. After 96 hours, MTT assay was carried out to understand the effect of the metal complexes on cells. HL 60 cells were incubated in a DMEM containing 10% FBS under partial pressure of 5% CO_2 at 37 º C. MTT assay was carried out by placing each cell into each well of 96-well plate; adding 0.05% DMSO containing samples into each well and incubating them for 72 h; adding 0.5 mg/mL MTT into each well and further incubating them for 4 h; dissolving produced formazan crystals in DMSO. All the statistical analyses were carried out using Graphpad Prism 5, and the test for significance was compared using one-way analysis of variance.

We have checked the cytotoxic activity of Cu(II), Ni(II), Co(II), Cd(II) and Zn(II) complexes with pyridylpyrazole ligand. Some of the results are shown in figure 16-24. The pharmacological properties of thiocyanate and selenocyante containing Cu(II) and Ni(II) complexes showed completely different activity than salt or ligand. The results showed that activity of $[CuL(NCS)]PF_6$ and $[NiL(SeCN)(H_2O)](ClO_4)_2$ complexes were mainly attributed to its ligand structure. This activity was quite comparable and dose dependent, indicating that these metal complexes can be a potent candidate for further exploration as an anti cancer agent.

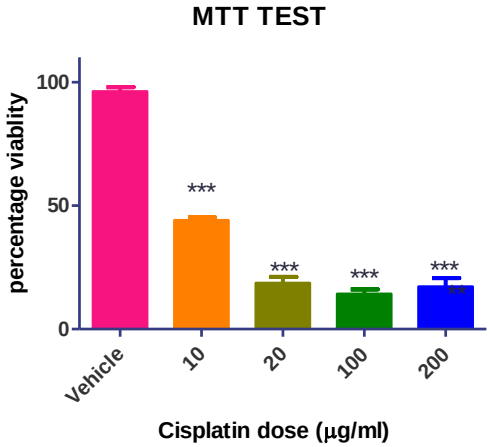

Fig.16

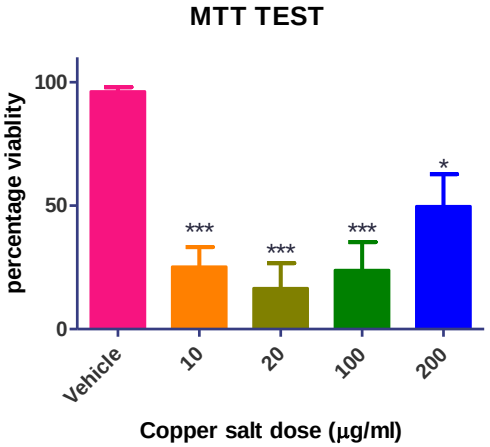

Fig.17

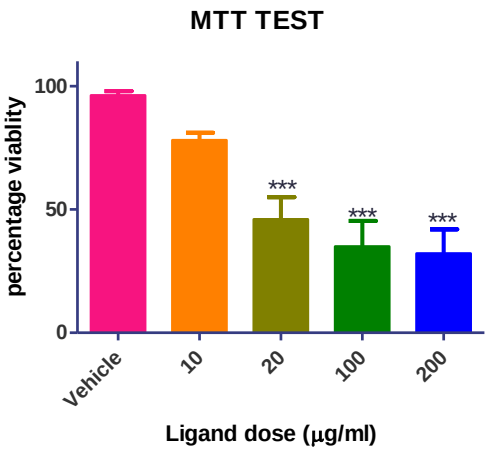

Fig.18

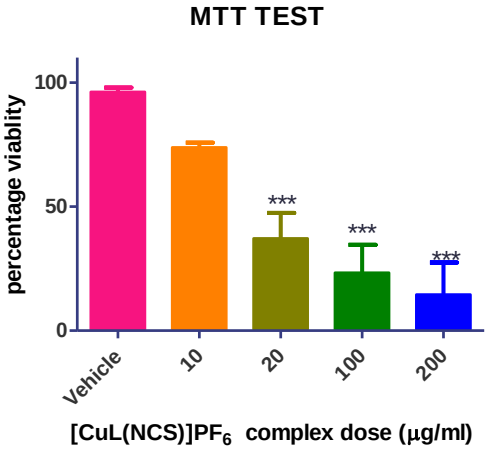

Fig.19

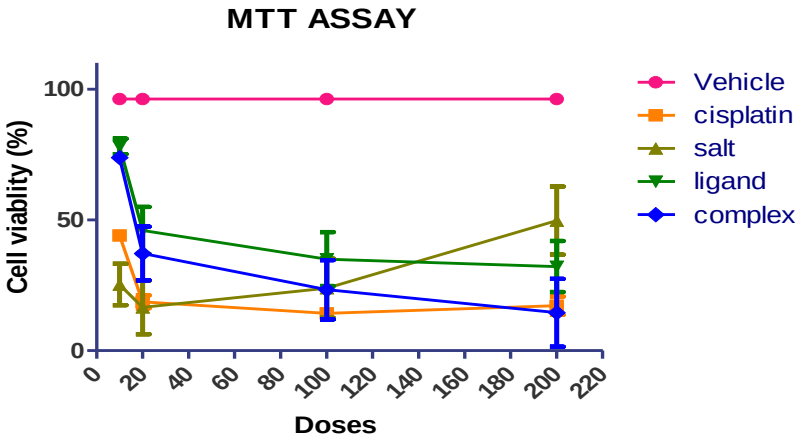

Fig.20

MTT assay of [CuL(NCS)]PF_6 complex.

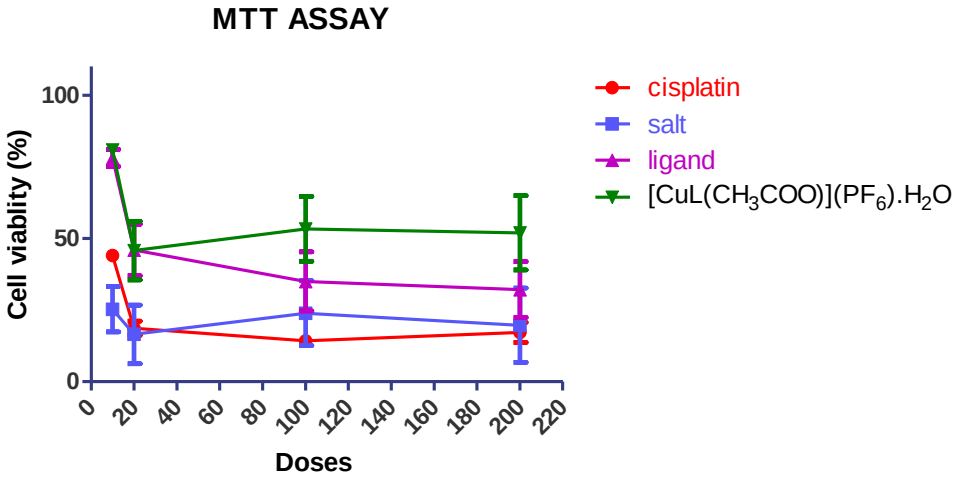

Fig.21 [CuL(CH_3COO)]PF_6 complex.

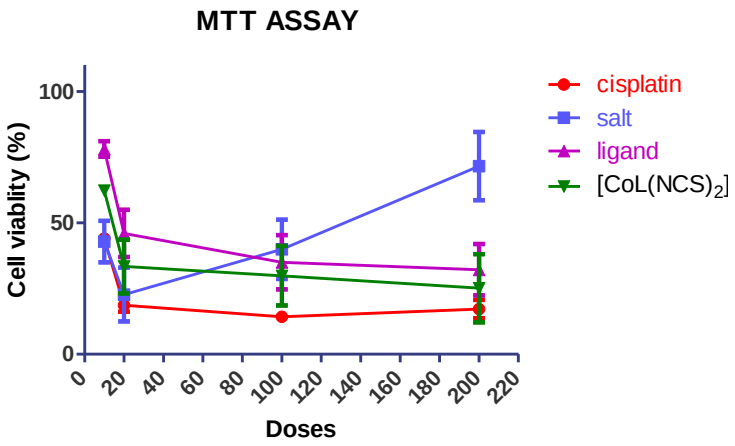

Fig.22 $[CoL(NCS)_2]$ complex.

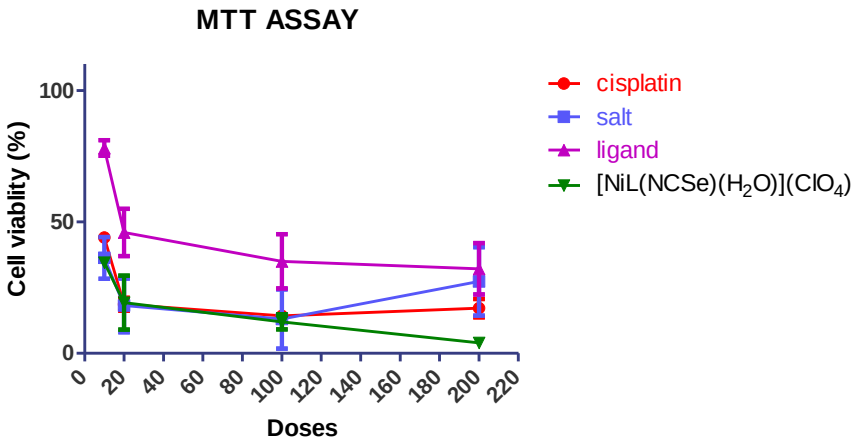

Fig.23 $[NiL(SeCN)(H_2O)](ClO_4)_2$ complex.

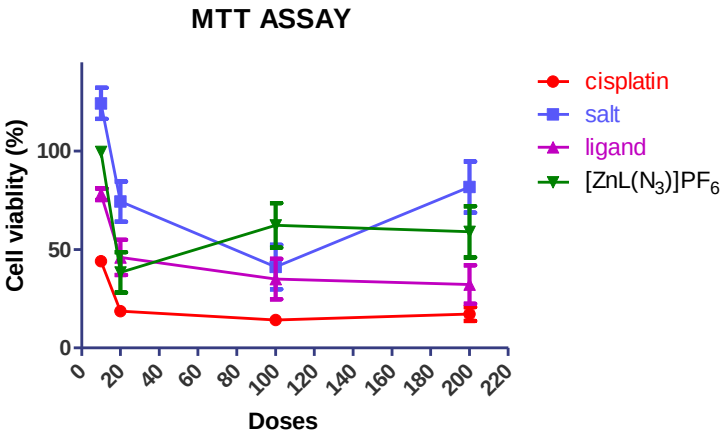

Fig.24 $[ZnL(N_3)]PF_6$ complex.

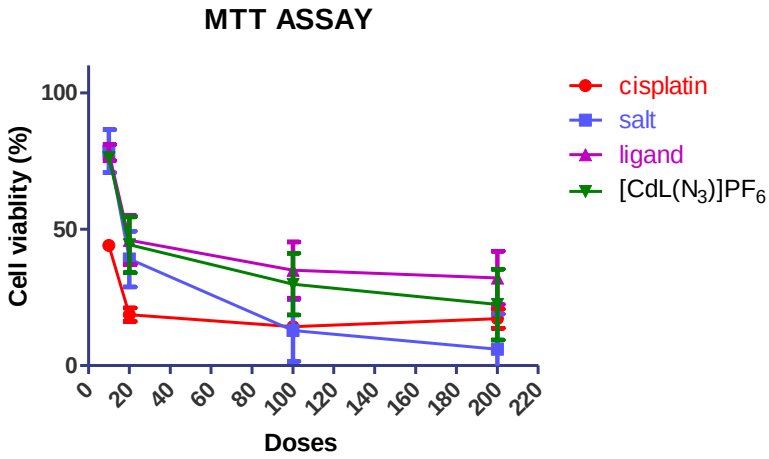

Fig.24 $[CdL(N_3)]PF_6$ complex.

List of Publication

1. Synthesis, characterization, structure and magnetic properties of azido-bridged nickel(II) and copper(II) complexes with a pyridylpyrazole-based ligand
   Mahendrasinh,. Zala.; Kumar, S B.; Suresh, E.; Ribas, *Trans. Met. Chem.*, 2010, *35*, 757
2. Isothiocyanate and selenocyanate complexes of Cu(II), Ni(II), and Co(II) with a pyridylpyrazole-based ligand:synthesis, characterization, and structure
   Mahendrasinh., Zala.; Kumar, S. B. Suresh, E.;. *J. Coord. Chem.*, 2011, *64*, 483.
3. Cayanato bridged Binuclear Nickel(II) and Copper(II) complexes with Pyridylpyrazole ligand: Synthesis, Structure and Magnetic properties
   Mahendrasinh, Zala.; Ankita, S.;. Kumar, S. B.; Escuer, A.; Suresh, E.
   (ICA-2011 press)
4. Chloride Bridge Binuclear Copper(II) Complex with Modified Ligand Structure and Different Coordination Environment:Synthesis, Characterization and Structure
   Mahendrasinh, Zala.; Ankita, S.; Kumar, S. B.; Suresh, E. (*Communicated)*
5. Sythesis, characterization, structure and cyatotoxic properties of thiocyanate containing copper (II) complexes with pyridylpyrazole ligand.
   Mahendrasinh, Zala.; Kumar, S. B.; A. Rangrej, P. Parikh.(communicated)
6. Synthesis, Characterization and Structure of mononuclear Copper(II) and Cobalt(II) complexes with a pyridylpyrazole based ligand.
   Mahendrasinh, Zala.; Kumar, S. B.; Suresh, E. (*manuscript under process)*
7. Azide containing Mononuclear Cadmium(II) Complex with Modified Ligand Structure:Synthesis, Characterization and Structure
   Mahendrasinh, Zala.; Kumar, S. B.; Suresh, E. (*Communicated)*
8. Synthesis, Characterization, Structure and Cytotoxic Properties of new Copper(II) complexes with pyridylpyrazole ligand.
   Mahendrasinh, Zala.; Kumar, S. B; Ayaz rangrej; Pragna Parikh.
   (*manuscript under process)*

Research Student **Research Guide**

(Zala Mahendrasinh Gajubha) **(Dr. Sujit Baran Kumar)**

Head of the Department

(Prof. B. V. Kamth)